Tree growth responses to different environmental conditions

NATASA KIORAPOSTOLOU

UNIVERSITÀ
DEGLI STUDI
DI PADOVA

Administrative unit: University of Padova

Department: **Land, Environment, Agriculture and Forestry (LEAF)**

PhD Program: **Land, Environment, Resources and Health (LERH)**

Batch: XXXII

Tree growth responses to different environmental conditions

PhD Program Coordinator: Prof. Davide Matteo Pettenella

Supervisor: Giai Petit

PhD candidate: Natasa Kiorapostolou

UNIVERSITÀ
DEGLI STUDI
DI PADOVA

Sede Amministrativa: Università degli Studi di Padova

Dipartimento; **Territorio e Sistemi Agro-Forestali (TESAF)**

CORSO DI DOTTORATO DI RICERCA: **Land, Environment, Resources, Health (LERH)**

Ciclo: XXXII

Risposte di crescita degli alberi a diverse condizioni ambientali

Coordinatore: Prof. Davide Matteo Pettenella

Supervisore: Prof. Giai Petit

Dottoranda: Natasa Kiorapostolou

Tree growth responses to different environmental conditions

Natasa Kiorapostolou

September 2019

PhD Thesis

Supervisor: Giai Petit

Reviewed by:

Gricar Jozica

Pavkova Lenka

PhD Course
LAND, ENVIRONMENT, RESOURCES AND HEALTH

Land, Environment, Resources and Health

(L.E.R.H.) PhD Program

UNIVERSITÀ DEGLI STUDI DI PADOVA

«Η φύσις, μηδέν μήτε ατελές ποιεί, μήτε μάτην»
Αριστοτέλης 384 – 322 π.Χ.

«Nature does nothing in vain»
Aristotle 384 – 322 BC.

Table of Contents

Summary

Increasing frequency and intensity of droughts affect forest ecosystems. There are already higher rates of tree mortality and forest drought-induced dieback. Since climate change affects the soil conditions, the precipitation rates and the growth seasons, it is expected that trees will develop acclimation and adaptation strategies in order to maintain vigor. Since the two most important reasons of mortality are carbon starvation and hydraulic failure, adjustments in physiological traits are expected to be related to the maintenance of the tree carbon and water balances.

This thesis focused on understanding how trees respond under different environmental conditions (e.g. wet vs dry) both at the intraspecific and interspecific level. The conducted studies focused on biomass allocation, xylem and phloem anatomies of stem and branches, xylem anatomy of leaves, plant hydraulics, and wood density. Mostly, data from personal measurements were used, but also published data to compare the results. The aim was to understand which structural traits are linked to the acclimation and adaptation strategies of trees and how. The structure of the thesis is: (i) general introduction, (ii) five main chapters based on different studies, (iii) one main chapter describing in short three more studies, (iv) overall conclusion, (v) additional information for each of the main chapters (if applicable), (vi) acknowledgments, (vii) anatomical images for some chapters, (viii) literature cited listed per chapter.

Sommario

L'aumento della frequenza e dell'intensità della siccità colpisce gli ecosistemi forestali. Esistono già tassi più elevati di mortalità degli alberi e di dieback indotto dalla siccità nelle foreste. Nelle condizioni climatiche previste, si prevede che gli alberi svilupperanno strategie di acclimatazione e adattamento al fine di mantenere il vigore. Poiché le due ragioni più importanti della mortalità sono la carenza di carbonio e il cedimento idraulico, si prevede che gli aggiustamenti dei tratti fisiologici siano correlati al mantenimento dei bilanci del carbonio e dell'acqua dell'impianto.

Questa tesi si è concentrata sulla comprensione del modo in cui gli alberi rispondono in diverse condizioni ambientali (ad esempio umido vs secco) sia a livello intraspecifico che interspecifico. Il lavoro svolto riguardava l'allocazione della biomassa, l'anatomia dello xilema e del floema dello stelo e dei rami, l'anatomia dello xilema delle foglie, l'idraulica delle piante e la densità del legno. Principalmente, sono stati utilizzati i dati delle proprie misurazioni, ma anche i dati pubblicati per confrontare i risultati. Lo scopo era capire quali tratti strutturali sono collegati alle strategie di acclimatazione e adattamento degli alberi e come.

La struttura della tesi è: (i) introduzione generale, (ii) cinque capitoli principali basati su diversi studi, (iii) un capitolo principale che descrive in breve altri tre studi, (iv) conclusione generale, (v) informazioni aggiuntive per ciascuno dei capitoli principali (se applicabile), (vi) riconoscimenti, (vii) immagini anatomiche per alcuni capitoli, (viii) letteratura citata elencata per capitolo.

Chapter 1. General introduction

Background

Increasing rates of heat waves and drought events due to climate change (IPCC, 2014) influence forest ecosystems (Reich et al., 2018). The increased frequency and intensity of droughts resulted already in an increasing trend of decline of vitality of current forest trees (Allen et al., 2010; Hartmann et al., 2018). Tree physiological processes are affected by droughts especially when they occur during the growing season. For instance, rates of photosynthesis are lower during drought (Reich et al., 2018) and trees have lower growth rates. However, how trees cope with droughts and how they alter their traits to maintain functionality, although important matters, are still unclear. Understanding the responses of trees, not only will allow us to predict the future status of Earth's forests, but also to include plant traits in climate models, which is of high importance since plants have a role in global geochemical cycles (Anderegg et al., 2018).

As reported in the work of Mc Dowell et al. (2008), the two physiological mechanisms leading to tree mortality are (i) carbon starvation and (ii) hydraulic failure. Thus, it can be expected that trees in order to survive will adjust the physiological characteristics that are linked to their carbon and water balances.

The survival of trees depends on a functional balance between carbon uptake and carbon cost for maintenance respiration of the living tissues and growth. Trees uptake carbon through leaf photosynthesis in the stomata that allow gas exchanges (Lack & Evans, 2005). Transpiration is sustained by water flowing from roots to leaves following a gradient of negative water potentials. In fact, the ascent of the sap is quite a "unique" process and was described by Dixon and Joly (1985) with the cohesion tension theory. According to this theory, water moves through elongated dead conduits in the xylem, driven by a gradient of negative pressures generated due to the transpiring leaves and without the consumption of energy. Because of the adhesion and cohesion of water molecules, the water columns remain intact. Water is under tension and below its vapour pressure (it is in a metastable state) being subjected to embolisation (Choat et al., 2018). Under drought, when soil water potentials are lower, xylem sap tension reaches a threshold in which air can be aspirated into xylem conduits (i.e. embolism formation). Embolism can spread in the xylem conduits and block the water transportation ultimately leading in hydraulic failure. Therefore, trees have on the one hand to efficiently transport water to maintain transpiration, and on the other hand to develop a safe water transport

system to avoid the risk of mortality due to hydraulic failure. However, a more efficient system has lower hydraulic safety (wider conduits) and thus, there is a trade-off between hydraulic safety and efficiency.

Xylem anatomy is strongly related to the total hydraulic safety and efficiency of the plant (Hacke & Sperry, 2001), and to plant performance under different soil water conditions. It is commonly found that under drier environments plants produce narrower and hydraulically safer conduits (von Arx et al., 2012; Pfautsch et al., 2016; Larter et al., 2017). In lieu, other studies showed that xylem cells widen from the apex towards the stem base according to a power scaling relationship ($y = \alpha \cdot x^b$, where α is the allometric constant and b is the exponent) that is very similar between different species and environments (Anfodillo et al., 2013). According to this scaling, conduits are narrower near the stem apex allowing for the independence of the resistance along the total path length. Scaling relationships are crucial and as suggested by Anfodillo et al. (2016), the death of a plant would be related to non-reversible departures from the general scaling between traits.

Carbon uptaken through photosynthesis is transported via the phloem sieve elements from the sources (areas with high sugar concentration, leaves) to the sinks (areas with lower sugar concentration) (Jensen et al. 2012) to be directly used for maintenance respiration of the living tissues or to be stored for usage upon requirements. Phloem sap moves following differences in turgor pressure between the sources and sinks according to the Münch's circulation hypothesis (Hölttä et al. 2006; De Schepper et al. 2013). Phloem sieve elements maintain hydration by compensating the negative water potentials in the xylem through osmoregulation (Savage et al. 2016), and thus the two tissues are coupled. In addition, phloem sieve elements are narrow at the treetop and progressively widen below until the stem base similar to the xylem (Petit and Crivellaro 2014).

Moreover, plant species are characterised by different values of minimum leaf water potential (Ψ_{L_MIN}). Species with lower leaf water potential are assumed to be more tolerant to drought as they can operate under lower (more negative) soil water potentials. Plant species can be classified into a continuum of isohydry (from isohydric to anisohydric) based on their stomata regulation (Martínez-vilalta & Garcia-forner, 2017). Plants that are characterised by a more isohydric behaviour have stronger stomatal control and close their leaf stomata at a defined Ψ_{L_MIN} to guarantee no water loss, while plants that have a more anisohydric

behaviour lower their Ψ_{L_MIN} to maintain a certain degree of leaf gas exchanges even under reduced soil water content (Attia et al., 2015). Isohydric species preserve their water transport system from conduit embolisation and sustain respiratory metabolism of living tissues with stored carbon reserves. Contrary, anisohydric species expose their water transport system to a higher risk of embolisation to maintain leaf transpiration and thus carbon assimilation, and do not necessarily rely upon stored reserves to survive during drought events (Mc Dowell, 2011).

Nevertheless, plants operate at leaf water potentials close to their thresholds of half loss of xylem conductivity due to embolism (Nardini and Salleo 2000; Choat et al., 2012), and for this reason, it is thought that embolism formation is a common phenomenon in everyday plant's life. Therefore, it is expected that plants evolved mechanisms to recover embolised conduits. Although the exact process of embolism recovery remains unknown (Brodersen & Mc Elrone, 2013), there are several hypothesis provided. For instance, Zwieniecki & Holbrook (2009) proposed the scenario of an active embolism refilling capacity, according to which when a conduit is embolised there is a higher sugar accumulation inside the conduit that attracts water molecules for refilling the conduit. In this case, xylem parenchyma cells should have an important role in this process providing the sugars and water needed. Another example is the replacement of embolised conduits with new xylem (Pratt et al. 2005).

Hence, characteristics of the xylem and phloem, and differences in biomass allocation can allow us to understand how trees maintain their carbon and water balances or why trees are losing vitality.

Aim and research questions

This thesis aimed to understand how trees respond to different environmental conditions (e.g. wet vs dry sites) focusing on traits that are possibly linked to the maintenance of the tree's carbon and water balances. The conducted studies focused on biomass allocation, xylem and phloem anatomies of branches and stems, xylem anatomy of leaves, plant hydraulics, and wood density.

According to the theoretical background described previously in this chapter, this thesis included the following research questions:

What are the differences in biomass allocation across and within species under different soil water availability?
What are the differences in the xylem and phloem anatomical traits within species under different soil water availability?
Is there a link between xylem embolism vulnerability and wood parenchyma fraction?
What is the effect of the axial gradient of xylem water potential considering the conduit widening?
What are the differences in xylem and phloem anatomies between declining and non-declining trees?

Structure of the thesis

In the rest of the thesis, the reader will find:

- Five main chapters aiming to provide answers to the research questions.
- One chapter describing in short three more studies relevant to the research questions.
- Overall conclusion.
- Additional information for each of the main chapters (if applicable).
- Acknowledgments.
- Anatomical images for some chapters.
- Literature cited listed per chapter.

Chapter 2. Structural and anatomical responses of *Pinus sylvestris* and *Tilia platyphyllos* seedlings exposed to water shortage

Authors:
Natasa Kiorapostolou*, Lucía Galiano-Pérez, Georg von Arx, Arthur Gessler, Giai Petit

Published in:
Trees (2018)

Corresponding author *

Abstract

Phenomena of tree decline and mortality are increasing worldwide as a consequence of the higher temperatures accompanying drought events. Studying changes in biomass allocation and xylem anatomy may shed light into the relative importance that C and water impairment have during drought, and can help to better understand how plants will respond to future droughts.

We measured the dry weight of the leaf, aboveground and belowground xylem biomass in tree seedlings of the drought avoidant *Pinus sylvestris* and drought tolerant *Tilia platyphyllos* exposed to different intensities of water shortage. Moreover, the area of vessels was measured at three positions along the stem.

In *P. sylvestris*, we found no differences in total biomass across treatments, but a preferential allocation to needle mass under drought, while there were no differences in xylem anatomy. *T. platyphyllos* under ambient and mild drought increased leaf and total xylem biomass according to an isometric pattern, whereas the largest vessels near the stem apex were found in seedlings under severe drought.

Our results suggest a categorisation of the two species regarding the coordination of carbon and hydraulic economies. *P. sylvestris* invests relatively more into leaf biomass to increase photosynthesis and thus decreases the risk of carbon starvation, while *T. platyphyllos* invests more into hydraulic efficiency to decrease the risks of embolisation.

Keywords: *Pinus sylvestris*, *Tilia Platyphyllos*, drought, biomass allocation, xylem anatomy, isohydry

Introduction

The average global temperature has already increased by 0.85 ˚C since 1880 (IPCC 2014), and even higher temperatures are expected in the future, implying warmer summers and winters thus longer growing seasons (Menzel and Fabian 1998), and possibly the occurrence of more frequent extreme drought events in various areas of the Earth due to more erratic precipitation regimes (IPCC 2014). Within such a perspective, species are expected to adopt acclimation and/or adaptation strategies to withstand the new climatic conditions (Jump and Penuelas 2005; De Micco and Aronne 2012). In recent years, however, higher rates of tree mortality and forest dieback have been reported at global scale after severe drought events (Allen et al. 2010). Although we still lack a clear understanding on the ultimate mechanism

leading to tree decline and mortality under drought (Mitchell et al. 2012), the coordination between carbon and hydraulic economies is emerging as a fundamental requirement for plant survival (Mencuccini 2014; Mitchell et al. 2014; Petit et al. 2016; Sterck and Zweifel 2016).

Plants are distributed across a continuum from drought avoidant to drought tolerant species, and according to their stomatal regulation under different soil water potentials (Martínez-Vilalta and Garcia-Forner 2017), from isohydric to anisohydric species. Relatively isohydric species close stomata at a defined minimum leaf water potential (Ψ_{L_MIN}) set at relatively moderate negative pressures, while relatively anisohydric species are able to lower their Ψ_{L_MIN} to maintain a certain degree of leaf gas exchange even under water deficits (Attia et al. 2015). These different modes of stomatal control are supposedly linked to different survival strategies under drought. Under this scenario, relatively isohydric species would preserve the transport system from xylem tensions potentially triggering conduit embolisation. This implies that these species most likely rely upon stored carbon reserves to sustain the respiratory metabolism under drought, and may therefore die of carbon starvation after substantial depletion of carbon resources during prolonged drought (McDowell et al. 2008). On the contrary, relatively anisohydric species probably need to keep water transport efficient to sustain leaf transpiration and carbon assimilation even under drought. Thus, anisohydric species would expose their xylem system to the risk of hydraulic failure because of excessive cavitation events triggered by the extreme high tensions that could develop under very intense water deficits, irrespective of their duration (Attia et al. 2015). These species do not necessarily rely upon stored reserves to survive during drought events (McDowell 2011).

Plants have been shown to allocate their functional/structural traits following allometric relationships that commonly follow power scaling functions:

$$Y = a \cdot X^b \qquad \text{eq. 1}$$

where Y and X are functional/structural traits, a the allometric constant and b the scaling exponent. According to optimality principles (West et al. 1999), these relationships between traits would imply a substantial convergence towards a common scaling exponent (b), reflecting the necessary balance between structures and functions to maintain a positive carbon balance (Anfodillo et al. 2016). On the contrary, differences in the allometric constant (a) would reflect modifications in the absolute proportion between traits (e.g. between leaf mass and

xylem mass) that may emerge in different environmental conditions (Weiner 2004). In this scheme, Anfodillo et al. (2016) suggested that the death of a plant would be related to non-reversible departures from the general scaling between traits (similar scaling exponent *b*), with high and low thresholds of the allometric constant (*a*) representing the limits to plant functionality. A sustainable balance of carbon production vs. consumption is reached when a given leaf mass provides at least the necessary carbon resources to sustain the maintenance cost of the living tissues in a given xylem mass, whereas the invested biomass to below- and aboveground xylem must guarantee an efficient soil water absorption and transport that meet the leaf transpiration requirements.

Water is transported under a negative pressure gradient through the elongated dead cells of the xylem, which can be compared to capillary tubes and therefore produce a frictional resistance to flow inversely proportional to the fourth power of their diameter (Hagen-Poiseuille law, Tyree & Ewer 1991). On the contrary, more adhesive forces for a unit of water volume can develop on smaller xylem conduits that can better cope with the metastable status of tensile water (Hacke et al. 2017). Therefore, xylem anatomy is strongly related to the total hydraulic safety and efficiency (Hacke and Sperry 2001), and thus to the plant performance under different soil water conditions. A common pattern often found in xylem anatomy studies is the production of narrower and hydraulically safer vessels in drier environments (von Arx et al. 2012; Pfautsch et al. 2016; Larter et al. 2017), with the reduced growth rate being the "cost" of their reduced hydraulic efficiency (Wheeler et al. 2005). Instead, other empirical evidence demonstrates that plant architecture is organised with conduit lumen areas widening from the stem apex towards the base according to a scaling pattern that is very similar between species in different environments (Anfodillo et al. 2013). The hydraulic consequence of such a pattern is that most of the resistance is concentrated within a short distance from the apex (Yang and Tyree 1993; Becker et al. 2000; Petit and Anfodillo 2009), thus making the apical anatomical features of particular importance for the whole plant conductance (Petit et al. 2011; Prendin et al. 2018) and also for hydraulic vulnerability (Prendin et al 2018b).

In this study, seedlings of two species (*Pinus sylvestris* L. and *Tilia platyphyllos* Scop.) were subjected to two water shortage intensities to test their performance under drought conditions in terms of biomass allocation to leaf, stem and root tissues, and also to evaluate the degree of plastic adjustment at the xylem anatomical level. As the species have

been shown to differ in terms of hydric behaviour, with *P. sylvestris* to be relatively isohydric (Irvine et al. 1998) and *T. platyphyllos* relatively anisohydric (Leuzinger et al. 2005; Galiano et al. 2017), we hypothesised that *P. sylvestris* will associate more needles to a given xylem biomass by prioritising allocation to needle biomass to prevent C reserve imbalances (e.g. C reserve depletion), while *T. platyphyllos* will maintain the structural balance between leaf and xylem biomass but will adjust its xylem anatomy to maintain an efficient water transport under drought.

Materials and methods

Plant materials and experimental design

Our two target species were selected based on different responses to drought conditions: *P. sylvestris L.* (PS) has a strong stomatal control and minimises stomatal conductance under drought, even if this can produce intense depletion of stored carbon reserves potentially leading to mortality events (Aguadé et al. 2015). Instead, *T. platyphyllos* Scop. (TP), a deciduous angiosperm with diffuse to semi-ring porosity, has a less strong stomatal control of transpiration and has been found to recover well after drought relief (Leuzinger et al. 2005).

Three-year old seedlings of the two species (N = 36), with a mean height of 28.16 ± 0.86 cm (mean ± se) for *P. sylvestris* and 30.59 ± 1.60 cm for *T. platyphyllos*, were planted in 3.5 L pots at the beginning of May 2014 in the greenhouse of the Swiss Federal Institute for Forest, Snow and Landscape Research WSL (47º 21′ 37″ N, 08º 27′ 21″ E; 500 m a.s.l.). The seedlings were planted before leaf development in *T. platyphyllos*. Greenhouse temperature ranged from 9 to 37 º C and air humidity from 22 to 74 %. Artificial illumination was applied (Master Green Power CG T 400W Mogul 1SL/12. Phillips Lighting Holding B.V., Eindhoven, The Netherlands) simulating the mean summer photoperiod of Swiss latitudes (~15 h light). During the acclimation period in the greenhouse, all seedlings were watered every second day to field capacity. Six pots from each of the two species were allocated to each of the three watering treatments paying attention that size variability between treatments was similar. The treatments started on 14th July in *T. platyphyllos* and 28th July in *P. sylvestris,* when seedlings showed vigorous conditions and leaves fully developed, and were applied continuously for approximately two months (until 14th September in *T. Platyphyllos* and 28th September in *P. sylvestris*), and were:

- Control (C): Normal watering with soil volumetric water content (VWC) maintained at field capacity ~ 23%.
- Moderate drought (MD): Watering adjusted to maintain VWC at 15%, which equalled the soil water potential (Ψ_{SOIL}) ~ -0.12 MPa.
- Severe drought (SD): Watering adjusted to maintain VWC at 8%, which equalled Ψ_{SOIL} ~ -1.3 MPa.

Measurements

At the end of the experiment, each plant was extracted from the pot and the root system cleaned from soil residues. The height of the plants was measured, then plants were divided into three different organs (leaves/needles, aboveground stem and branches including the bark, and belowground roots), which were carefully separated and dried in an oven at 60 °C for 72 hours. The dry mass of all leaves/needles (*LM*), aboveground stem and branches (*AM*), and roots (*RM*) were obtained using a balance (Acculab ALC-1100.2) to the nearest 0.1 g. Total leaf area (LA_{TOT}) was measured in scanned images with ROXAS v2.1 (Arx and Dietz 2005; von Arx and Carrer 2014). Total biomass (BM_{TOT}), the ratio *LM:(AM+RM)*, and specific leaf area (*SLA*) were later computed. Stem segments were then collected at 3 different heights (stem base, 20 cm from the apex, 2 cm from the apex) from each of the 6 seedlings per species and watering treatments (total samples = 108). Sample preparation and anatomical analyses followed the guidelines proposed by von Arx et al. (2016). Micro sections were created using a rotary microtome LEICA RM 2245 (Leica Biosystems, Nussloch, Germany) at 15 μm thickness, stained with a solution of safranin and Astra Blue (1% and 0.5% in distilled water respectively), and permanently fixed on glasses with Eukitt (BiOptica, Milan, Italy). Overlapping images (around 25%) of the entire cross section of each sample were taken with a digital camera mounted on a Nikon Eclipse 80i microscope (Nikon, Tokyo, Japan), and then stitched with PTGui (New House Internet Services B.V., Rotterdam, The Netherlands). Stitched images were then analysed with ROXAS v2.1 (Arx and Dietz 2005, von Arx and Carrer 2014) for the automatic measurement of the lumen area (*CA*) of all the vessels in the outmost ring, and their frequency distribution in *CA* size classes of 20 μm^2 for *P. sylvestris* and 30 μm^2 for *T. platyphyllos*.

Statistical analysis

LM, *AM*, *RM*, BM_{TOT}, LA_{TOT}, *SLA*, and *LM:(AM+RM)* were all normally distributed. One-way ANOVA with Tukey post hoc comparisons were

used to test differences across watering treatments (C, MD, SD). To test the differences of *CA* size classes in the apical part of the branches (2 cm from the apex), a Kruskal-Wallis test was performed to the non-parametric data of the six largest *CA* size classes. All statistical analyses were conducted with standard methods (Zar 1999) using the software IBM SPSS Version 21 and Minitab 18.

Results

Pinus sylvestris

The overall structure of *P. sylvestris* seedlings did not seem to be changed at the end of the experiment. Mean final plant height (29.15 ± 0.93 cm) was not significantly different from the initial and we did not find significant differences in the height of the plants across treatments ($p > 0.05$). Moreover, the seedlings did not show any significant difference in BM_{TOT}, *LM*, *AM*, and *RM* across watering treatments (Fig 1a; Table 1). However, when we compared the allocation to leaf vs. xylem biomass, we found that the individuals exposed to severe drought (SD) showed a preferential allocation to the needle mass, resulting in a significantly higher ratio of *LM*:(*AM*+*RM*) (Fig 1c and Fig 2).

At the wood anatomy level, the distribution of tracheids in classes of lumen areas (*CA*) did not change much among treatments for stem distance from the apex (Fig 3). Mean cell lumen areas (*MCA*) increased from the stem apex to the base in all watering treatments (the so called conduit widening) (Fig 3, reference lines).

Table 1. Mean values (standard error) for each single variable across control (C), moderate drought (MD) and severe drought (SD) treatments in *P. sylvestris* (PS, upper panel) and *T. platyphyllos* (TP, lower panel). Letters (a,b) show significant grouping differences.

PS	*LM* (g)	*AM* (g)	*RM* (g)	LA_{TOT} (cm²)	*SLA* (cm²/g)
C	3.06 (0.23) a	2.50 (0.28) a	3.69 (0.34) a	132.99 (100) a	43.53 (107) a
MD	2.71 (0.25) a	2.13 (0.12) a	3.03 (0.37) a	110.76 (83) a	41.19 (92) a
SD	3.44 (0.22) a	2.15 (0.17) a	2.83 (0.21) a	151.70 (95) a	44.17 (63) a

TP	*LM* (g)	*AM* (g)	*RM* (g)	LA_{TOT} (cm²)	*SLA* (cm²/g)
C	1.85 (0.19) a	3.23 (0.33) a	8.66 (2.73) a	509.32 (96) a	300.95 (39) a
MD	0.95 (0.09) b	2.25 (0.30) a	4.11 (1.29) b	276.58 (26) ab	331.83 (45) a
SD	0.77 (0.12) b	2.05 (0.41) a	3.95 (1.46) b	255.26 (69) b	389.93 (106) a

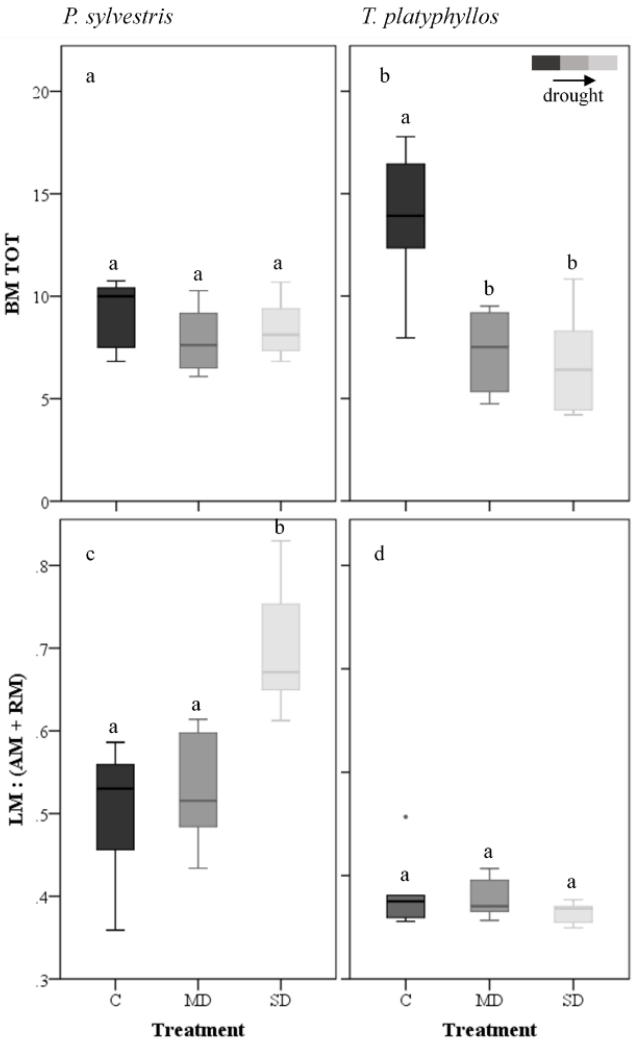

Fig. 1: Total biomass (BM_{TOT}) (g) for *P. sylvestris* (PS) (a) and *T. platyphyllos* (TP) (b), and the ratio Leaf mass / Stem and Root mass (*LM:(AM+RM)*) for PS (c) and TP (d) across control (C), moderate drought (MD), and severe drought (SD) treatments. Letters above the bars show the grouping with a p-value < 0.05 performed with Tukey post-hoc tests.

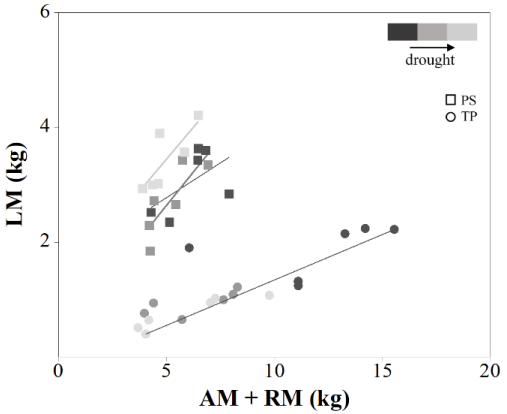

Fig. 2: Leaf biomass (g) against combined Stem and Root biomass (g) for *P. sylvestris* (PS, squares) and *T. platyphyllos* (TP, circles) across watering treatments (C, MD, SD). Statistics for PS: (C) $y=1.1444x^{0.5376}$, $R^2 = 0.3803$, p = 0.26, (MD) $y=0.558x^{0.96}$, $R^2 = 0.6726$, **p=0.042***, (SD) $y=1.2006x^{0.6554}$, $R^2 = 0.6539$, p=0.053. Statistics for TP: $y=0.1791x^{0.8933}$, $R^2 = 0.7071$.

Tilia platyphyllos

In *T. platyphyllos* seedlings, the application of water shortage treatments affected the overall plant structure and xylem anatomy. The mean final height (31.24 ± 1.55 cm) did not differ significantly from the initial and across treatments ($p > 0.05$). Instead, the drought treatments significantly and negatively affected the total biomass production. Indeed, the BM_{TOT} was significantly lower (by approximately 50%) under both moderate (MD) and severe drought (SD) treatments compared to the control (C) (Table 1; Fig 1b). However, the ratio *LM*:(*AM+RM*) did not differ across watering treatments (Fig 1d; $b = 0.89$, 95% CI = 0.7197, 0.9936). LA_{TOT} tended to be lower and *SLA* higher with increasing drought but only LA_{TOT} was significantly different in the severe drought (SD) relative to the control (C) (Table 1).

At the wood anatomy level, we found some differences among watering treatments (Fig 3). In particular, the analysis of the anatomical structure at 2cm from the stem apex revealed that seedlings exposed to the severe drought (SD) produced more vessels in the six widest CA classes (Kruskal-Wallis, $x^2 = 39.5$, $p < 0.001$) (Fig 3). However, the mean cell lumen area (*MCA*) at the different positions along the stem did not vary

much between watering treatments, but slightly increased from the apex downwards (Fig 3, reference lines).

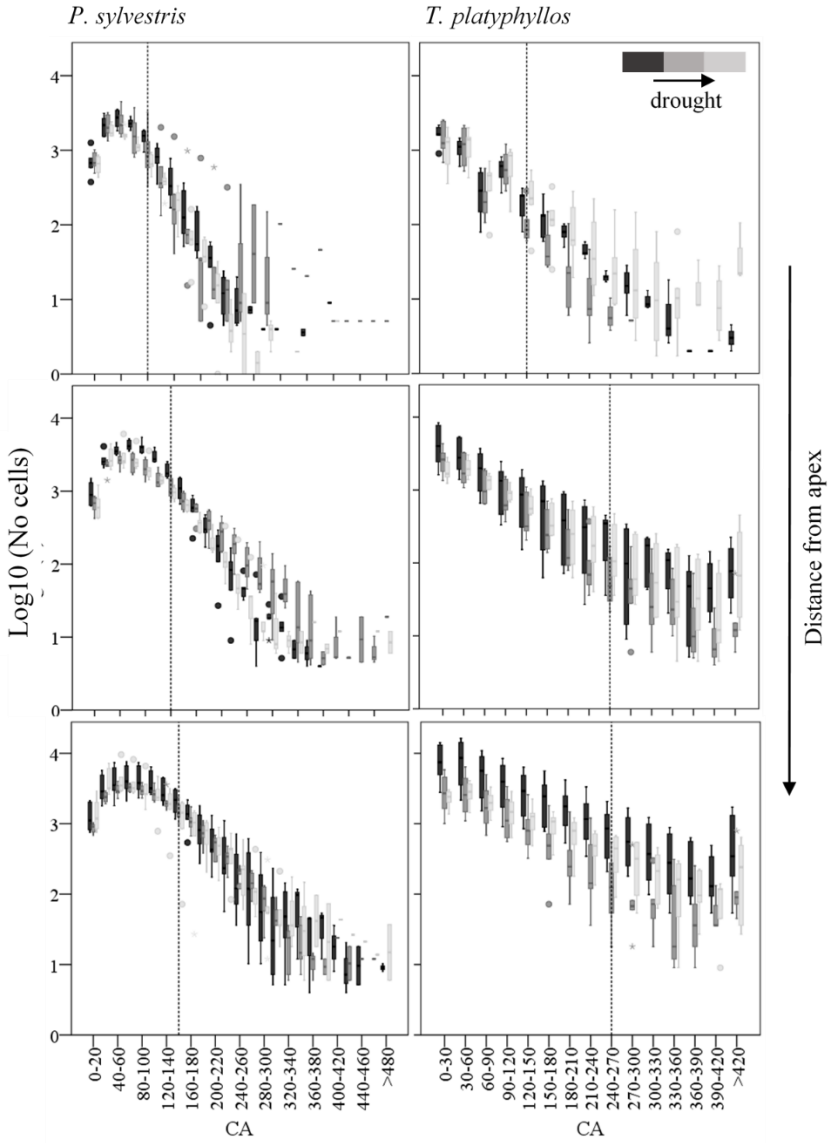

Fig. 3: Size classes of cell lumen areas (*CA*) for *P. sylvestris* (left panels) and *T. platyphyllos* (right panels) at different distances from the stem apex (2 cm upper panels, 20 cm middle panels, ~ 40 cm lower panels) and across watering

treatments (C, MD, SD). The reference lines show the mean *CA* of each distance from the apex and widening from the apex towards the base.

Discussion

Our greenhouse experiment revealed that the seedlings of the relatively isohydric *P. sylvestris* and the relatively anisohydric *T. platyphyllos* responded differently to drought exposure in terms of biomass allocation to the different organs and of wood anatomy.

In our *P. sylvestris* seedlings, we found little but not significant modifications in the overall plant biomass allocation and xylem anatomy. Because of the restricted size variation between seedlings, we could not assess a clear scaling relationship between *LM* and *AM+RM* explaining how *LM* must be adjusted to sustain the cost of maintenance associated to the living tissues in the xylem (Anfodillo et al. 2016). However, our results suggest that drought slightly affected the mass balance between C-producer (*LM*) and C-consumer (*AM+RM*) tissues (Fig 1c and Fig 2). Whatever the process mostly affected under drought was, either the accumulation of NSC in the needles or the slower production of fine roots (Galiano et al. 2017), our results suggest that drought-exposed pine seedlings modified the balance between *LM* and *AM+RM* in a way that a higher needle mass was associated to a given mass of tissues consuming carbon. A higher NSC concentration in the leaves (see also Galiano et al. 2017) may have provided the necessary osmoregulation to keep stomata open also under drier conditions. Alternatively, such a result is consistent with a recent hypothesis (Anfodillo et al. 2016) according to which species that cannot lower their leaf water potential (Ψ_L) enough to maintain the stomata open during reduced soil water (like *P. sylvestris*), must provide the carbon required for respiration by increasing the proportion of leaf/needle mass (see also Petit et al. 2016). Regarding the anatomical characteristics, we did not find any substantial difference in the size of xylem conduits along the stem across the three watering treatments. However, it is likely that cambial phenology was almost complete at the time of the experiment, and we cannot exclude the possibility that *P. sylvestris* modifies also its xylem anatomy when drought occurs before or during the intense cambial activity at the beginning of the season.

In *T. platyphyllos* seedlings, the two drought treatments negatively affected total biomass production (Fig 1b), in agreement with other studies referring to other species (e.g. Maseda and Fernández 2016). We found a nearly isometric relationship (i.e., a power scaling with

exponent *b* not significantly different from *b*=1) between *LM* and *AM+RM* irrespective of the watering treatment (Fig 2). This means that drought did not affect the proportionality between leaf biomass (C-producer) and biomass of aboveground plus belowground xylem (C-consumer) (Fig 1d, Fig 2). Therefore, differently from *P. sylvestris*, the maintenance costs of a given unit of xylem biomass in *T. platyphyllos* is sustained by a given unit of leaf biomass irrespective of soil conditions. The isometric relationship between *LM* and *AM+RM* suggests maintenance of the functional balance between leaf photosynthesis and xylem water transport. The fact that *T. platyphyllos* maintained the same proportion between different functional tissues (leaf and xylem biomass) also under drought conditions (Fig 1d) suggests that this species has a rather conservative strategy in the differential allocation between functional tissues (Reich et al. 2008, Anfodillo et al. 2016). Under drought this implies an adjustment in Ψ_L and/or an increase in total xylem conductance to maintain leaf transpiration. On the one hand, *T. platyphyllos* reduced Ψ_L slightly more under drought than *P. sylvestris* (Galiano et al. 2017), thus being relatively more anisohydric. On the other hand, we found an increase in the lumen area (*CA*) of apical conduits under severe drought (SD). Such a result strongly suggests an increase in xylem conductance in response to drought (see also Petit et al. 2016), in agreement with previous reports revealing the fundamental importance of the xylem anatomy close to the apex for the efficiency of the whole hydraulic transport system (Petit et al. 2011; Prendin et al. 2018).

Taken together, *T. platyphyllos* has a lower leaf biomass associated to a given xylem biomass than *P. sylvestris* (i.e., lower *y*-intercept in Fig 2). We can assume that the C-cost associated to tissue respiration is at least similar between species, since the amount of living, and thus respiring, xylem parenchyma is certainly not higher in *P. sylvestris* than *T. platyphyllos* (Schweingruber 1990). Therefore, our results would suggest that a unit of leaf mass in *T. platyphyllos* must provide more carbon than *P. sylvestris* needles (Galiano et al. 2017), i.e. they must be photosynthetically more efficient because the amount of assimilated carbon per leaf biomass required for the maintenance costs of a given xylem biomass (leaf-based maintenance costs) is higher in *T. platyphyllos* as it has higher SLA values (Table 1). In agreement with this, *P. sylvestris* showed relatively stronger stomatal control of water losses by transpiration than *T. platyphyllos* (Galiano et al. 2017), with Ψ_{L_MIN} commonly being less negative, suggesting an earlier interruption

of leaf gas exchange and thus photosynthesis under water deficit conditions (Irvine et al. 1998). In addition, we can speculate that the seedlings of *T. platyphyllos* acclimated to soil drought by reducing the investment in growth because of the high leaf-based maintenance costs (low *y* intercept in Fig 2). This would imply that leaf transpiration and photosynthesis are also maintained under water shortage. Consistently, we found a slightly higher number of vessels in the largest classes of lumen area (*CA*) near the apex under severe drought (SD). Since the xylem cell conductance scales to the second power of its area (according to Hagen-Poiseuille: Tyree & Ewers 1991), and apical conduits represent the hydraulic bottleneck of the entire xylem transport system (Petit et al. 2010), such a result would suggest an attempt to increase the overall conductive capacity of the xylem transport system by investing the least carbon into the new xylem biomass. This result is highly relevant, as it provides evidence that future acclimation of a species that tolerates drought implies prioritised investment in xylem efficiency vs. safety. This is supported by recent investigations (Petit et al. 2016) reporting that under reduced soil water availability, *Fraxinus ornus* L. trees reduce the C costs associated to growth while producing wider vessels to maintain an efficient leaf specific conductance. However, this finding is in contrast to the literature reporting narrower and safer conduits in drier environments (e.g. Wheeler et al. 2005; Lens et al. 2007; von Arx et al. 2012; Pfautsch et al. 2016; Larter et al., 2017). In this context, it is worth highlighting that most studies simply ignored the existence of a substantial axial variation of vessel/tracheid lumen area from the apex downwards (Petit and Anfodillo 2011), and such a pattern must be filtered out through a proper standardisation procedure when assessing the effect of any environmental factor on wood anatomical properties (Lechthaler et al. 2017 submitted).

Conclusion

Based on our results, *P. sylvestris* seems to respond morphologically and *T. platyphyllos* anatomically to ultimately adapt their carbon and hydraulic economies to drought conditions.

P. sylvestris has less xylem biomass associated to a unit of needle/leaf biomass than *T. platyphyllos*, and therefore it has less corresponding living tissues. The species prioritises allocation to needle vs. xylem biomass under drought, likely to enhance the total assimilation per time unit of stomata opening, while maintaining safe conditions against the risk of xylem cavitation. However, such a strategy may lead in the long

run to carbon reserve depletion and ultimately to death from carbon starvation.

Instead, the high leaf-based maintenance costs of *T. platyphyllos* impose a strategy to maintain a more continuous carbon assimilation and consequently transpiration, also under drier conditions. Therefore, the hydraulic efficiency (i.e., conductance) of the xylem transport system is prioritised over safety, exposing the xylem to lower water potential under drought, even if this could lead to wide spread cavitation events.

Chapter 3. Similarities and differences in the balances between leaf, xylem, and phloem structures in *Fraxinus ornus* along an environmental gradient

Authors:
Natasa Kiorapostolou*, Giai Petit

Published in:
Tree physiology (2018)

Corresponding author *

Abstract

The plant carbon balance depends on the coordination between photosynthesis and the long-distance transport of water and sugars. How plants modify the allocation to the different structures affecting this coordination under different environmental conditions has been poorly investigated. In this study, we evaluated the effect of soil water availability on the allocation to leaf, xylem, and phloem structures in *Fraxinus ornus*.

We selected small individuals of *F. ornus* (height, *H*~2 m) from sites contrasting in soil water availability (wet vs dry). We measured how the leaf (*LM*) and stem+branch biomass (*SBM*) are cumulated along the stem. Moreover, we assessed the axial variation in xylem (*XA*) and phloem tissue area (*PA*), and in lumen area of xylem vessels (*CAxy*) and phloem sieve elements (*CAph*).

We found a higher ratio of *LM:SBM* in the trees growing under drier conditions. The long-distance transport tissues of xylem and phloem followed axial patterns with scaling exponents (*b*) independent of site conditions. *PA* scaled isometrically with *XA* (*b*~1). While *CAxy* was only marginally higher at the wet sites, *CAph* was significantly higher at the drier sites.

Our results showed that under reduced soil water availability, *F. ornus* trees allocate relatively more to the leaf biomass and produce more conductive phloem likely to compensate for the drought-related hydraulic limitations to the leaf gas exchanges and the phloem sap viscosity.

Keywords: *Fraxinus ornus*, soil moisture, biomass allocation, wood anatomy, xylem, phloem, allometry, conductance

Introduction

The survival of vascular plants under different environmental conditions primarily depends on the maintenance of a positive carbon (C) balance of C gain through photosynthesis minus the C consumptions for maintenance respiration and the C allocation for growth (i.e. new biomass) and storage of the different organs (Klein and Hoch 2015).

Gas exchanges between the mesophyll cavities and the atmosphere occur through open stomata; thus the assimilation of CO_2 through photosynthesis pays a high cost in terms of water losses with evapotranspiration (*ET*). According to the hypothesis of the continuum

soil-plant-atmosphere, the transpiration stream is sustained by the water flowing from roots to leaves through the xylem vasculature (*Fx*), following an axial gradient of negative water potentials (i.e. in a metastable state at sub-atmospheric pressures) (Sperry et al. 2003). According to Darcy's law, the xylem sapflow rate (*Fx*) is proportional to the water potential difference between the transpiring leaves (i.e. when stomata are open) and the rootlets in the soil ($\Delta\Psi$), and to the total xylem conductance (*K*) (Tyree and Ewers 1991):

$$Fx=\Delta\Psi\cdot K \qquad \text{eq. 1}$$

Since the conductance of the xylem (*K*) is a static property and cannot be adjusted without producing new conductive elements, the functional balance of $ET=Fx$ can be actively regulated by the stomatal conductance (Aston and Lawlor 1979), with the decrease in the guard cells' hydration reducing stomata aperture and compensating for the excessive evapotranspiration from the leaf mesophyll (Franks et al. 1998). Alternatively, the soil-to-leaf difference in water potential can be amplified through leaf osmoregulation.

Sugars produced with photosynthesis in the leaves (C-source) are flowing in aqueous solution through the phloem (*Fp*) to the sink sites in the different parts of the plant (Jensen et al. 2012). These sugars are used for the maintenance respiration of all living tissues, and for the biosynthesis of new biomass in the different organs (Maier 2001), or are stored as non-structural carbon reserves in the parenchyma cells (Plavcová et al. 2016). Phloem sap is flowing according to the M*ü*nch's circulation hypothesis following gradients of turgor pressure between the source (higher sugar concentrations) and sink sites (lower sugar concentrations) (Hölttä et al. 2006; De Schepper et al. 2013).

The hydraulic systems of long-distance transport of water and sugars operate at an overall hydraulic equilibrium between xylem and phloem (Thompson and Holbrook 2003; Hölttä et al. 2009), with phloem cells maintaining hydration by compensating the negative water potential in the xylem through osmoregulation (Savage et al. 2016).

The functional coupling of xylem and phloem hydraulics is also mirrored in their similar axial scaling of tissue area and conduit diameter. Jyske and Hölttä (2015) found a sub-isometric scaling (exponent $b \sim 0.9$) between the areas of the outmost ring and of the conducting phloem. In addition, both xylem conduits and phloem sieve elements are narrow at the treetop and progressively widen below until the stem base in a similar fashion (Petit and Crivellaro 2014; Jyske and Hölttä 2015).

The xylem network system has been more deeply investigated and commonly found to be very similar across species and tree sizes (Anfodillo et al. 2013), and stable during ontogeny (i.e. reiterated according to the similar axial widened pattern every year of growth) (Prendin et al. 2018b). Along the outmost ring, xylem conduits have a narrow lumen diameter at the stem apex and widen basally along the longitudinal axes of stem and branches until the stem base. Among all the possible combinations of conduit size and number along the stem axis providing a given conductance (*K*), the evolution of a widened xylem architecture allowed the minimisation of the C costs associated to the production of a safe and efficient long-distance transport system (Mencuccini et al. 2007), with smaller conduits at the apex to be more resistant to embolism formation under more negative water potentials (Nardini et al. 2017) developing in proximity of the transpiring leaves. Instead, since the resistance of a conductive pipe is inversely proportional to the fourth power of its diameter (Hagen-Poiseuille's law) (Tyree and Ewers 1991), wider conduits towards the stem base add negligible frictional forces to the total hydraulic resistance, thus making the conductive capacities of the current year xylem and the functional phloem nearly independent of tree height (Petit and Anfodillo 2009; Savage et al. 2017).

Although emerging evidence is supporting that the architectural design and the hydraulic functioning of xylem and phloem are tightly coupled, less clear is how plants adjust these structures to maintain efficient coordination of water and sugar transport under the limitations imposed by environmental variability.

For what concerns the effect of drought on xylem physiology, it is well known that lower water potentials expose plants to the risk of losing xylem conductance by embolism formation (Brodersen and McElrone 2013). Depending on the stomatal control of leaf transpiration, plants can either avoid excessive leaf dehydration and the development of risky high xylem tensions or osmoregulate to maintain stomata open and gas exchanges even if it comes at a higher risk of embolism formation. Under drier conditions, gas exchanges are more limited by the prolonged stomatal closure, especially in drought avoidant (isohydric) species. Therefore trees require a relatively larger leaf biomass/area to sustain a given cost of maintenance respiration (Anfodillo et al. 2016; Kiorapostolou et al. 2018), which is not affected by the stomata opening. Although a large body of literature reports that under drier conditions trees have a safer xylem, often characterised by

smaller xylem conduits (von Arx et al. 2012, Pfautsch et al. 2016, Larter et al. 2017), more recent analyses that accounted for the effect of axial conduit widening showed that carbon economy and hydraulic efficiency, but not safety, are rather pursued under more stressful conditions (e.g. drought, taller statures). This result suggests that the production of average larger conduits can be coupled with a reduction in their number to maintain xylem efficiency while further reducing its overall C production costs (Petit et al. 2016; Kiorapostolou et al. 2018; Prendin et al. 2018a). Moreover, it has also been hypothesised that further C economisation can be determined by the reduction in stem elongation, resulting in the contribution of more sapwood rings to the total *K* (Petit et al. 2016; Sterck and Zweifel 2016).

Soil drought has been hypothesised to impose limitations to phloem transport at two levels. On the one hand, unless leaves osmoregulate to lower their water potential, a lower soil water potential reduces the steepness of the water potential gradient along the xylem (Venturas et al. 2017), affecting in turn the steepness of the coupled hydrostatic pressure gradient along the phloem (Hölttä et al. 2006; Hölttä et al. 2009). On the other hand, phloem osmoregulation to equilibrate its hydric status with the lower xylem water potential (Savage et al. 2016) would increase the phloem sap viscosity (Mencuccini et al. 2015), with negative impact on the sugar transport velocity (according to the Hagen-Poiseuille's law, the hydraulic resistance is proportional to the fluid viscosity: Tyree and Ewers, 1991). In order to sustain plant metabolism, phloem conductance has been supposed to increase in response to drier conditions to compensate for the effect of higher phloem sap viscosity (Sevanto 2014; Sevanto et al.).

In this study, we evaluated the effect of soil water availability on the allocation to photosynthetic, xylem and phloem tissues in *Fraxinus ornus* L. trees. We tested the hypotheses that under drier conditions plants: (i) invest relatively more into leaf biomass to compensate for a longer stomatal closure, and (ii) produce more conductive xylem and phloem architectures to compensate for the more limiting axial gradient of xylem water potential and maintain an efficient long distant transport of water and sugars.

Materials and methods

Plant material and study sites

We selected our target species *Fraxinus ornus* L. (FO) based on its ability to adapt to different environments (De Micco et al. 2008). We

sampled five trees of similar size (2-3 m in height), in five different sites (N = 25) within the Province of Trieste (Northeastern of Italy) towards the end of growing season 2017 (mid-September). Trees had an age of 18 (± 7) years, and the stem diameter at the tree base was approximately 2-4 cm. We selected five sampling sites (Table 1) not much differing in annual temperature and precipitation regimes, but differing in available soil water content (AWC) according to the soil map of the Regional Agency of Agriculture Development (ERSA FVG, http://www.ersa.fvg.it/tematiche/suoli-e-cartederivate/cartografia-derivata). We divided our sites into two groups (wet (W) and dry (D)) according to the species response to the site's conditions in terms of stomatal conductance and minimum leaf water potential (Ψmin) (Gortan et al. 2009).

Biomass measurements

For each tree, we selected five to seven points evenly distributed along the main stem axis and measured their distance from the apex (*Dap*). Distal to each point, we measured the dry leaf biomass (*LM*, g) and the dry biomass of stem and branches (*SBM*, g), with a precision balance calibrated to the nearest 0.1g. (Acculab ALC-1100.2), after drying in an oven for 72 hours at 60° C. On a subset of randomly selected fresh leaves (approximately 50 leaves per tree), we also measured the leaf area (*LA*) on scanned images acquired with an EPSON GT-20000 scanner (Seiko Epson Corporation) and analysed with Fiji (Fiji Is Just ImageJ) v 1.49 (*Schindelin* et al. 2012). The specific leaf area (*SLA*) was then calculated as *LA:LM*.

Xylem and phloem anatomical measurements

For each sampling point along the stem axis, we extracted segments and preserved them into a solution of 50% alcohol. Sample preparation and anatomical analyses followed the guidelines described by von Arx et al. (2016). Transverse micro-sections for each stem segment were cut using a rotary microtome LEICA RM 2245 (Leica Biosystems, Nussloch, Germany) at 15-18 μm, stained with a solution of safranin and Astra Blue (1% and 0.5% in distilled water respectively), and permanently fixed on glass slides with Eukitt (BiOptica, Milan, Italy). Images from the micro-sections spanning from pith to bark were acquired at 100x magnification, using a D-sight slide scanner (Menarini Group, Florence, Italy). These images were analysed with ROXAS v 3.0.139 (von Arx and Carrer 2014b; von Arx and Carrer 2014a). The

analysis was performed on a wedge of known angle (α) centred at the pith. A first manual editing of the images to outline the contour of different sectors (i.e. the pith, each xylem ring, the conductive and the non-conductive phloem) was carried out. For each outlined sector in the wedge, ROXAS automatically measured the area (*RA*) and the mean conduit area (*CA*). The total xylem area (*XA*), and the total phloem area (*PA*) were up-scaled to the whole cross-section by multiplying the corresponding *RA* measurement by 360/*α*. For the phloem only, we restricted the ROXAS estimate of the mean area to the 20 most integer phloem sieve elements (*CAph*) among the widest in the functional, non-collapsed phloem, i.e. the youngest 1-2 phloem rings which are the most functional for the sugar transport (Evert 1990).

Site (Abbreviation)	symbol	latitude	longitude	altitude	drainage	AWC	*Ψmin*
Monrupino (MR)	■	45°43'09''	13°48'35''	336	LD	77	~-1.2
Bosco Bovedo (BO)	●	45°40'54''	13°45'49''	166	LD	86	~-2.7
Monte Valerio (MV)	◆	45°39'41''	13°47'44''	152	LD	80	~-3.25
San Lorenzo (SL)	◀	45° 37' 43''	13° 51' 46''	384	HD	44	~-3.55
Cernizza (CE)	✳	45° 46' 49''	13° 35' 31''	23	HD	42	~-3.7

Table 1. The five research sites and their characteristics. Symbols for each site were used on the Figures. Drainage refers to low soil drainage (LD) and high soil drainage (HD). The available water content (AWC, mm) is retrieved from the Regional Agency of Agriculture (ERSA FVG) and the minimum leaf water potential (Ψmin, MPa) of the species in these specific sites were taken from Gortan et al. (2009).

Statistical analysis

We analysed the scaling relationships between the different traits (i.e. *XA*, *PA*, *CAxy*, *CAph*, *LM*, *SBM*) and the distance from the apex (*Dap*), and the relationship between *XA* and *PA* as linear regressions of Log_{10}-transformed data, to comply with the assumption of normality and homoscedasticity. We tested for possible site effects on the *y*-intercept and slope (i.e. interaction: *b*) of the different scaling relationships by using general linear regression models. Differences between the means at wet and dry sites were tested with Kruskal – Wallis and Tukey post hoc tests. All statistical analyses were performed using R version 3.4.2 (R Core Team, 2017).

Results

Allocation to leaf and xylem biomass

We assessed how *F. ornus* trees cumulate the biomass of stem and branches (*SBM*) and the leaf biomass (*LM*) along the stem axis moving from the apex downwards. We observed a similar axial scaling (i.e. similar slope, *b~1.88*) of *SBM* vs the distance from the apex (*Dap*) between sites, but an overall higher *SBM* (higher *y*-intercept) in trees growing at the drier sites (see Supplementary Figure 1; Table 2). Instead, *LM* is cumulated along the stem axis from the apex downwards differently between dry and wet sites, with the former ones showing a lower *y*-intercept and a higher slope (*b*) (see Supplementary Figure 2; Table 2).

The total leaf biomass per individual tree (*LMind*) was significantly higher at the drier sites (Figure 1a; Kruskal – Wallis, $P < 0.05$). The total leaf area (*LA*) calculated for a subset of leaves was not significantly different between sites (Figure 1b; $P > 0.05$), and the derived calculation of the specific leaf area (*SLA*) resulted to be significantly lower at the drier sites (Figure 1c; Kruskal – Wallis, $P < 0.05$).

We assessed the relative allocation to leaf vs stem+branch biomass as the ratio *LM:SBM*, which resulted significantly higher at the drier sites (Figure 1d; Kruskal – Wallis, $P < 0.05$).

Xylem and phloem anatomies

We estimated the axial variation in the anatomical traits such as tissue area and average conduit lumen area of xylem and phloem.

Both xylem area (*XA*) and phloem area (*PA*) increased from the stem apex downwards to the base according to similar scaling exponents

(*b*=0.88 for *XA* vs *Dap* and *b*=0.89 for *PA* vs *Dap*) independent of site conditions, but with an offset of +0.5 in the *y*-intercept at the drier sites for both *XA* and *PA* (Figure 2; Figure 3; Table 2). This resulted to the tight, site independent and substantially isometric relationship between *XA vs PA* (Figure 4; b = 0.96, 95% CI = 0.9090-1.0199, R^2= 0.91; P < 0.0001).

At the cell level, we found that the mean lumen area of both xylem vessels (*CAxy*) and phloem sieve elements (*CAph*) increases from the stem apex downwards according to a scaling pattern independent of site conditions (*b*=0.42 for *CAxy* vs *Dap* and *b*=0.17 for *CAph* vs *Dap*) (Figure 5, Figure 6, Table 2). Moreover, we found a marginally significant higher *y*-intercept in *CAxy* vs *Dap* at the wetter sites (Figure 5; Table 2) and a highly significant higher *y*-intercept in *CAph vs Dap* under drier conditions (Figure 6; Table 2).

Table 2. Outputs of linear regression models. The models equal Log10(variable) ~ Log10(*Dap*) + site + Log10(*Dap*)*site, where variable = *SBM* or *LM* or *XA* or *PA* or *CAxy* or *CAph*, and site = W and D. Non-significant interactions are not shown in the table. W sites were taken as a reference and equal the y_0 and *b*.

Model information		***Estimates (± SE)***	***t-value***	***P***
SBM vs Dap	Intercept (y_0)	- 4.14 (0.12)	-35.70	< 0.001***
R^2 = 0.95, DF=122	Log10(Dap) (*b*)	1.88 (0.04)	49.00	< 0.001***
Sites	W	y_0		
	D	y_0 + 0.36 (0.03)	11.11	< 0.001***
LM vs Dap	Intercept (y_0)	- 1.41 (0.14)	- 9.98	< 0.001***
R^2 = 0.89, DF=122	Log10(Dap) (*b*)	0.88 (0.05)	18.33	< 0.001***
Sites	W	y_0		
	D	y_0 - 1.11 (0.22)	- 5.18	< 0.001***
Interactions	W	*b*		
	D	*b* + 0.50 (0.07)	6.83	< 0.001***
XA vs Dap	Intercept (y_0)	- 0.84 (0.09)	- 9.80	< 0.001***
R^2 = 0.86, DF=128	Log10(Dap) (*b*)	0.85 (0.03)	27.29	< 0.001***
Sites	W	y_0		
	D	y_0 + 0.32 (0.05)	6.96	< 0.001***
PA vs Dap	Intercept (y_0)	- 1.49 (0.08)	-17.57	< 0.001***
R^2 = 0.87, DF=120	Log10(Dap) (*b*)	0.86 (0.03)	27.54	< 0.001***
Sites	W	y_0		
	D	y_0 + 0.33 (0.05)	7.27	< 0.001***
CAxy vs Dap	Intercept (y_0)	1.75 (0.05)	38.80	< 0.001***
R^2 = 0.85, DF=128	Log10(Dap) (*b*)	0.44 (0.02)	27.05	< 0.001***
Sites	W	y_0		
	D	y_0 - 0.05 (0.03)	-2.48	< 0.02*
CAph vs Dap	Intercept (y_0)	1.71 (0.05)	37.42	< 0.001***
R^2 = 0.54, DF=111	Log10(Dap) (*b*)	0.15 (0.02)	8.82	< 0.001***
Sites	W	y_0		
	D	y_0 + 0.16 (0.03)	7.02	<0.001***

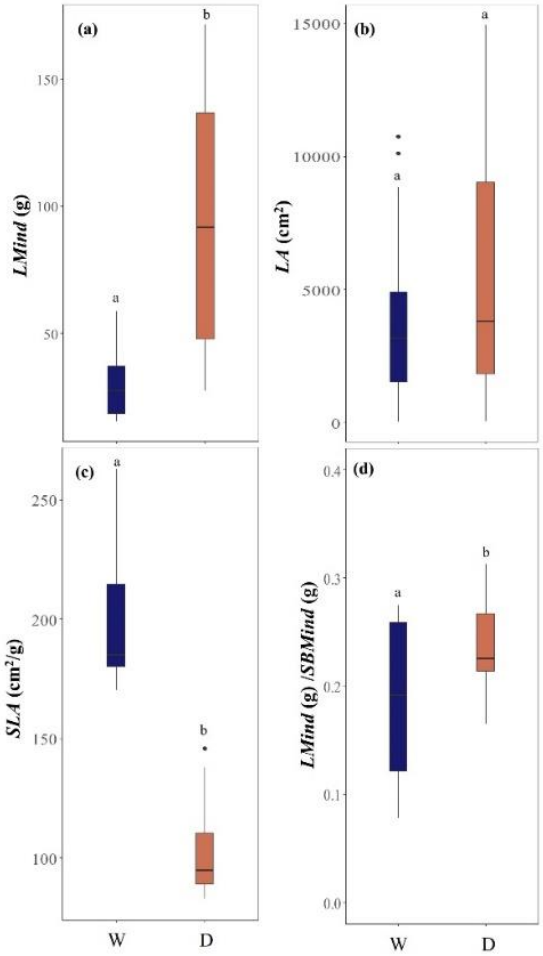

Figure 1. (a) Leaf mass (*LMind*, g) along the wet (W) (i.e. MR, BO, MV) and the dry (D) (i.e. CE, SL) sites. (b) Leaf area (*LA*, cm^2) along the W and D sites. (c) Specific leaf area (*SLA*, cm^2/ g) along the W and D sites. (d) Leaf mass (*LMind*, g) to stem+branch mass (*SBMind*, g) along the W and D sites. Letters above the boxes show the grouping with a *P*-value < 0.05 performed with Tukey post hoc tests.

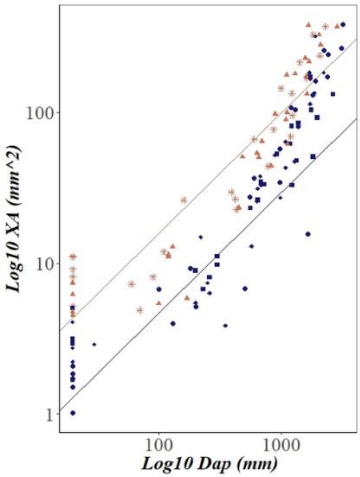

Figure 2. Xylem area (*XA*, mm^2) against the distance from the stem apex (*Dap*, mm) across the different sites. Blue colour for wet and orange for dry sites. Site symbols are shown in Table 1.

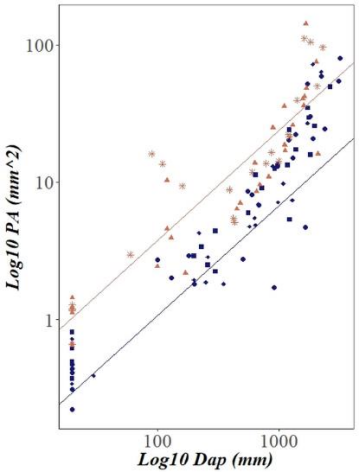

Figure 3. Phloem area (*PA*, mm^2) against the distance from the stem apex (*Dap*, mm) across the different sites. Blue colour for wet and orange for dry sites. Site symbols are shown in Table 1.

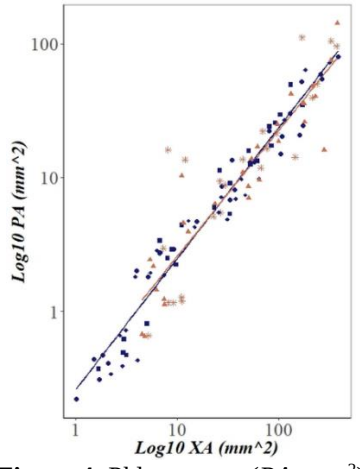

Figure 4. Phloem area (*PA*, mm^2) against xylem area (*XA*, mm^2) across the different sites. Blue colour for wet and orange for dry sites. Site symbols are shown in Table 1.

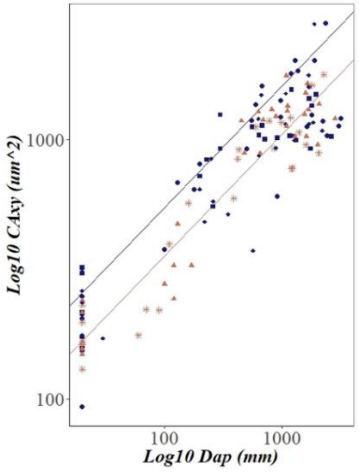

Figure 5. Mean xylem vessel area (*CAxy*, μm^2) against distance from the stem apex (*Dap*, mm) across the different sites. Blue colour for wet and orange for dry sites. Site symbols are shown in Table 1.

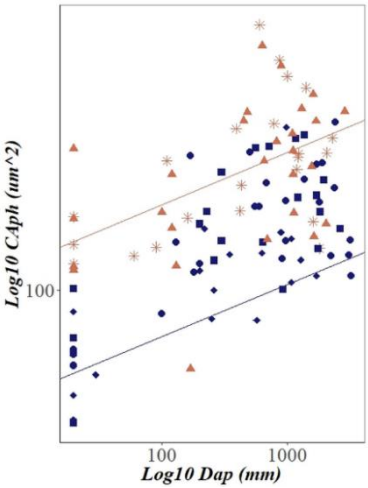

Figure 6. Mean phloem cell area (*CAph*, μm^2) against distance from the stem apex (*Dap*, mm) across the different sites. Blue colour for wet and orange for dry sites. Site symbols are shown in Table 1.

Discussion

Our analyses revealed that *F. ornus* trees growing on sites characterised by lower soil water availability invested relatively more into leaf vs stem+branch biomass. At the anatomy level, trees at drier sites had larger phloem sieve elements likely to increase the phloem conductance to compensate for the potential limitations in the long distance sugar transport due to the higher phloem sap viscosity. On the contrary, we found that the xylem architecture did not significantly vary between dry and wet sites in terms of axial scaling of both xylem area and mean vessel diameter.

We found a relatively higher allocation to leaf vs stem+branch biomass in *F. ornus* trees growing under drier soil conditions (Figure 1d), in agreement with a recent study reporting larger needle vs below+above xylem biomass in *Pinus sylvestris* L. seedlings exposed to prolonged water shortage (Kiorapostolou et al. 2018). A larger leaf biomass could be interpreted as a compensation mechanism for the reduced leaf-based daily/seasonal C assimilation. Indeed, physiological measurements on the same species growing at the same sites revealed lower stomatal (g_S) and leaf conductance (*Kleaf*) under drier soil conditions (Gortan et al. 2009), likely to avoid the unbalance of higher leaf evapotranspiration than xylem water flow rate (Aston and Lawlor 1979; Franks et al. 1998). These likely limited the leaf C assimilation and the seasonal C

budget, supporting our hypothesis. Moreover, the minimum leaf water potential (Ψmin) was lower at the drier sites (Gortan et al. 2009), indicating that water was flowing through the xylem at higher tensions. These results would provide empirical support to the recent hypothesis of Anfodillo et al. (2016), predicting larger photosynthetic biomass to provide the necessary C resources for the maintenance respiration of a given stem+branch biomass by compensating for the negative effects of reduced stomatal conductance or prolonged stomatal closure. Nevertheless, the leaf lamina expansion was lower in the drier sites, resulting in a lower specific leaf area (*SLA*), as commonly reported for several species (e.g. Marron et al. 2003, Wright et al. 2001). Consequently, the total leaf area per individual tree was not significantly different between sites (Figure 1b).

Our analyses on the geometry and anatomy of the long-distance transport systems of xylem and phloem strongly support the hypothesis that the hydraulic functioning of these tissues is tightly coupled (Thompson and Holbrook 2003; Hölttä et al. 2006). In both xylem and phloem, the axial increase in tissue area and conduit lumen area with the increasing distance from the apex (*Dap*) seemed to follow similar axial scaling patterns. Their scaling exponents (*b*) were unaffected by site conditions (Figure 2-5; Table 2), suggesting a stable axial configuration of the long-distance transport systems of both xylem and phloem.

Along the stem's axial path, the xylem and phloem areas were significantly larger at the drier sites (Figure 2; Figure 3; Table 2), and the relationship between the two areas revealed a substantially isometric pattern (Figure 4). Such observed parallel axial geometry of the xylem and phloem architectures would suggest that in our trees the relative variation in xylem and phloem conductivity along the main stem axis (i.e. from apex to base) is of the same magnitude. This coordinated configuration would guarantee an optimal dynamic equilibrium between xylem and phloem flows (Hölttä et al. 2006; Hölttä et al. 2009).

The mean lumen area of xylem vessels (*CAxy*) increased from the stem apex downwards (Figure 5). Such a widened pattern (b=0.42) was higher than the average value of b~0.2 reported for most empirical observations (Anfodillo et al. 2013), but consistent with the axial pattern found for several angiosperm trees within the first meters from the apex (Anfodillo et al. 2006; Petit et al. 2010; Petit and Crivellaro 2014). Such a widening confines the smallest and most embolism

resistant vessels (Cai and Tyree 2010; Nardini et al. 2017) towards the stem apex, where the tensions are the highest because of the proximity to the transpiring leaves. We reported not significant differences in this axial scaling exponent (*b*) between sites, but a marginally significant difference in the *y*-intercept, suggesting that trees under more favourable soil conditions have slightly larger conduits (Figure 5; Table 2). Overall, results would suggest the species convergence towards a rather precise axial geometry of the xylem path (Olson et al. 2014), which represents the best compromise in terms of hydraulic efficiency (i.e. it guarantees a given path length conductance (Petit and Anfodillo 2009)) and safety (i.e. high resistance against tension-induced conduit implosion, especially at the apex where tensions are the highest (Hacke et al. 2001)), and for the carbon economy (i.e. it minimises the C costs associated to the production of the necessary wall material of all the xylem cells (Mencuccini et al. 2007)). In the wetter sites the vessel lumen area was only marginally larger, suggesting that not much carbon resources can be invested for plastic adjustments aimed at increasing the efficiency (in wetter conditions) or safety (in drier conditions) of the xylem transport system (Figure 5; Table 2). Trees growing in moister climates were often reported to be characterised by larger xylem conduits (Pfautsch et al. 2016; Hacke et al. 2017). However, those studies adopting a standardisation procedure to filter out the path effect on xylem anatomy showed either negligible variations in vessel diameter across aridity gradients (Lechthaler et al 2018) or even that trees acclimating to more severe water stress conditions such as big statures (Prendin et al. 2018a) or reductions in water availability (Petit et al. 2016; Kiorapostolou et al. 2018), slightly enlarge their xylem conduits while reducing their number, likely in the attempt of maintaining the xylem conductance at lower C costs. We hypothesise that the discrepancies of these results arise from the fact that trees sampled across environmental gradients simply grew under the stable limitations imposed by the different but stable local conditions, whereas changing climatic conditions during the ontogenetic growth likely impose changing allocation patterns to comply with hydraulic and carbon requirements (Petit et al. 2016; Petit et al. 2018).

We found along the main stem's longitudinal axis both a larger phloem area and larger lumen areas of the sieve elements under drier conditions (Figure 3 and Figure 6). These come in agreement with a recent study also reporting higher phloem conductance under drought (Sevanto et al. 2018).

Phloem conduits progressively increased in lumen area from the stem apex to the base, in agreement with previous studies (Petit and Crivellaro 2014; Jyske and Hölttä 2015). The exponent of the power scaling of phloem conduit area (*CAph*) vs. the distance from the apex (*b*=0.17) was similar to those reported by Petit and Crivellaro (2014) (Figure 6; Table 2). The lumen area of phloem sieve elements (*CAph*) was significantly larger at our drier sites (Figure 6; Table 2). Since the hydraulic resistance of a sieve element scales proportionally to the fluid viscosity and the fourth power of its diameter (Savage et al. 2017), such an increase in phloem conductance in drier conditions would likely compensate for the increase in phloem sap viscosity (Sevanto 2014) due to its likely higher osmolality due to higher sugar concentration or/and tissue dehydration (Lintunen et al. 2016). At the same time, we can also speculate that a higher phloem conductance would maximise the translocation of sugars during the reduced time windows when stomata are open, i.e. when phloem sap can efficiently flow in coordination with water flow along the xylem compartments (Hölttä et al. 2006; Hölttä et al. 2009).

In conclusion, we demonstrated that under reduced soil water availability, *F. ornus* trees allocated relatively more biomass to leaves rather than to the rest of the body biomass and produced larger phloem and larger sieve elements. More leaves are needed to compensate for the negative effects of lower stomatal conductance and/or prolonged stomatal closure on the seasonal carbon balance, while the likely larger phloem conductance guarantees an efficient delivery of sugars for the maintenance of the metabolic activities of the living cells in the different tissue.

Chapter 4. Vulnerability to xylem embolism correlates to wood parenchyma fraction in Angiosperms but not in Gymnosperms

Authors:
Natasa Kiorapostolou*, Luca Da Sois, Francesco Petruzzellis, Tadeja Savi, Patrizia Trifilò, Andrea Nardini, Giai Petit

Published in:
Tree Physiology (2019)

Corresponding author *

Abstract

Understanding which structural and functional traits are linked to species vulnerability to embolism formation (*P50*) may provide fundamental knowledge on plant strategies to maintain an efficient water transport.

We measured *P50*, wood density (*WD*), mean conduit area (*MCA*), conduit density (*CD*), percentage areas occupied by vessels (*VA*), parenchyma cells (PA_{TOT}), and fibres (*FA*) on branches of angiosperm and gymnosperm species. Moreover, we compiled a dataset of published hydraulic and anatomical data to be compared with our results.

Species more vulnerable to embolism had lower *WD*. In angiosperms, the variability in *WD* was better explained by PA_{TOT} and *FA*, which were highly correlated. Angiosperms with a higher *P50* (less negative) had a higher amount of PA_{TOT} and total amount of non-structural carbohydrates (*NSC*). Instead, in gymnosperms, *P50* vs PA_{TOT} was not significant.

The correlation between PA_{TOT} and *P50* might have a biological meaning, and also suggests that the causality of the commonly observed relationship of *WD* vs *P50* is indirect and dependent on the parenchyma fraction. Our study suggests that angiosperms have a potential active embolism reversal capacity in which parenchyma has an important role, while in gymnosperms this might not be the case.

Keywords: embolism, xylem anatomy, parenchyma, wood density, hydraulic failure, refilling

Introduction

In plants, water is transported over long distance through elongated dead xylem conduits while under negative pressure, and is hence maintained in the liquid phase while below its vapour pressure (Tyree 1997). This mechanism exposes plants to the risk of embolism formation at critical xylem tension, when gas bubbles from surrounding compartments are aspirated into the water-filled xylem conduits and expand occupying the whole conduit volume (Nardini et al. 2011, Vilagrosa et al. 2012). Embolism can spread between adjacent conduits, thus decreasing the xylem hydraulic conductance (*K*) (Jacobsen et al. 2005, Domec et al. 2006), with negative effects on sap flow rate and thus plant performance (growth, reproduction, and survival). In fact, carbon assimilation with photosynthesis ultimately depends on the functional balance between

the water absorbed from the soil and transported across the xylem to the leaves (sap flow rate, *F*), and the water lost via leaf transpiration (*T*) (i.e. *F=T*). *F* depends on the difference of water potential between the leaves and the soil and on the xylem hydraulic conductance (i.e. $F=\Delta\Psi*K$). Therefore, any decrease in *K* due to embolism can alter this balance, potentially leading to turgor loss and stomatal closure due to progressive leaf dehydration.

Plants frequently operate at leaf water potentials close to critical thresholds of conductivity loss by embolism formation (Nardini and Salleo 2000, Choat et al. 2012), suggesting that this latter phenomenon is not a rare occurrence in every day plant's life. Hence, plants have evolved strategies to avoid emboli spread, or to tolerate embolism until the production of new xylem conduits (Pratt et al. 2005), or they have developed mechanisms to recover the hydraulic functionality after embolism formation (Salleo et al. 2004). Species vulnerability to xylem embolism can be quantified by means of 'vulnerability curves' and derived values of xylem pressure causing 50% loss of hydraulic conductance of xylem (*P50*). In earlier studies, *P50* was linked to several physiological/anatomical traits in an effort to understand which factors are linked to vulnerability to embolism formation. Among the several structural-functional relationships emerging from these studies focused on different species' assemblages, the one reported most commonly is the negative relationship between wood density (*WD*) and *P50* (Hacke et al. 2001, Lachenbruch and McCulloh 2014, Rosner 2017), with denser wood being more resistant to embolism formation. Nevertheless, the mechanistic basis for this relationship, and the identification of which wood traits are mostly driving it, are still uncertain. Higher resistance to embolism has been also commonly found in species with narrower conduits, often characterised by smaller pit areas (Becker et al. 2003, Lazzarin et al. 2016), which would make conduits safer against air seeding (Hacke et al. 2006, Martínez-Cabrera et al. 2009). In addition, according to the rules of xylem spatial distribution (xylem packing) the conduit area (*CA*) is inversely related to the conduit density (*CD*: number of conduits per unit xylem area) (Martinez-Vilalta et al. 2012), so that narrower and denser conduits are commonly reported to be more resistant to embolism formation (Hacke et al. 2017).

According to Johnson et al. (2012) plants operate at different distances from their hydraulic safety margins, resulting in the formation of different degrees of embolism. Hydraulic safety margin is defined as the

difference between the leaf water potential at stomata closure (i.e. the daily/seasonal minimum xylem pressure, *Pmin*) and *P50*. Gymnosperms were found to have larger safety margins than angiosperms (Choat et al. 2012), suggesting that tight stomatal control in this group of species may help to safeguard the xylem from embolism formation better than angiosperms. The low safety margins of angiosperms would suggest that most of them regularly experience a certain degree of xylem embolism, exposing their hydraulic system to a risk of high loss of hydraulic conductance (Choat et al. 2012), with negative consequences on transpiration and carbon assimilation. While non-lethal loss of xylem hydraulic conductance can be recovered by the production of new xylem potentially characterised by adaptive changes in hydraulic properties (Petit et al. 2016, Secchi et al. 2017), it is conceivable that the ability to repair embolism and recover full gas exchange rates might confer an adaptive advantage to some woody species, especially angiosperms (Klein et al. 2018).

Some species have been reported to refill embolized conduits with water upon drought relief (Nardini et al. 2017). However, the occurrence of this phenomenon has been questioned by some studies due to methodological uncertainties (Cochard and Delzon 2013, Klein et al. 2018), while other studies showed the inability of species to recover embolised conduits (Choat et al. 2018; Johnson et al. 2018; Creek et al. 2018) and, thus, the phenomenon remains at present controversial. Xylem embolism reversal has been reported in both angiosperms and gymnosperms (Brodersen and McElrone 2013, Mayr et al. 2014), although gymnosperms have been found to have a long recovery process (Secchi et al. 2017). Short-term embolism reversal has been hypothesised to depend on active metabolic processes that requires a source of energy and a source of water. According to the current paradigm, soluble carbohydrates released in xylem conduits by surrounding living cells would accumulate and reclaim water from surrounding tissues via an osmotic mechanism (Salleo et al. 2004, Zwieniecki and Holbrook 2009). Therefore, wood parenchyma cells are expected to play a fundamental role in the process of embolism reversal (Brodersen and McElrone 2013, Trifilò et al. 2019), as main sources of non-structural carbohydrates (*NSC*) (Plavcova et al. 2016) and stored water to be diverted inside the refilling conduits (Rosner et al. 2018). In this context, starch degradation is hypothesised to provide sugars (Tomasella et al. 2017). In parallel, parenchyma cells may be necessary to sustain physiological processes while the recovery mechanism is

active (Secchi et al. 2017). In this scheme, it can be expected that the plant's capacity to recover the water transport system from emboli formed in the conduits correlates with the volume of parenchyma cells in the xylem (Secchi et al. 2017). Hence, a higher abundance of parenchyma cells in the xylem (i.e. a higher amount of stored starch and water) is hypothesised to be required in species more vulnerable to embolism formation with low safety margins, in which the refilling mechanism would be of higher importance for their survival, especially under prolonged drought (Ogasa et al. 2013, Trifilò et al. 2015).

In this study, we performed anatomical analyses and measured the *P50* and wood density (*WD*) of branches in different angiosperm and gymnosperm species, examining correlations between key structural and functional traits related to embolism vulnerability. We also gathered available data from previous studies to perform a global analysis and compare our experimental results. We aimed to understand which of the wood characteristics explain better the variability of *P50*. We addressed the following hypotheses: (i) there are differences in the traits related to embolism vulnerability between angiosperms and gymnosperms; (ii) the wood composition (i.e. the percentages of wood tissues) and the xylem anatomical traits correlate to species' embolism vulnerability; (iii) there is a relationship between embolism vulnerability and the fraction of the living tissues, at least in angiosperms.

Material and methods

We performed measurements on branch segments of angiosperm (N=75) and gymnosperm species (N=14) (Table 1) growing at the Botanical garden of the University of Padova (45.3996° N, 11.8805° E), in the Karst region (Trieste) (45.6495° N, 13.7768° E) and in Messina (Sicily) (38.1938° N, 15.5540° E), in Italy. We measured the wood density (*WD*), the percentage areas occupied by: parenchyma cells, fibres, conduits, and measured the conduit anatomical characteristics (see below). For some of the species we measured the *P50* value, while for others the same parameter was derived from previously published studies (see below). We also compiled a global dataset summarizing *P50*, amount of total non-structural carbohydrates (*NSC*, including starch) stored in the wood, *WD*, and xylem parenchyma amount (PA_{TOT}), as reported from previous published studies focused on very diverse species' assemblages.

Parenchyma amount and wood anatomy

One to three branch segments from different individuals were sampled. We used the replicates to ensure that there is a low intraspecific variability between individuals growing under similar environmental conditions. For each segment, we cut transverse and tangential micro-sections at 25 μm with a rotary microtome LEICA RM 2245 (Leica Biosystems, Nussloch, Germany), stained them with a solution of safranin and Astra Blue (1% and 0.5% in distilled water respectively), and permanently fixed on glass slides with Eukitt (BiOptica, Milano, Italy). Images from the transverse micro-sections were acquired at 100x and for the tangential at 40x magnification, using a D-sight slide scanner (Menarini Group, Florence, Italy).

Table 1. The 15 angiosperm species for which we performed hydraulic experiments, their maximum vessel length (VL_{max}) (cm), their water potential of 50% loss of hydraulic conductivity (*P50*) (MPa), and the number of segments used for the estimation of *P50* (n). SE shown in brackets next to the mean values. VL_{max} for *Fraxinus ornus* is non-applicable due to data loss.

Spp	***VL_{max}* (cm) (SE)**	***P50 (MPa)* (SE)**	**n**
Acer monspessulanum L.	13.7 (0.9)	- 4.99 (0.38)	4
Carpinus orientalis Mill.	5 (1.7)	- 3.81 (0.53)	4
Corylus avellana L.	19.6 (3.5)	- 2.86 (0.20)	3
Ficus carica L.	25 (15)	- 1.74 (0.36)	3
Fraxinus ornus L.	na	- 3.48 (0.37)	3
Hedera helix L.	4.8 (0.2)	- 2.84 (0.81)	2
Morus alba L.	77.2 (13.5)	- 0.9 (0.05)	2
Ostrya carpinifolia Scop.	5 (1.7)	- 4.31 (0.27)	5
Pistacia terebinthus L.	63.8 (8.9)	- 2.71 (0.38)	4
Prunus mahaleb L.	25.5 (3.5)	- 5.54 (0.37)	4
Quercus ilex L.	57.0 (7)	- 3.56 (0.85)	4
Quercus pubescens Willd.	67.7 (2.8)	- 2.37 (0.80)	3
Robinia pseudoacacia L.	79.8 (14.3)	- 2.59 (0.24)	3
Tilia cordata Mill.	15.4 (4.4)	- 1.64 (0.10)	3
Whisteria sinensis (Sims) Sweet	84.6 (5.9)	- 1.19 (1.17)	3

The images of transverse and tangential sections were analysed with ImageJ 2.0.0 (Schneider et al. 2012) for the estimation of the percentages of the areas occupied by parenchyma cells. For each image, we selected an area of approximately 1 mm^2 (A_{IMAGE}) with intact tissues (i.e. not affected by artificial cracks caused by cutting), and manually outlined the areas occupied by parenchyma cells. For the transverse sections, we outlined and measured only the total area of axial parenchyma cells (PA_A), including both apotracheal and paratracheal cells, whereas in the tangential sections, the total area of radial parenchyma cells (PA_R) was measured. Both PA_A and PA_R were then converted into percentage amounts (%PA_A and %PA_R respectively) by dividing with A_{IMAGE}.

Since the axial and radial parenchyma cells orientate perpendicularly to our transverse and tangential sections respectively, the percentage area occupied by parenchyma cells was estimated as:

$$PA_{TOT} = (\%PA_A + \%PA_R)*(\%XA/100) + \%Apith \quad \text{eq. 1}$$

where %*Apith* is the percentage of pith area and %*XA* is the percentage of xylem area estimated by ROXAS (see below) on the complete transverse section.

Images from the transverse sections were further used for the automatic anatomical measurements in ROXAS v3.0.139 (von Arx and Dietz 2005, von Arx and Carrer 2014). The analysis was performed on a wedge of known angle (α) centred at the pith for each image. A first manual editing of the images to outline the contour of the pith and of each ring was carried out. For each outlined sector in the wedge (i.e. pith or rings), ROXAS automatically measured the area (*RA*), the conduit number (*CNo*), the mean conduit area (*MCA*), and the conduit hydraulic diameter (*Dh*). Then, traits' data (Y') of pith area (*Apith*), total xylem area (*XA*), and total conduit number (*CNo*) were up-scaled to the whole cross-section as $Y=Y'/\alpha \times 360$. Conduit density (*CD*) was calculated from the up-scaled total conduit number and total xylem area. The percentage of pith area was calculated as $\%Apith = (Apith/(Apith+XA))*100$ and of xylem area as $\%XA = 100-\%Apith$. We, furthermore, estimated the total area occupied by vessels as a percentage over the total xylem area ($VA = CNo$ * MCA*100/*XA*), and the percentage area occupied by fibres as the total area (100 %) minus the percentage area occupied by parenchyma cells, the percentage area occupied by vessels and the pith area ($FA = 100 - PA_{TOT} - VA - \%Apith$).

Wood density

The *WD* of one to three branch segments (~ 2-8 mm in diameter) - the same that were used in the anatomical analysis - of 51 angiosperms and 13 gymnosperms was measured using the water displacement method according to the Archimedes' principle. The branch segments were boiled in a container filled with water until they sank upon rehydration, and then debarked. Another container was filled with water, placed on a digital balance calibrated to the nearest 0.01 g (Acculab ALC-1100.2) and re-zeroed. Each segment was connected from the pith to a needle attached to a thread and carefully immersed in water. The weight of water displaced was equal to the segment wet volume of xylem+pith and 1g of displacement was equivalent to 1 cm^3. After measuring their volume, the segments were put in the oven at 60º C for 72 h. The dry weight was measured with the same digital balance (Acculab ALC-1100.2) immediately when the samples were taken out of the oven and cooled. *WD* was then calculated as *dry weight (g) / volume (cm^3).*

Measurements of *P50*

Hydraulic measurements were performed on 15 species of angiosperms (Table 1) during summer 2018 (June-August). Before the estimation of *P50*, we assessed the maximum vessel length (VL_{max}) for each species (Table 1) to avoid experimental artefacts (Ennajeh et al. 2011). For each species, we cut at least three branches (1 – 2 m long) originating from different individuals. Both the basal and apical parts (about 15cm from the apex) of the branch were then trimmed 3 times underwater with a razor blade, and connected from the apical part to a tubing system. Air was perfused from the apical end of the branch at a pressure of 10 kPa while the basal end was immersed in a water tank and observed with a magnifying lens for the presence of air bubbles. The basal end of the branch was cut progressively by 1 cm until air bubbles were observed. VL_{max} for each branch was equal to the length of the branch when at least two evident streams of air bubbles were observed indicating that at least two vessels were open at both ends. The species VL_{max} was estimated as the average value of VL_{max} of the three replicates.

For the estimation of *P50*, vulnerability curves were determined with the air-injection method (Ennajeh et al. 2011). At least three branches 1 to 2 m long depending on the species VL_{max}, were collected early in the morning from at least three individuals per species. Three branches per species were used when the variability in *P50* was low (except from *Hedera helix* and *Morus alba* for which only two branches were used),

while for higher variability the number of replicates was increased (same as in Savi et al. 2018). The branches were immediately placed with the distal end in a bucket filled with water, and covered with a plastic bag for at least 2h before the measurements to relax the tension and avoid the artefact of inducing embolism (Wheeler et al. 2013). Before the measurement, each branch was recut underwater (final length > VL_{max}), debarked at both ends for 2 cm and connected to a hydraulic apparatus (Xyl'EM xylem embolism meter, Bronkhorst, Montigny-Les-Cormeilles, France). All the leaves were removed cutting the stalk underwater. Branches were flushed with a filtered poly-ionic solution enriched with a 10-mmolL^{-1} KCl solution at a pressure of 0.18 MPa for 30 minutes. Then the branch was submerged in water, and the bark was removed from a central portion that was later connected to a double-ended pressure chamber (Ennajeh et al. 2011). The cut ends were slightly trimmed again, and the basal area of the segment was connected to a 1 m long tube, which was wide enough to allow the escape of air bubbles. Maximum conductance (K_{max}) was then measured at low pressure (4.8 kPa). After measuring the K_{max}, increasing pressures at steps of 0.2-1 MPa were applied to the branches and the branch conductance at each step (Kp) was measured. The percentage loss of conductance at each pressure was calculated as:

$$PLC = 100*(K_{max}-K_p)/K_{max} \quad \text{eq. 2}$$

The measurements were repeated for each branch until reaching a PLC of at least 70-80%. Vulnerability curves, consisting of 7-12 points each, were assessed using the packages Rcmdr version 2.4-4 (Fox 2005, Fox 2017, Fox and Bouchet-Valat 2018) and fitplc version 1.1-7 (Duursma and Choat 2017) in R Studio version 1.1.423 (RStudio team 2015) and the water potential at which the PLC equals 50% (*P50*) was estimated accordingly. Only sigmoidal shaped curves were taken into consideration (example shown in Supplementary Figure 1). For few branches the curves resulted to be non-sigmoidal (r-shaped), then these curves were discarded and another replicate was repeated for the species. This was done not only to have a uniform analysis as most curves were sigmoidal, but also and most importantly because non-sigmoidal (r-shaped) curves are possibly the result from open vessels' artefact and lead to an overestimation of *P50* (Cochard et al. 2013; Wang et al. 2014; Savi et al. 2018). Some studies suggested that non-sigmoidal curves may accurately describe species vulnerability to embolism formation (Jacobsen and Pratt 2012, Sperry et al. 2012, Hacke et al. 2015), but methods different from the air-injection were

used by them to evaluate the *P50*. Sigmoidal and non-sigmoidal curves were recognised by eye based on Figure 1 of Cochard et al. (2013). Values of *P50* for all the other species were obtained from Choat et al. (2012).

Global dataset

We compiled a global dataset (Supplementary Table 1) including species-specific data of branches (and when not available we used stem data) for 107 species (68 angiosperms and 39 gymnosperms). In this dataset, we included PA_{TOT} data collected from Morris et al. (2016), *P50* collected from Choat et al. (2012), *WD* data that were taken from the Global Wood Density Database (Chave et al. 2009, Zanne et al. 2009), and the total *NSC* content (sugars and starch) that were obtained from several published studies (listed in Supplementary Table 1).

Statistical analysis

We assessed the relationship between *P50* and *WD* in angiosperms and gymnosperms. We then tested the relationships *P50* vs *MCA* and *P50* vs *CD*. Moreover, we tried to understand if *FA*, *VA*, and PA_{TOT} explain the variation in the distribution of *WD* and of *P50* in angiosperms. We assessed these relationships with linear regressions and tested the normality and homoscedasticity of the residuals. In case of non-parametric data, we applied a log10 transformation. We used the absolute values of *P50* for its log10 transformation. For angiosperms, we tested for differences in the slopes (*b*) and the y-intercepts between our measurements and the compiled global dataset in the relationships *P50* vs PA_{TOT} and *P50* vs *WD*, and we assessed the relationship of *P50* vs *NSC* in the compiled dataset. We applied the Bonferroni adjustment in these models, and quantile plots to test for statistically significant outliers (i.e. outside the 95% confidence envelope) (Supplementary Figures 2, 3, and 4). In gymnosperms the total sample number was too low to allow for valid results. All the statistical analyses were performed in R version 3.4.2 (R Core Team 2017).

Results

***P50* and wood density**

We found a significant negative relationship between *P50* and *WD*, with species being less vulnerable to embolism formation (i.e. lower *P50*) producing denser wood (Figure 1a). The relationship was significant for both angiosperm ($R^2 = 0.17$, $P < 0.001$) and gymnosperm species ($R^2 =$

0.18, $P < 0.01$). The comparison between the different sources of data (global dataset vs. our own measurements) revealed that the relationship is significant in angiosperms in both datasets, although we observed a marginally significant offset in the *y*-intercept (Supplementary Figure 5a; Supplementary Table 2). In gymnosperms, the relationship was not significant when testing the two datasets separately (Supplementary Table 2).

P50 and xylem anatomy

We assessed the effects of mean conduit area (*MCA*) and conduit density (*CD*) on the vulnerability to embolism formation (*P50*). In angiosperms, we found a significant positive relationship between *P50* and *MCA* (Figure 1b, $R^2 = 0.27$, $P < 0.001$), suggesting that angiosperms with wider vessels are more vulnerable to embolism formation. In addition, we also found a negative relationship between *P50* and *CD* (Figure 1c; $R^2 = 0.19$, $P < 0.001$), indicating that species with denser vessels are less vulnerable to embolism formation. However, *MCA* was negatively related to *CD* according to a highly significant power scaling with $b \sim -1$ (Supplementary Figure 6c; $R^2 = 0.72$, $P < 0.001$). In contrast, in gymnosperms, we did not find any significant relationship. However, the sample size was likely low to obtain robust results (N=14).

We furthermore explored correlations between other wood structural properties (i.e. percentage areas occupied by: vessels, *VA*; parenchyma cells, PA_{TOT}; fibres, *FA*) and *P50*.

We found that PA_{TOT} was significantly related with *P50* in angiosperms (Figure 2a; $R^2 = 0.16$, $P < 0.001$), with more vulnerable species having larger amounts of parenchyma. The assessed relationship comprised data from literature and our own measurements, as we found no significant difference in the parameters of the fitting equation between the different groups of source data (Supplementary Figure 5b; Supplementary Table 2). However, this relationship was not significant in gymnosperms ($P > 0.05$) (Fig. 2a; Supplementary Table 2).

For the angiosperms only, the percentage area occupied by vessels (*VA*) did not vary much across species (13.27 ± 5.85, N = 74) (mean, ± SD) (Figure 3a triangles) whereas PA_{TOT} and *FA* showed a highly significant negative relationship ($R^2 = 0.80$, $P < 0.001$; Figure 3a circles). Accordingly, we also found a highly significant negative relationship between *P50* and *FA* (Figure 3b; $R^2 = 0.22$, $P < 0.001$), whereas *VA* was not related to *P50* ($P > 0.05$).

WD and % of wood tissues

We analysed the variation in wood structure as a function of *WD* for the different angiosperm species. We found that *FA* significantly increased (Figure 4 triangles; $R^2 = 0.33$, $P < 0.001$) and PA_{TOT} significantly decreased with increasing *WD* (Figure 4 circles; $R^2 = 0.25$, $P < 0.001$). However, *VA* was not significantly related to *WD* ($P > 0.05$).

P50 and non-structural carbohydrates

We assessed the relationship between *P50* and total amount of non-structural carbohydrates (*NSC*) in the stem using data available from literature, and found a significant positive relationship (Figure 2b; $R^2 = 0.09$, $P < 0.05$) that suggests that species more vulnerable to embolism formation have on average a higher amount of *NSC* stored in wood compartments.

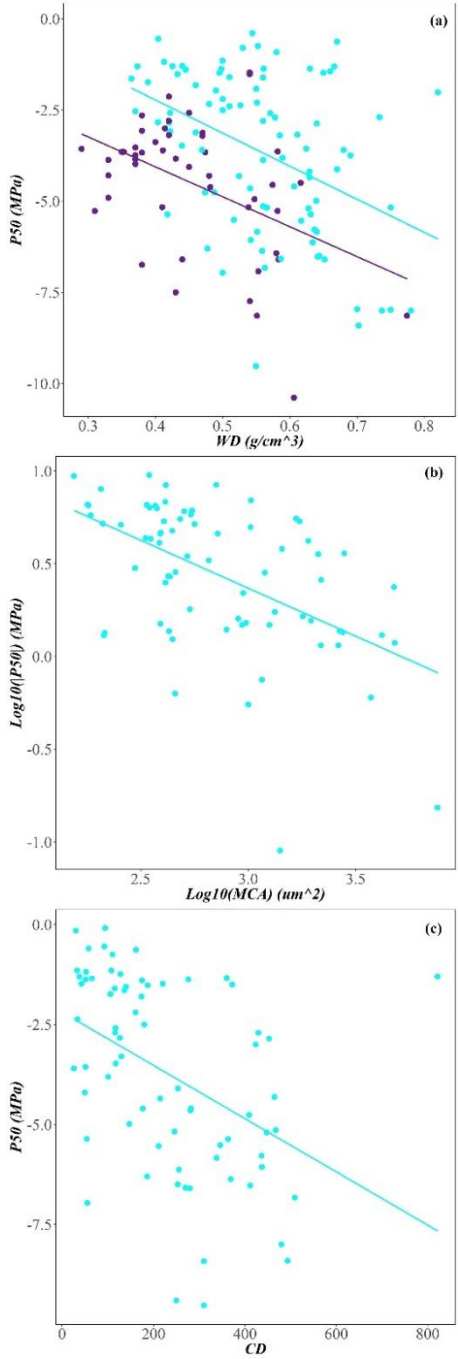

Figure 1. (a) Vulnerability to embolism (*P50*) against the Wood Density (*WD*) for angiosperms in light cyan and gymnosperms in dark purple color. The data are from our own measurements and from literature. **(b)** *P50* against the Mean Conduit Area (*MCA*) for angiosperm species. **(c)** *P50* against the Conduit Density (*CD*) for angiosperm species.

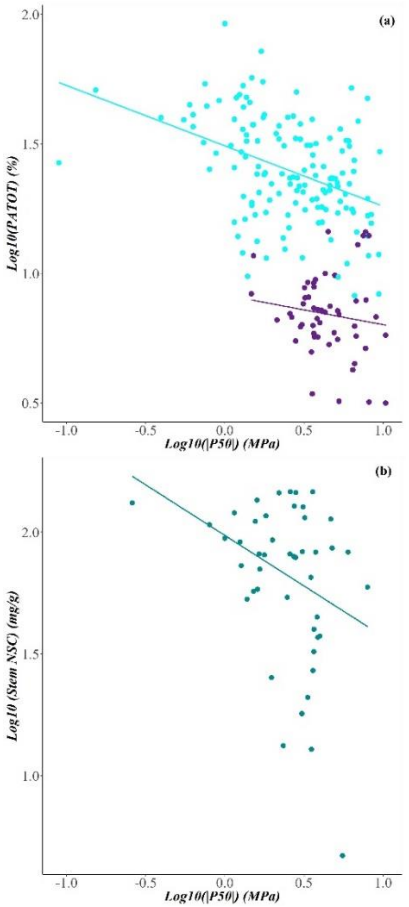

Figure 2. (a) Percentage area occupied by parenchyma cells (PA_{TOT}) against the vulnerability to embolism (*P50*) for angiosperms in light cyan and gymnosperms in dark purple color. The data are from our measurements and from literature. **(b)** Total amount of structural carbohydrates in the stem (*Stem NSC*) against the vulnerability to embolism (*P50*) for angiosperm species. The data are collected from literature.

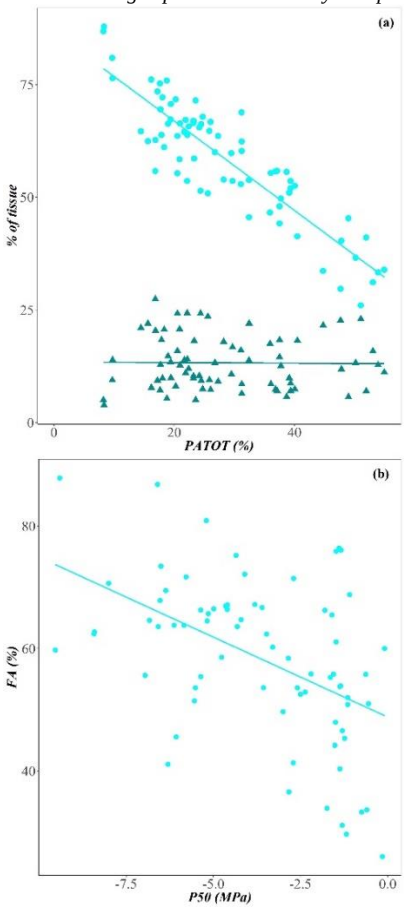

Figure 3. (a) Percentage area occupied by fibers (*FA*) (light cyan solid circles) and Percentage area occupied by vessels (*VA*) (dark cyan triangles) against the percentage area occupied by parenchyma cells (PA_{TOT}). **(b)** Percentage area occupied by fibers (*FA*) against the vulnerability to embolism (*P50*).

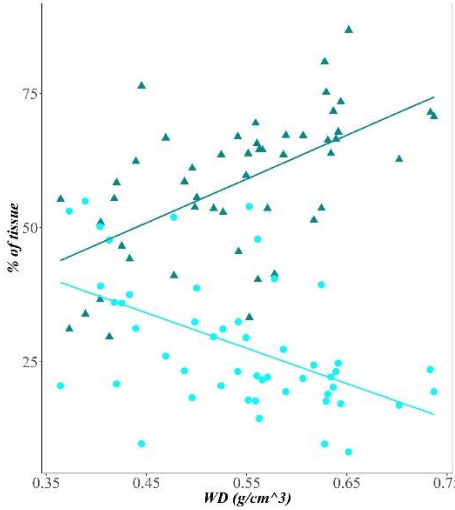

Figure 4. Percentage area occupied by fibres (*FA*) (dark cyan triangles) and percentage area occupied by parenchyma cells (PA_{TOT}) (light cyan solid circles) against the wood density (*WD*).

Discussion

Our results show that xylem vulnerability to embolism formation is significantly related to different wood structural traits, although they singularly explain a minor proportion of the total *P50* variability, and often are mutually correlated.

We found clear differences between the wood composition in angiosperm vs. gymnosperm species. Species in the first functional group present a xylem composed of a rather constant amount of conductive vascular elements, i.e. 10-20% of the total volume. The remaining 80% of xylem volume can largely vary in the relative amount of parenchyma cells and fibre elements, according to a tight negative relationship (Figure 3a), which was found to be the main driver for the variation in wood density (*WD*) (Figure 4). Instead, gymnosperms had a relatively fixed and low amount of parenchyma cells (PA_{TOT} ~ 5-10 % of the total volume). This would suggest that the variation in *WD* in conifer wood substantially depends on the frequency distribution of tracheid diameters and their cell wall thickness (*CWT*). Although the number of gymnosperm species was low to support any significant relationship between *WD* and conduit density (*CD*) or *CWT*, other more

detailed analyses are clearly in agreement with this hypothesis (Rosner 2017).

In general, species with higher wood density (*WD*) were less vulnerable to embolism (more negative *P50*) (Figure 1a), consistent with earlier studies (e.g. Hacke and Sperry 2001, Jacobsen et al. 2005, Lens et al. 2013, Rosner 2017). However, our anatomical analyses would suggest that the relationship between *P50* and *WD* is functionally different between angiosperms and gymnosperms, where in the former it was driven by the variation in the amount of parenchyma vs. fibres, whereas in the latter *P50* would seem to be more likely related to the scaling of tracheid number vs. diameter. Tracheid diameter was found to scale isometrically with pit aperture (Becker et al. 2003, Lazzarin et al. 2016), an ultrastructural feature of the cell wall supposedly proportional to the susceptibility of torus displacement under tension, and thus to the vulnerability to air seeding (Martínez-Cabrera et al. 2009). Moreover, larger conduits with thinner cell walls are less resistant against tension-induced implosion (Hacke et al. 2001). Therefore, conifer species with lower wood density usually have larger tracheids and are more vulnerable to embolism formation (less negative *P50*) (Hacke and Sperry 2001, Larter et al. 2017). Also for angiosperm vessels a relationship between diameter and *P50* has been often found at both interspecific (Hacke et al. 2006) and intraspecific level (Nardini et al. 2017), but also among different sized vessels within the xylem (Jacobsen et al. 2019), consistent with our results and potentially underlining a relationship between pit traits and vessel size, as for gymnosperms. Indeed, previous studies reported that narrower vessels with smaller pit areas are less vulnerable to air seeding (Sperry and Tyree 1988, Tyree and Sperry 1989, Cochard and Tyree 1990, Hacke et al. 2006, Martínez-Cabrera et al. 2009, Christman et al. 2012). In addition, denser (and therefore smaller) cells (Sperry et al. 2008) (cf. Supplementary Figure 6c) are thought to be hydraulically safer against losses of xylem conductance, because water can more easily bypass embolized conduits (Venturas et al. 2017). Accordingly, angiosperm species with narrower and denser vessels were also those with a lower (i.e. more negative) *P50* (Figures 1b and 1c).

We found that gymnosperm species were not varying much in their amount of parenchyma tissue (i.e. PA_{TOT} ~ 5-10 % of a given volume of wood). On the contrary, a significant proportion of the higher $\%PA_{TOT}$ variability in stem and branches of angiosperms was explained by the species' vulnerability to embolism formation (*P50*) (Figure 2a),

meaning that more vulnerable angiosperms have a higher amount of parenchyma in the wood. This tissue not only provides a storage compartment for sugars and water to be used upon requirements (Spicer 2014, Scholz et al. 2011, Jupa et al. 2016), but also represents a cost for the plant carbon balance due to its metabolic activity as it is a living tissue. Hence, since vulnerable angiosperm species would frequently operate at conditions favouring embolism formation (Choat et al. 2012), it is intriguing that these species, potentially limited in gas exchange due to periodical reductions in xylem conductance, have developed a large and carbon expensive wood parenchyma.

It is worth mentioning here that in the study of Pratt et al. (2007), roots of angiosperms had more parenchyma and fewer fibres than stems, but even with a higher amount of parenchyma they were more vulnerable to embolism formation. This fact might be explained by the axial increase of vessels' size and connectivity (Lechthaler et al. 2018), with wider vessels in the roots being more vulnerable to embolism, since embolism vulnerability is related to conduit size (e.g. Brodersen and McElrone 2013). At the same instant, roots are in less need of mechanical stability (i.e. fewer fibres) and this might be the reason that plants invested in the production of more parenchyma cells, and thus a higher storage of sugars, in roots.

A first possible explanation for our result is that large Non-Structural Carbohydrate (*NSC*) reserves stored in the abundant parenchyma during favourable periods help these species to avoid carbon starvation due to stomatal closure during periods of prolonged water shortage. Also, the relationship between PA_{TOT} and *P50* would be consistent with the hypothesis that parenchyma has a fundamental role in xylem embolism reversal by actively translocating into the embolized conduits the necessary amount of sugars needed to osmotically attract water molecules from the surrounding compartments (Zwieniecki and Holbrook 2009). In this view, abundant parenchyma cells would provide the necessary sugars and energy to trigger the whole refilling process (Secchi and Zwieniecki 2011, Trifilò et al. 2019) in species frequently exposed to conditions favouring embolism formation.

Since PA_{TOT} was tightly related to the amount of fibres in the wood (Figure 3a), *FA* and wood density (*WD*) were also related to *P50*. While *FA* and *WD* do not really provide a functional explanation for the variation in *P50* (Lachenbruch and McCulloh 2014), these results would strongly suggest that these parameters are indirectly related to *P50*, as more vulnerable species would require a higher amount of parenchyma

for carbon storage and/or for efficient embolism reversal. Consistent with this hypothesis, we found that angiosperms more vulnerable to embolism not only had a higher percentage of parenchyma cells in the wood, but also a higher storage of *NSC* (Figure 2b). These results agree with a recent study of Plavcova et al. (2016), who found that the amount of parenchyma tissues is a strong determinant of the amount of stored *NSC*.

In conclusion, we found global-wide patterns in differences of wood structure between angiosperm and gymnosperm species that correlate with their vulnerability to embolism formation (*P50*). In particular, in gymnosperms the relationship between *P50* and *WD* is likely driven by the scaling between conduit number and diameter, and thus cell wall thickness. In contrast, in angiosperms, the relative amounts of parenchyma cells and fibres were significantly related to embolism formation. The amount of parenchyma volume in the xylem, which may be involved in the maintenance/repair of plant hydraulic systems, was significantly related to *P50*. Angiosperm species more vulnerable to embolism formation had wider and less dense vessels, but also had a higher amount of parenchyma, consistent with hypothesis around embolism reversal mechanisms, where parenchyma and the amount of *NSC* would play a central role.

Chapter 5. The total path length's hydraulic resistance according to known anatomical patterns: what is the shape of the root-to-leaf tension gradient along the plant's longitudinal axis?

Authors:
Silvia Lechthaler, Natasa Kiorapostolou*, Andrea Pitacco, Tommaso Anfodillo, Giai Petit

To be submitted

Corresponding author *

Abstract

Xylem conduit diameter widens from leaf tip to stem base and how this widening affects the total hydraulic resistance (R_{CUM}) and the gradient of water potential (Ψxyl) has never been thoroughly investigated.

Data of conduit diameter of *Acer pseudoplatanus*, *Fagus sylvatica* and *Picea abies* were used to model the axial variation of R_{CUM} and Ψxyl.

The majority of R_{CUM} (from 79 to 98%) was predicted to be confined within the leaf/needle. Consequently, a steep gradient of water potentials was predicted to develop within the leaf/needle base, whereas lower in the stem water potentials approximate those of rootlets.

Our analyses suggest that the xylem conduits of stem and roots, accounting for nearly the total length of the hydraulic path, provide a nearly negligible contribution to plant's water relations, which in turn are controlled by living cells at the hydraulic path's extremities (rootlets and leaves).

Keywords: hydraulic resistance, leaf, xylem, stem, water potential, tension gradient, conduit widening.

Introduction

According to the cohesion-tension theory, water within the xylem flows against gravity from the soil to the canopy due to the lower water potential developed in the transpiring leaves (Dixon & Joly 1895; Angeles et al. 2004). The evaporation of water in the mesophyll and the consequent vapor diffusion into the atmosphere (i.e. leaf transpiration) is the main mechanism driving the water uplift. The surface tension at the liquid/vapor interface does not overcome the adhesion forces in the nanopores of the mesophyll cell walls inside the substomatal cavities (estimated in the range of 5-10 nm, Tyree & Zimmermann, 2002), determining the formation of water menisci inside these cavities and the transmission of subatmospheric pressures along the whole hydraulic path until the rootlets. The water lost with transpiration is replenished by the bulk water flowing from roots to leaves in a metastable state, through a network of dead and hollow conduits (i.e. the xylem) (Nobel 2012; Brown 2013).

Plant's water relations are widely studied based on the analogy to electric circuits, where water flow (F) is analogous to the electric current generated by a difference in potential energy of water (water potential, Ψ, MPa) between the two extremities of the circuit (soil-to-

root and leaf-to-atmosphere interfaces), the media through which water flows are resistances connected in series (e.g., xylem conduits), and other plant structures may serve as capacitors (e.g., parenchyma cells) (Tyree & Zimmermann 2002). According to the Darcy's law, the water flow is determined by the ratio between the difference in water potential between two points along the hydraulic path ($\Delta\Psi$) and the total hydraulic resistance (R) of the medium passed through (Reid et al. 2005):

$F = \Delta\Psi / R$ Eq. 1

The $\Delta\Psi$ between leaves and soil (Ψ_{leaf} - Ψ_{soil}) is strongly influenced by the surrounding environmental conditions. When the atmosphere is dry and hot, the transpiring leaves loose more water from the mesophyll cell walls, with even lower water potential (i.e. higher tension) being propagated down along the xylem path. Instead, when soil gets drier, the xylem water potential decreases accordingly, determining a reduction in $\Delta\Psi$ between leaves and soil.

The total hydraulic resistance of the plant's hydraulic architecture can be simplified as the sum of resistances connected in series along the hydraulic path (Fig. 1). For the nearly entire path length, water flows through a complex network of conductive elements, similar to capillary tubes (i.e., the dead, hollow and thick-walled xylem conduits). Instead, at the extremities of the hydraulic path, water moves for very short distances along different structures. In both the leaf mesophyll and rootlets, water does not flow through "tubes", but must cross cell membranes and walls of a series of living cells (Tyree & Zimmermann 2002).

Between the two extremities where water must flow through the living cells of rootlets and leaves, the total hydraulic resistance of the whole xylem architecture connecting roots to leaves is essentially determined by conduit number and conduits' anatomical traits, such as their size (lumen diameter and length) and their pits' properties (density and pore size) (Hacke & Sperry 2001; Choat et al. 2008). According to the Hagen-Poiseuille's law, the hydraulic resistance (r) of a single xylem conduit's lumen can be assimilated to that of a capillary tube (Tyree & Ewers 1991):

$r = \frac{128 \cdot \eta \cdot l}{\pi \cdot d^4}$ Eq. 2

where η is the dynamic viscosity of water (10^{-9} MPa·s at 20°C), l is the length and d the diameter of the conduit. It follows that changes in

conduit size, especially *d*, along the hydraulic path can have a great effect on its total hydraulic resistance.

At the stem level, it has been widely demonstrated that the diameter of xylem conduits continuously varies along the stem, being rather narrow at the tree top and becoming progressively wider towards the stem base (see Anfodillo et al. 2013 for a review). The scaling of conduit diameter with the distance from the stem apex commonly follows a trend well approximated to a power function ($Y=a \cdot X^b$), with the rate of conduit enlargement per unit of path distance being steeper close to the tree apex and gradually approaching a plateau towards the stem base. The scaling exponent (*b*) of the basipetal widening of stem's xylem conduits has been commonly reported to converge to the value of 0.2 irrespective of species, tree size or environmental conditions (Anfodillo et al. 2006; Anfodillo et al. 2013; Olson et al. 2014). Belowground, the axial variation in conduit diameter had been scarcely investigated. While the continuous increase in conduit diameter from the root collar towards the rootlets had been found in a few conifer trees (Petit et al. 2009; Lintunen & Kalliokoski 2010), other researchers observed more complex axial patterns in conduit diameter in both conifer (Lintunen & Kalliokoski 2010; Prendin et al. 2018) and angiosperm roots (Jacobsen et al. 2018). In any case, xylem conduits of roots were always wider than those of stem in both broadleaved (McElrone et al. 2004; Petit et al. 2010; Jacobsen et al. 2018) and conifers (Petit et al. 2009; Lintunen & Kalliokoski 2010; Prendin et al. 2018). The hydraulic consequence of such an axial configuration is that the overall increase in conduit diameter basally would theoretically strongly compensate for the path length effect to the total hydraulic resistance. As a consequence, the increase in the hydraulic resistance cumulated from the distal unit of the hydraulic path downwards (R_{CUM}) would be much less than linear, so that most of R_{CUM} remains confined within a very short distance from the stem apex (West et al. 1999; Petit & Anfodillo 2009; Petit et al. 2010). A few studies provided empirical hydraulic measurements supporting that the axial distribution of resistances along the longitudinal stem/branch axis were very consistent with modeled distribution of resistances due to the axial widening of xylem conduit diameters (Yang & Tyree 1993; Petit et al. 2008). Although other ultrastructures of xylem conduits (e.g., type of wall thickening, end-wall anatomy, pit structures, pit size and number) effectively contribute to the total xylem resistance, yet they were often reported to contribute

to the total conduit resistance in proportion to the lumen resistance (Martre et al. 2000; Sperry et al. 2005; Pittermann et al. 2006; Christman & Sperry 2010). Consistently, pit number and size have been reported to be strongly correlated to conduit diameter (Becker et al. 2003; Sperry et al. 2006; Lazzarin et al. 2016; Losso et al. 2018; Jacobsen et al. 2018).

The elements of the stem xylem are directly connected to the elements composing the leaf xylem network, where conduits are on average narrower than those in the stem (Lintunen & Kalliokoski 2010; Petit & Anfodillo 2013), and decrease in diameter from the petiole to the narrow minor veins (Coomes et al. 2008; Sack et al. 2012; Petit & Anfodillo 2013).

Nonetheless, the contribution of leaves to the total plant resistance remains still controversial. Recent studies have highlighted that the total leaf's hydraulic resistance is substantially determined in equal proportion by the resistances in series of the leaf xylem and of the outside-xylem paths in the mesophyll (Cochard et al. 2004; Trifiló et al. 2016; Scoffoni et al. 2017). Moreover, it has been argued that the dissipation of very low water potential within the short distances inside the leaf would require very high hydraulic resistances (Buckley & Sack 2019). On the contrary, other studies based on empirical hydraulic measurements reported instead a lower contribution of leaves to the total hydraulic resistance compared to stem and branches (e.g., Tsuda & Tyree, 1997; Sobrado, 2007).

Despite the existence of the abovementioned axial variations in xylem anatomy, yet their effects on the axial gradient of xylem water potential (Ψxyl) along the soil-plant-atmosphere continuum (SPAC) have never been deeply investigated. Most commonly, the total xylem resistance has been considered as a sort of "unit resistance", intrinsically assuming no axial variations in resistivity (i.e., resistance per unit length), thus implicitly assuming Ψxyl to vary linearly between the two extremities of the hydraulic path (e.g., Venturas *et al.*, 2017).

This work aims to evaluate the effect of the axial variation in conduit diameter along the whole leaf-to-stem hydraulic path in shaping the stem-to-leaf gradient of water potential (Ψx). We combined our own measurements on axial variation in conduit diameter along the main leaf/needle axial vein with published and unpublished data on the axial variation from the stem apex to base for two angiosperms (*Acer pseudoplatanus* L., Petit et al., 2008, and *Fagus sylvatica* L., Petit et al.

unpublished data) and one gymnosperm species (*Picea abies* (L.) Karst., Petit et al. unpublished data). The published data include anatomical information on the conduit diameter variation with tree height, obtained from several anatomical sections performed at different heights along the stem. We implemented these data into a simple hydraulic model to assess the effect of the distribution of resistances along a single root-to-leaf chain of conduits in shaping the gradient of water potential along the entire vascular path from the ultimate (i.e., distal) element of the leaf/needle venation network to the rootlets (Fig. 1).

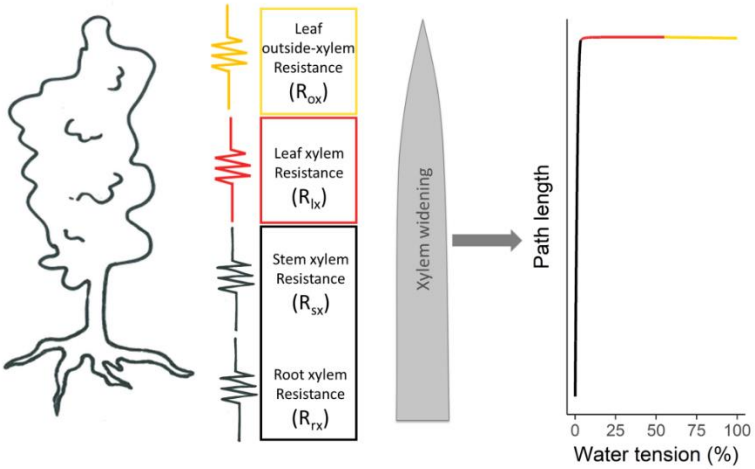

Figure 1. Graphic representation of the distribution of the different hydraulic resistances connected in series along the aboveground hydraulic path from the rootlets to the leaf mesophyll. Due to the axial variation of conduit diameter along the axes of leaves (yellow) and stems (black) and to the magnitude of the outside-xylem resistance in the leaves (red), almost the total water tension gradient is confined within the leaf (red, yellow lines) whereas the variation in the stem is almost negligible (black line).

Material and methods

Anatomical analyses

We focused our analyses on two angiosperms (*Acer pseudoplatanus* L. and *Fagus sylvatica* L.) and one gymnosperm (*Picea abies* (L.) Karst). At the end of the growing season 2017 (to ensure that the leaves were fully developed), we collected three to seven leaves/needles per species from trees growing at the botanical garden of the University of Padova

(http://www.ortobotanicopd.it/en). For each leaf/needle, we cut 3-10 segments at different distances from the leaf/needle tip, and embedded them in paraffin (Anderson & Bancroft 2002). Stem cross-sections for *F. sylvatica* and *P. abies* individuals were cut at different distances from the tree apex (Petit *et al.* unpublished). Micro-sections of both stem and leaves were then cut with a rotary microtome Leica RM 2245 (Leica Biosystems, Nussloch, Germany) at 14-15 μm. For the leaves, we performed sections every 2 cm along the midrib and petiole whereas the needles of *P. abies* were cut along the longitudinal axis at every ~1mm (for more information on cut frequencies for the stem sections see Table S1 not available in this thesis). All sections were stained with a solution of safranin and Astra blue (1% and 0.5% in distilled water, respectively) and permanently fixed on glass slides with Eukitt (BiOptica, Milan, Italy). Slides of leaf sections were scanned with a D-Sight 2.0 scanner (A. Menarini diagnostic, Firenze, Italy) at 100x magnification. Images of stem cross-sections were captured at 100× magnification using a light microscope connected to a digital camera (Nikon Eclipse 80i, Nikon, Tokyo, Japan) and considering the outermost ring. Relative images of leaf and stem sections were analyzed with ROXAS v. 3.0.139 (von Arx & Dietz 2005; von Arx & Carrer 2014) for the automated measurement of the xylem vessel diameters. Slides of the needle sections were observed under a light microscope (Nikon Eclipse80i; Nikon, Tokyo, Japan) connected to a digital camera at 400x magnification, and the diameter of the six biggest tracheids was manually measured using a linear measurement tool. For each leaf/needle section, the hydraulic diamter (*Dh*) was calculated as:

$$Dh = \Sigma d^5 / \Sigma d^4 \qquad \text{q. 3}$$

where *d* is the diameter of a given vessel.

For *A. pseudoplatanus*, we obtained from published data the estimated *Dh* at different distances from the stem apex (Table S1 not available in this thesis).

Statistical analyses

Data of *Dh* and distance from the leaf/needle tip (*L*) were Log10-transformed in order to meet the normality and homoscedasticity assumptions, and fitted with a linear regression to estimate the *y*-intercept and the widening coefficient (i.e., the slope *b*) for each species and organ (leaf/needle or stem) (Table 1).

Hydraulic model

For each species, the estimated basal widening pattern of conduit diameter along the leaf midrib/needle axis and further below along the stem were implemented into a hydraulic model for the assessment of the axial variation in the cumulative path resistance and in the xylem water potential along the longitudinal hydraulic path of a theoretical tree, simplified as a single pipe of chained conduits of 30 m of total length.

We calculated the theoretical hydraulic resistance (r) of each conductive element at each 1 mm of the hydraulic path according to Hagen-Poiseuille (Eq. 2). The cumulative path resistance (R_{CUM}) was calculated as the sum of all conduits starting from the apical (i.e., distal) element and moving down until the stem base.

R_{CUM} was calculated according to three different patterns of axial variation in conduit diameter: (i) according to our empirical observations of axial conduit widening along the stem (R_{sx}); (ii) according to our empirical observations of axial conduit widening along the stem and leaf midrib/needle (R_{sx} + R_{lx}); (iii) according to our empirical observations of axial conduit widening along the stem and leaf midrib/needle, plus the resistance of the outside-xylem path (R_{ox}) added as the most distal element of the hydraulic path (R_{sx} + R_{lx} + R_{ox}), with a value of 50% of the total leaf/needle resistance (i.e., R_{ox}=R_{sx} + R_{lx}) (Cochard et al. 2004; Trifiló et al. 2016; Scoffoni et al. 2017).

At each mm along the hydraulic path, the water potential was estimated according to Eq. 1, and the estimation of water flow (F) under the assumption of the conservation of mass. The total path resistance was calculated as the sum of each single element resistance and an arbitrary $\Delta\Psi$ was applied between the most distal and the proximal element of the hydraulic path. The water potential at the base of a given xylem element (Ψ_{X1}, considered cylindrical) was calculated as:

$$\Psi_{X1} = F * r + \Psi_{X0} \qquad \text{Eq. 4}$$

where r is the conduit resistance and Ψ_{X0} is the water potential at the base of the next xylem element.

We then expressed Ψ_X as relative variation in tension between the most apical (distal) element of the hydraulic path (i.e., 100% of tension) and the stem base (0% of tension).

The model also simulated the theoretical effects of different soil ($\Psi soil$ from 0 to -2 MPa) and air dryness (Ψair from -40 to -80 MPa) (Brown & van Haveren 1972) on the variation in the water potential (Ψ_X) along

the whole hydraulic path from the substomatal cavities until the soil/root interface, assuming full functionality of all xylem conduits (i.e., no losses of conductance due to embolism formation). The water potential calculated for the apical element of the hydraulic path, (i.e., at the outside xylem level) accounted also for the leaf osmotic adjustment to compensate for the gravitational pressure drop of 0.01 MPa/m.

Results

The hydraulic diameter of xylem conduits (*Dh*) in the angiosperm leaves increased along the midrib from the leaf tip to the petiole (Fig. 2, 3) following a power trajectory characterized by a scaling exponent of *b*=0.41 (CI 95%: 0.37; 0.44, Table 1) in *A. pseudoplatanus* and *b*=0.33 in *F. sylvatica* (CI 95%: 0.18; 0.47, Table 1). On the contrary, the tracheid *Dh* of the analyzed *P. abies*' needles remained around 3.5 µm without showing significant axial trends (Fig. 2, 3, Table 1).

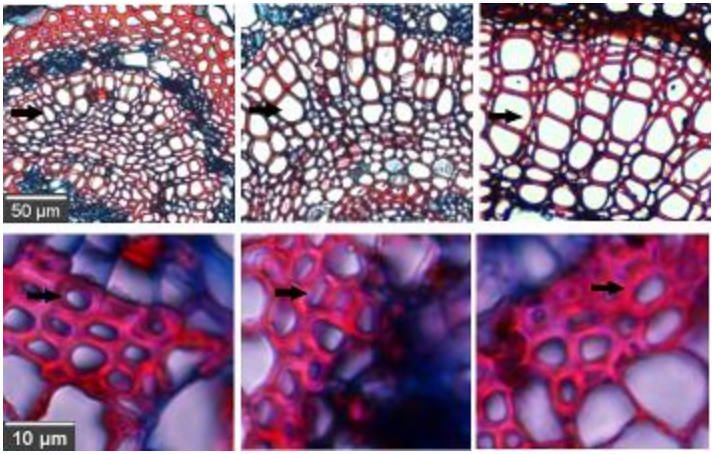

Figure 2. Anatomical sections taken at 20, 60, 180 mm from the leaf tip for Acer pseudoplatanus (upper images) and at the tip, middle and base of a Picea abies needle of 15 mm in length. The black arrows indicate the xylem conduits.

The pattern of xylem's *Dh* variation along the axis of the whole hydraulic path with leaves/needles and stem connected in series, revealed for *P. abies* a steep increase in *Dh* at the needle junction into the stem apex, whereas in both angiosperms the *Dh* variation from the leaf petiole to the stem apex was rather smooth (Fig. 3, Table 1).

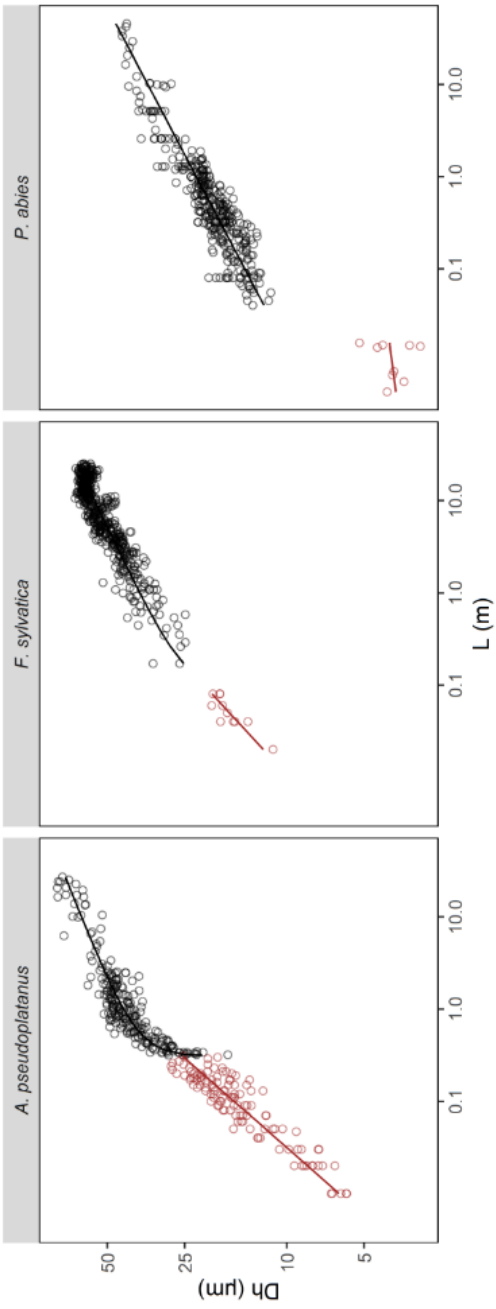

Figure 3. Variation of the hydraulic diameter (Dh) with the distance from the apex of leaf/needle (L) along the leaf/needle (red symbols) and stem (black symbols, data from Anfodillo et al., 2006; Petit et al., 2008) axes. Power scaling parameters of the relationship between Dh and axial length (L) assessed separately for leaves and stems are reported in table 1.

Table 1: Parameters (y-intercept, a; slope, b; their 95% confidence intervals; R^2 and p-value) of the linear regressions of Log10Dh vs. Log10L describing the conduit widening along the leaf/needle or stem longitudinal axis, where L (in mm) is the distance from the apical element of the leaf/needle or stem, respectively. Data of Dh along the stem were taken from literature (Acer pseudoplatanus, Petit et al., 2008) and from unpublished works (Fagus sylvatica, Picea abies).

Species		*a*	*b*	R^2	*p-value*	*a 95% CI*	*b 95% CI*	*Citation*
Acer pseudoplatanus	*Leaf*	0.39	0.41	0.85	**9.32e-49**	0.32; 0.45	0.37;0.44	
	Stem	1.22	0.14	0.85	**4.68e-94**	1.20; 1.25	0.13; 0.15	Petit et al., 2008
Fagus sylvatica	*Leaf*	0.66	0.33	0.75	**2.4e-6**	0.41; 0.90	0.18;0.47	
	Stem	1.34	0.13	0.79	**3.3e-164**	1.32; 1.35	0.13;0.14	Unpublished
Picea abies	*Leaf*	0.54	0.04	0.02	0.36			
	Stem	0.85	0.16	0.82	**7.1e-140**	0.83;0.87	0.16;0.17	Unpublished

The estimated variation in the cumulative resistance (R_{CUM}) with the increasing path length (L) showed that the hydraulic resistances are not homogeneously distributed along the hydraulic path (Fig. 4), but elements of highest resistance are located in the apical part of the hydraulic path.

Along the longitudinal axis of the stem, R_{CUM} increased from the apex downwards at rates progressively decreasing towards the stem base (Fig. 4a). When the contribution of leaf/needle conduits (*Rlx*) to the total path resistance was added to that of stem's conduits (*Rsx*), the model predicted that 65% and 95% of the total hydraulic resistance was confined within the needle in the conifer and within the leaf midrib in angiosperms, respectively (Fig. 4b). When also the contribution of the outside xylem resistance (*Rox*) was considered for the build-up of the total path resistance (i.e. 50% of the total leaf/needle resistance), almost the entire R_{CUM} (98% for *A. pseudoplatanus*, 92% for *F. sylvatica* and 85% for *P. abies*) was confined at the leaf level (Fig. 4c).

Accordingly, the same trends were predicted for the variation in tension (expressed as the percentage of Ψxyl from the leaf tip to the stem base, with most of the gradient confined within the leaf/needle (Fig. 4d).

By running a series of simulations for considering all the resistances along the hydraulic path (*Rsx+Rlx+Rox*), and applying virtually possible conditions of soil water potentials ($\Psi soil$=0 to -2 MPa) and air water potentials in the substomatal cavities (Ψair=-40 to -80 MPa), the model predicted that the gradient of xylem water potential rapidly increases along the leaf midrib from the tip to the petiole (Fig 5, dotted line, simulation made for *A. pseudoplatanus*). Notably, at the petiole base, the Ψx was predicted not to reach very low values, and was mostly dependent on $\Psi soil$ and much less influenced by air dryness (Ψair).

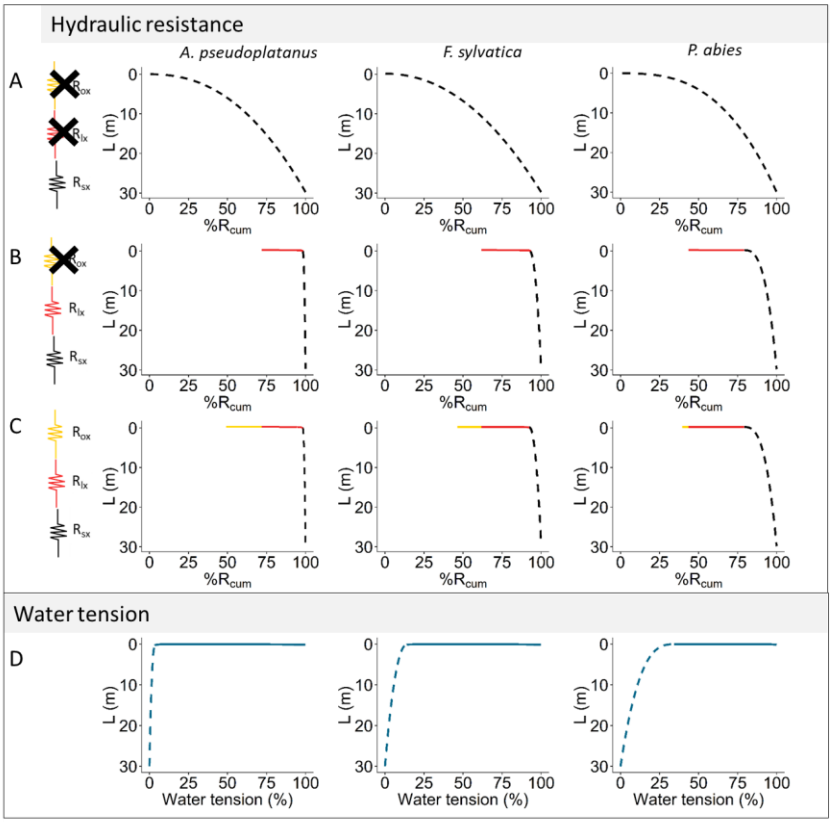

Figure 4. Relative axial variation of the cumulated resistance (R_{cum}) with the path length (L) considering (a) only the stem vasculature ($R_{sx,}$ black dotted line), (b) the integrated vasculatures of stem and leaves/needles (R_{sx} + $R_{lx,}$ black + red line), and (c) the total pathway, i.e. accounting also for the outside-xylem resistance in the leaves/needles (R_{sx} + R_{lx} + $R_{ox,}$ black + red+yellow line). (d) Relative variation in tension between the most apical (distal) element of the hydraulic path (i.e., the air/liquid interface on the mesophyll cell walls, 100% of tension) and the stem base (0% of tension). The dotted and solid lines represent the hydraulic path along the branch/stem/root and leaf/needle axes, respectively.

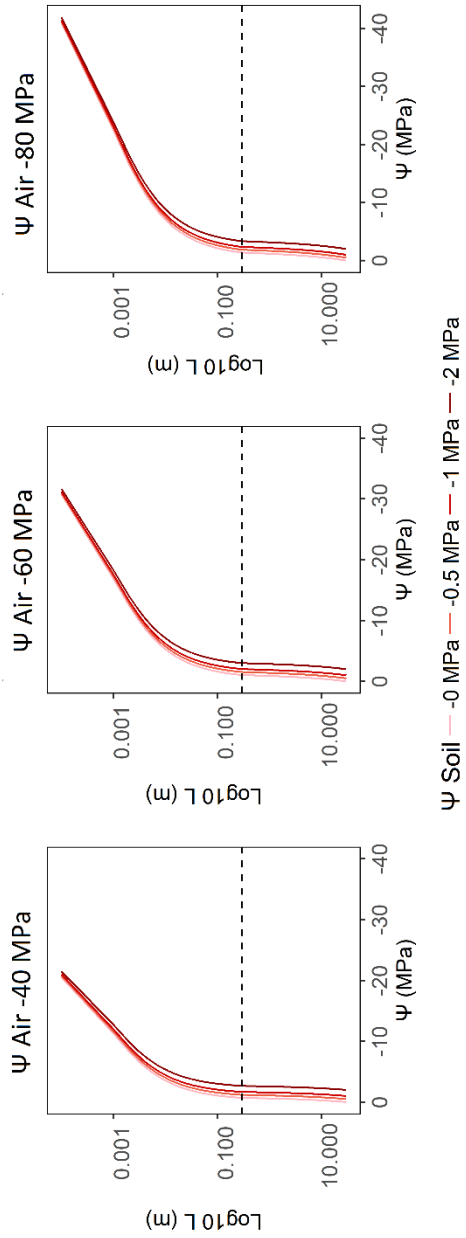

Figure 5. Theoretical effects of different soil (Ψsoil from 0 to -2 MPa) and air dryness (Ψair from -40 to -80 MPa) on the variation in the water potential (Ψ) along the whole hydraulic path from the most apical (distal) element of the hydraulic path (i.e., the air/liquid interface on the mesophyll cell walls) until the soil/root interface (L = 30 meters). The dotted line indicates the separation between the hydraulic paths along leaf and stem.

Discussion

Our results provided empirical evidence that the whole xylem vascular system is composed by conduits of different diameter with the smallest vascular elements being located at the distal extremity of the hydraulic path (i.e., in leaves/needles), in connection with the stem vasculature with conduits progressively enlarging in diameter moving away below the stem apex. This whole axial anatomical organization is likely to affect the distribution of resistances along the hydraulic path. This would theoretically determine a characteristic shape of the water potential gradient from the terminal element of the leaf/needle down to the stem base and further below until the root/soil interface, with potentially important implications for the exposure of xylem conduits to more or less risky water potentials for embolism formation.

Our anatomical analyses revealed that the xylem vascular system of angiosperms' leaves is characterized by an axial scaling of conduit diameter with an exponent of b~0.4, i.e., much higher than that reported for the stem of our trees (b~0.14), consistent with previous studies (Coomes et al. 2008; Petit & Anfodillo 2013). On the contrary, needles showed no axial trends in conduit diameter. Overall, the whole vascular system of either the angiosperms and the conifer seemed to conform to the principle that the size of conduits substantially depends on their position along the hydraulic path (Anfodillo et al., 2013; Lintunen et al., 2010; Olson et al., 2014, 2018).

We used our anatomical observations to derive information on the hydraulic properties of the whole transport system. Although our anatomical data were limited to only three species, it is worth mentioning that the reported axial scaling exponents estimated either along the leaf midrib or along the stem, were consistent with the convergent axial patterns found in both leaf venations (Coomes et al. 2008; Petit & Anfodillo 2013) and stems (Anfodillo et al. 2013; Olson et al. 2014).

At the stem level, the total hydraulic resistance (R_{CUM}) progressively cumulated from the stem apex downwards, but much less than linearly (Petit & Anfodillo 2009). Although our model oversimplified the xylem architecture, this result is fully consistent with some detailed physiological data. Indeed, measurements of axial hydraulic resistances carried out on stems of *Acer saccharum* Marsh. (6-9 m in length) of progressively reducing length by removing segments from the apex (Yang & Tyree 1993) are surprisingly consistent with our anatomical

based data (Fig. 6). Seemingly, but with the opposite approach (i.e., reducing stem/branch length starting from the base), the axial components of the total hydraulic resistance of stem and branches in *Acer pseudoplatanus* L. assessed with hydraulic measurements well matched the predictions based on the axial variation in vessel diameter (Petit et al. 2008).

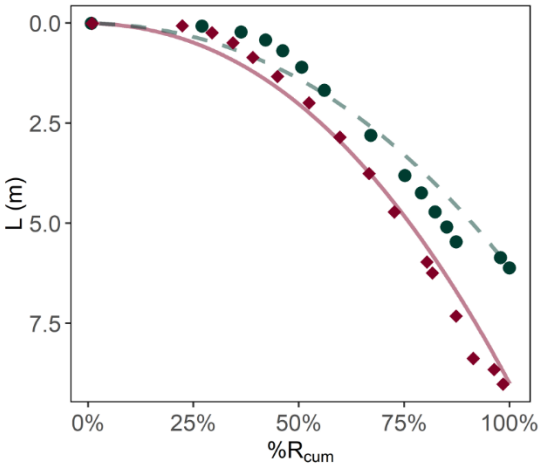

Figure 6. Relative axial variation of the cumulated resistance ($\%R_{cum}$) with path length (L (m)) in two branches of Acer saccharum. Dark green circles and purple diamonds are real data obtained from Yang & Tyree 1993 for two branches of 6 and 9 meter in length. We considered vessel widening with an exponent 0.14 as for our Acer trees (see table 1). Dark green dashed line and solid purple line are model expectation.

These good matching of physiological data and intra-individual variation in conduit diameter implies that the contribution of other conduit ultrastructures to the total conduit resistance is a constant fraction of lumen resistance. Indeed, it had been often reported that different cell's ultrastructures, such as wall-thickening type, end wall angle and morphology, size and density of pits, effectively contribute to the total conduit resistance in proportion to the lumen resistance (Martre et al. 2000; Sperry et al. 2005; Pittermann et al. 2006; Christman & Sperry 2010). with a proportion estimated as 56-64% in both angiosperms and gymnosperms (Sperry et al. 2005; Pittermann et

al. 2006). However, detailed analyses on how this proportion varies along the hydraulic path have still to be carried out.

We found that the leaf/needle length, its conduit widening, and the variation in conduit size at the junction between leaf/needle and stem were the main factors affecting the increase in R_{CUM} from the leaf/needle tip down along the hydraulic path to the stem base. The overall axial trend in conduit diameter along both leaf/needle and stem in series suggested a hydraulic segmentation of the foliar element, along which most of R_{CUM} would remain concentrated (~80%), thus minimizing the contribution of the stem's xylem to R_{CUM} (Fig. 4a). Notably, such a contribution became even weaker when we accounted also for the contribution of the living cells of the outside-xylem hydraulic pathway to R_{CUM} (Fig. 4a). In our simulations we implemented a conservative approximation of the outside-xylem resistance (R_{OX}), being equal to 50% of the total leaf/needle hydraulic resistance in both angiosperms and conifer. However, R_{OX} had been reported to vary between 40 to 88 % of the total leaf resistance across angiosperm species (Cochard et al. 2004; Trifiló et al. 2016; Scoffoni et al. 2017), but no data are available for conifer needles. Nevertheless, these results would suggest in general that the higher is the contribution of R_{OX} to the total leaf resistance then the lower is the contribution of the stem's xylem to the total hydraulic resistance of the whole transport system (R_{CUM}). This theoretical scenario is consistent with the classical view that the major component of the whole plant's hydraulic resistance is concentrated in the leaves (Tyree et al. 1993; Yang & Tyree 1994; Nardini & Salleo 2000; Sack & Holbrook 2006), although other empirical hydraulic measurements reported that leaf resistance is significantly lower than the resistance of both stem and roots (Tsuda & Tyree 1997; Sobrado 2007). In addition, our anatomical observations would strongly support a recent hypothesis that a very steep gradient of negative water potential likely occurs within the leaves (Buckley & Sack 2019), and agrees with empirical water potential measurements reporting a steep gradient of water potential developing during the day along the midrib of compound leaves, with more negative Ψ_{leaf} measured at the apical leaflet than that of the whole compound leaf at the level of the midrib's petiole (Petit & Anfodillo 2013). More specifically, the model predicted that the remaining drop in water potential between the stem apex and rootlets is very small, so that the actual stem water potential strongly depends on the water potential of

rootlets. This result conflicts with the classical view according to which the water potential along the stem increases linearly from leaves (Ψ_{LEAF}) to soil (Ψ_{SOIL}) (e.g.,Venturas *et al.*, 2017).

Steep variations in hydraulic resistivity have been suggested to determine hydraulic segmentations of different portions of the hydraulic path, with important consequences for the axial gradient of water potential and for the spread of gas emboli (Tyree & Zimmermann 2002b). According to the reported axial anatomical patterns, leaves/needles have been predicted to be nearly hydraulically "decoupled" from the stem, with the former accounting for nearly the total hydraulic resistance and therefore containing most of the total gradient of water potential (Nardini & Salleo 2000; Buckley & Sack 2019), whereas down along the latter the gradient would become rather flat, with water potential approximating that of rootlets (Fig. 4d and Fig. 5). Consequently, our model would predict that in case of water sub-saturation of soil (Ψ_{SOIL} ~0 MPa), the water potential developing along the whole stem axis would not be very low, even with very dry air. Such a segmentation would seem to be very effective in limiting the risks of embolism formation due to high transpiration rates (Martin-StPaul et al. 2017). However, much would depend on the relative contribution of rootlets to the total plant resistance. Hydraulic measurements on root segments suggested a minor contribution to the total hydraulic resistance (Martínez-Vilalta et al. 2002; McElrone et al. 2004b), consistent with anatomical observations of larger conduits below- than aboveground (McElrone et al. 2004b; Petit et al. 2009; Lintunen & Kalliokoski 2010; Petit et al. 2010; Prendin et al. 2018; Jacobsen et al. 2018). On the contrary, hydraulic measurements of the entire root system revealed a major contribution of the belowground transport system to the total plant resistance (Pratt et al. 2010). Further investigations are needed to more precisely understand the water relations of whole roots, as they imply the bypassing of impermeable barriers (i.e., the Casparian bands in the endodermis cell walls) through symplastic pathways, where aquaporins actively play a key role in strongly modulating root resistance upon physiological needs (Steudle & Peterson 1998).

In conclusion, we provided evidence for typical anatomical axial patterns between the upper and lower extremities of the hydraulic path, theoretically confining nearly the whole tension gradient within the leaf/needle segments. However, while the axial variation of xylem

conduit diameter is recognized to determine the hydraulic properties of the stem, the water relations at the extremities of the hydraulic path remain controversial and require further investigations to clearly understand their relative contribution to the total plant's hydraulic resistance. Based on empirical data of xylem anatomy, we hypothesize that roots and leaves respectively contribute negligibly and substantially to the total hydraulic resistance, so that the total hydraulic resistance is substantially independent of path length and a negligible tension gradient develops along branches, stem and roots, with water potentials remaining in the range of that at the soil/root interface, determining the highest safety against embolism formation during transpiration.

Chapter 6. Scots pine trees react to drought by increasing xylem and phloem conductivities

Authors:
Natasa Kiorapostolou*, Jesus Julio Camarero Martínez, Marco Carrer, Frank Sterck, Brigita Brigita, Gabriel Sangüesa-Barreda, Giai Petit

Submitted in:
Tree Physiology

Corresponding author *

Abstract

Drought limits the long-distance transport of water in the xylem due to the reduced leaf-to-soil water potential difference and possible embolism-related losses of conductance, and of sugars in the phloem due to the higher viscosity of the dehydrated sugary solution. This condition can have cascading effects in water and carbon fluxes that may ultimately cause tree death. We hypothesize that the maintenance of xylem and phloem conductances is fundamental for survival also under reduced resource availability, when trees may produce effective and low C cost anatomical adjustments in the xylem and phloem close to the treetop where most of the hydraulic resistance is concentrated.

We analyzed the treetop's xylem and phloem anatomical characteristics in Scots pine trees symptomatic and non-symptomatic of drought-induced dieback. We selected the topmost 55 cm of the main stem and selected several sampling positions at different distances from the stem apex to test for differences in the axial patterns between the two groups of trees. We measured the annual ring areas (*RA*), the tracheids' hydraulic diameter (*Dh*) and wall thickness (*CWT*), and the average lumen area of phloem sieve elements (*CAph*).

Declining trees grew less than the non-declining ones, and despite the similar axial scaling of anatomical traits, had larger *Dh* and lower *CWT*. Moreover, declining trees had wider *CAph*.

Our results demonstrate that even under drought stress, maintenance of xylem and phloem efficiencies is of primary importance for survival, even if producing fewer larger tracheids maybe also more vulnerable to embolism formation.

Keywords: Scots pine, wood anatomy, forest dieback, tree mortality, hydraulic failure, phenotypic plasticity, xylem, phloem.

Introduction

Drought events and heat waves are increasing worldwide in frequency and intensity due to the effects of climate change (Dai 2013). The resulting soil water shortage and high evaporative demand impose serious limitations to leaf transpiration and C uptake, inducing challenging conditions for the survival of trees. Indeed, an increased frequency of forest dieback and tree mortality events has been reported worldwide in the last decades (Allen et al. 2010, 2015).

Tree survival depends on the positive carbon balance, i.e., the difference between C uptake through photosynthesis and C used for all

the different physiological processes. Maintenance respiration consumes approximately 50% of the total C fixed with photosynthesis (Waring et al. 1998), whereas another significant amount is transferred to the environment as root exudates (~10%) (Jones et al. 2009) and volatile organic compounds (VOCs) (~10%) (Peñuelas & Llusià 2003). Importantly, with drought plants require a higher tissue osmoregulation to maintain tissue hydration, especially at the root level (O'Brien et al. 2014). Alongside, a higher amount of C is released to the soils (Preece et al. 2018), which is commonly supposed to be a strategy to ameliorate the rhizosphere condition by attracting symbiotic microorganisms, like mycorrhizas (Walter 2018). Moreover, also VOCs emissions have been reported to increase in response to drought (Ameye et al. 2018).

Carbon assimilation is linked to transpiration. The water diffused to the atmosphere through the leaf stomata needs to be replaced by water absorbed by roots and flowing along the xylem transport system to the leaves (Taiz & Zeiger 2006). The difference of water potential between leaves and roots ($\Delta\Psi=\Psi_{LEAF}-\Psi_{SOIL}$) represents the "engine" triggering the water flow. According to the Darcy's law (Tyree & Ewers 1991), the flow rate ($F=\Delta\Psi\times K$) is also proportional to the total xylem conductance (K), which is the resultant of the hydraulic contribution of every single xylem conduit constituting the water transport system. Since K cannot be promptly modified because xylem conduits are dead hollow cells, a reduction in $\Delta\Psi$ due to soil drought can be limiting for F, and therefore for gas exchange. If this situation persists until the tree depletes all the C reserves, decline and finally death by C starvation would occur. Other major mechanism of dieback and death implies widespread xylem embolism leading to plant desiccation by hydraulic failure (McDowell et al. 2008). However, the evaporation from cellular interstices in the leaf mesophyll cavities implies that water flows along the xylem at sub-atmospheric pressure and therefore in a metastable liquid phase (Tyree 1997). When water potential drops below a certain threshold, air bubbles can penetrate and expand into a xylem conduit, which becomes air-filled and no longer conductive (Cochard 2006). Vulnerability of conduits to embolism formation is variable and depends on different anatomical structures (e.g., pit size and number) (Tixier et al. 2014). In general, embolism resistance decreases with increasing conduit size (Hacke et al. 2006, Sperry et al. 2006), especially at the intraspecific level (Larter et al. 2017). Accordingly, the smallest xylem conduits along the roots-to-leaves hydraulic path are found at the stem apex (Petit et al. 2009, 2010), where the water

potential is the lowest due to the proximity to the sites of evaporation (i.e., leaves) (Venturas et al. 2017). Below the apex, conduits increase progressively until the stem base according to a universal axial pattern across species, size, and environment (Anfodillo et al. 2013).

In parallel to water flowing upwards to the leaves along the xylem architecture, the solution of sugars produced with photosynthesis flows in the opposite direction along the phloem, where conduits increase in diameter from stem apex to base seemingly to those of xylem (Petit & Crivellaro 2014, Jyske & Hölttä 2015, Savage et al. 2017). The flow occurs under the positive pressure between the sites of sugar loading (leaves, with higher sugar concentration) and sink sites, where sugars are consumed (De Schepper et al. 2013). This drop in the positive pressure is sustained by sugar loading at the leaf level. Consequently, sugar transport is dependent on C assimilation and thus on leaf transpiration (Hölttä et al. 2006, 2009). Under drought, not only phloem sap flow is limited by the prolonged stomatal closure, but also its overall efficiency (i.e., conductance) can be further limited by the higher sap viscosity due to tissue dehydration (Sevanto 2014).

What mechanism is mostly involved in determining irreversible conditions and exposing trees to pathogens attacks and ultimately mortality has been the object of intense research in the last decade (McDowell et al. 2013, Gaylord et al. 2015). On the one hand, a relevant loss of hydraulic conductance (> 60%) due to widespread embolism formation has been commonly reported in trees at significant stressful conditions preceding drought-induced mortality (Adams et al. 2017). On the other, the tree reaction to drought has been investigated either through comparative analyses of coexisting declining and non-declining trees, or retrospectively by reconstructing time series of xylem anatomical traits (e.g., Pellizzari et al. 2016). The first and most evident reaction to drought is the reduction in both primary and secondary growth rates (Maier 2001). Since anatomical traits (e.g., vessel diameter and grouping) vary axially according to a rather rigid design (Lechthaler et al. 2018), the commonly used protocols of measuring anatomical traits at one single position along the stem/branch with a fixed age, led to the most obvious result that trees with smaller xylem conduits are more embolism-resistant but less efficient in water transport (i.e., have a lower xylem conductance), with consequent limitations to secondary growth rates (von Arx et al. 2012, Pfautsch et al. 2016, Schuldt et al. 2016, Martínez-Sancho et al. 2017). Drought dependent limitations to growth rate are also reported from

retrospective analyses of ring width (Weemstra et al. 2013, Cailleret et al. 2017), with deeper anatomical investigations supporting the hypothesis that declining trees imprint their long-term reaction to drought by producing narrower conduits (Pellizzari et al. 2016).

The overall picture described above conflicts with other analyses carried out according to different sampling approaches, accounting for the general and predictable axial design of the xylem and phloem architectures. These studies supported the alternative hypothesis that trees react to drought by maintaining or even increasing the efficiency of the long-distance transport systems of both xylem and phloem. The underlying hypothesis is that to increase the survival probability, a tree must maintain a positive C balance and, hence, compensate for potential limitations to C assimilation (and therefore to transpiration and water flow) and sugar transport. At the xylem level, plants were reported to either react to soil drought by producing wider xylem conduits at the stem apex (Petit et al. 2016, Kiorapostolou et al. 2018) or to prevent any plastic adjustment of conduit size (Kiorapostolou & Petit, 2018). Furthermore, it has been shown that also tall trees, compared to small ones, can produce slightly larger conduits at the stem apex, likely to compensate for the hydraulic limitations imposed by the longer path length (Prendin et al. 2018). Interestingly, the authors showed with a simple hydraulic model that such a hydraulic compensation would be effective also if a tall tree would produce smaller conduits towards the stem base, as often observed in tall mature trees (Mencuccini et al. 2007). In addition, recent investigations on the reaction of phloem to drought revealed contrasting results, with sieve elements found to be either narrower in young *Fagus sylvatica* L. individuals (Dannoura et al. 2018) or wider in *Fraxinus ornus* L. (Kiorapostolou & Petit 2018) in individuals exposed to drought stress.

The aim of this study was to compare the xylem and phloem anatomy of the stem's leader shoot of declining vs. non-declining Scots pine (*Pinus sylvestris* L.) trees in a site experiencing drought-triggered dieback. The apical region is exposed to the lowest xylem water potentials (Venturas et al. 2017), and its xylem and phloem conduits, the narrowest of the whole transport paths, basically represent tight hydraulic bottlenecks (Petit & Anfodillo 2009, Ryan & Robert 2017). The target population was already object of a retrospective dendro-anatomical analysis revealing that the production of narrower conduits at 1.3 m started decades before evident signals of dieback such as needle loss and growth decline (Pellizzari et al. 2016). The null hypothesis was

that declining Scots pines produced wider tracheids close to the stem apex, as opposite to what was found at the stem base (Pellizzari et al. 2016), allowing to compensate to some extent for the limitations to gas exchanges imposed by soil water shortage. Moreover, phloem anatomy is expected to be characterized by a higher conductive area and wider sieve elements to guarantee an adequate efficiency of the long-distance transport of a more viscous phloem sap under drier soil conditions.

Materials and methods

Plant material and study site

In late April of 2017, we sampled three declining (with reduced foliage cover, on average less than 28% of crown cover) and three non-declining trees (crown cover > 90%) of similar height in a site (0º 59' 18'' W, 40º 26' 32'' N, 1260-1289 m a.s.l.) located near Corbalán, Aragón (E. Spain), where many trees started defoliating and dying after the severe drought of 2012. Since then, mean mortality rates are 12% yr^{-1} (J.J. Camarero, pers. observ.). Trees from this site had been already subject of dendro-anatomical analyses by Camarero et al. (2015) and Pellizzari et al. (2016). All sampled trees were measured (diameter at breast height, height), and their age at 1.3 m and crown cover were estimated (Table 1).

Table 1. Diameter at breast height (*Dbh*), height (*H*), crown cover, and age of the three declining and three non-declining sampled trees.

Condition	*Dbh* (cm)	*H* (m)	Crown cover (%)	Age (years)
Declining	23.0	9.5	40	126
	21.3	10.7	20	115
	27.0	12.3	25	135
Non-declining	19.5	9.28	100	61
	21.0	10.5	90	90
	20.0	9.0	100	62

We cut 4-15 stem segments at different axial positions to a maximum distance of 55 cm from the apex. The segments were cut just above the annual intervals and, thus, the range in the segment number depends on individual's growth. Transverse micro-sections from stem segments were cut using a rotary microtome LEICA RM 2245 (Leica Biosystems, Nussloch, Germany) at 15-18 μm, stained with a solution of safranin and Astra Blue (1% and 0.5% in distilled water, respectively), and permanently fixed on glass slides with Eukitt (BiOptica, Milan, Italy). Images of micro-sections were acquired at 100x magnification, using a

D-sight slide scanner (Menarini Group, Florence, Italy), and analysed with ROXAS (von Arx & Carrer 2014). The analysis was performed on a wedge of known angle (α) centred at the pith. A first manual image editing implied to outline the contour of the pith and of each xylem ring to allow ROXAS to automatically measure the area of each xylem ring (*RA*), the average conduit hydraulic diameter ($Dh = \Sigma d^5/\Sigma d^4$, where *d* is the conduit diameter), and the cell wall thickness (*CWT*). Then, each *RA* was up-scaled to the whole cross-section as $Y=Y'/\alpha \times 360$ (where *Y* is the up-scaled *RA*, Y' the *RA* of each ring, and α the wedge angle). Moreover, we measured for each segment the average area of phloem sieve tubes (*CAph*) retrieved from the 20 biggest sieve elements from the analysed conductive phloem (i.e. the youngest 1-2 phloem rings).

Statistical analysis

We performed a comparative analysis of the scaling relationships between different traits (i.e., dependent variables: *RA, CWT, Dh, CAph*) against the distance from the apex (*Dap*) in declining and non-declining trees for the wood produced after the drought of 2012 (the last 5 annual rings of the sections). We used Standardized Major Axis (SMA) models and tested for possible differences on the elevation (*y*-intercept) and slope (exponent *b*) of the different scaling relationships (Warton et al. 2006, 2012). When necessary, variables were transformed in natural logarithm (log in R) to meet the assumptions of normality and homoscedasticity. All statistical analyses were performed using R version 3.4.2 (R Core Team, 2017).

Results

In both declining and non-declining trees, the annual allocation into xylem biomass followed an axial scaling relationship between the xylem ring area (*RA*) and the distance from the stem apex (*Dap*). The scaling exponent (i.e., the slope of the log-log relationship was higher in declining compared to non-declining trees (Figure 1a; Table 2). However, declining trees grew significantly less than non-declining trees, as shown by their lower y-intercept in the relationship between *RA* and *Dap* (Figure 1a; Table 2), and by their lower stem elongation rates (mean ±SE = 2.37 ± 0.2 vs. 5.77 ±1.13 cm yr^{-1}).

The tracheid cell wall thickness (*CWT*) increased with increasing distance from the apex for the declining trees, whereas for non-declining trees the axial variation for the topmost 55 cm was negligible (Figure 1b; not significant slope). The declining trees had thinner cell

walls closer to the stem apex, as shown by the significantly lower y-intercept in the relationship *CWT* vs. *Dap* (Figure 1b; Table 2).

The conductive xylem and phloem elements revealed clear axial patterns. Both the mean tracheid hydraulic diameter (*Dh*) and the mean area of sieve elements (*CAph*) increased with increasing distance from the stem apex (*Dap*), according to power scaling relationships with slopes not significantly different between declining and non-declining trees (Figures 2a and 2b; Table 2). However, declining trees produced either wider tracheids than non-declining ones (significantly higher y-intercept in *Dh* vs *Dap*: Figure 2a; Table 2), either wider phloem sieve elements (higher y-intercept in *CAph* vs *Dap*; Figure 2b; Table2).

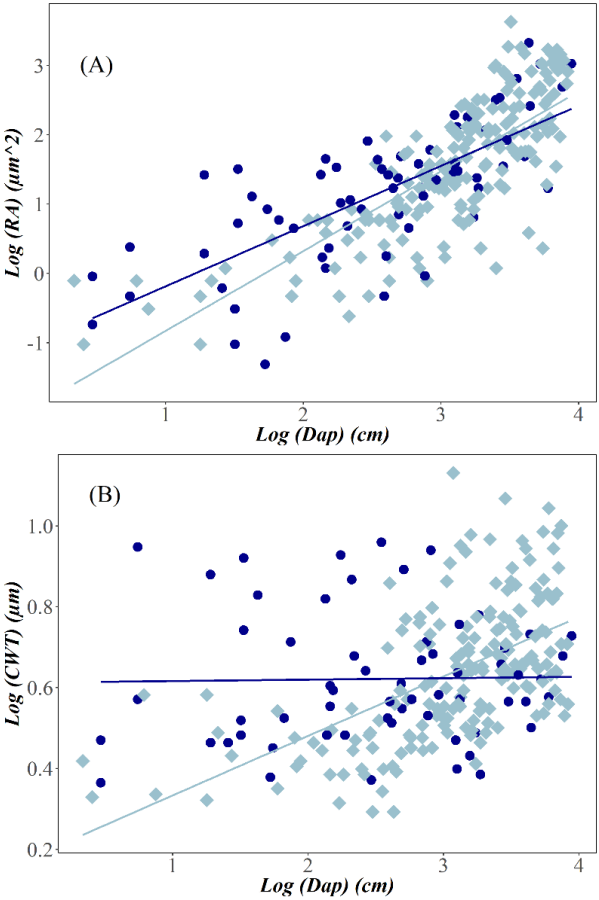

Figure 1. (a) Total ring area (*RA*, mm^2) for the last five years (after the drought of 2012) against distance from the stem apex (*Dap*, cm) in dark blue circles for non-declining trees and light blue diamonds for declining trees. (b) Conduit cell wall thickness (*CWT*, µm) for the last five years (after the drought of 2012) against distance from the stem apex (*Dap*, cm) in dark blue circles for non-declining trees and light blue diamonds for declining trees.

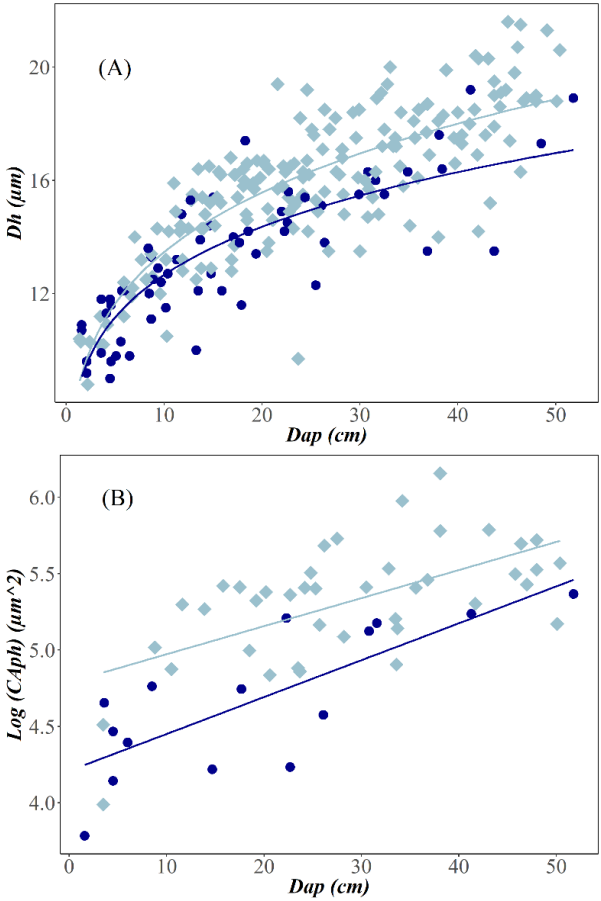

Figure 2. (a) Conduit hydraulic diameter (*Dh*, µm) for the last five years (after the drought of 2012) against distance from the stem apex (*Dap*, cm) in dark blue circles for non-declining trees and light blue diamonds for declining trees. (b) Mean phloem cell area (*CAph*, μm^2) for the last five years (after the drought of 2012) against distance from the stem apex (*Dap*, cm) in dark blue circles for non-declining trees and light blue diamonds for declining trees.

Table 2. Outputs of Standardized Major Axis (SMA) models. The models equal: *variable ~ Dap + conditions* to test for differences in elevation (y-intercept), and *variable ~ Dap*conditions* to test for differences in slopes (exponent *b*) (Warton et al. 2012). Data in Log transformed when needed. In the models variable = *RA* or *CWT* or *Dh* or *CAph*, and conditions = declining and non-declining.

Model information		Intercept	Slope
Log RA vs Log Dap	*Declining*		
	Estimate	-2.763	1.480
	Lower limit	-3.126	1.350
	Upper limit	-2.400	1.623
	Non-declining		
	Estimate	-2.416	1.187
	Lower limit	-2.771	1.005
	Upper limit	-2.061	1.404
P-value		<0.01	0.02
Log CWT vs Log Dap	*Declining*		
	Estimate	-0.099	0.255
	Lower limit	-0.183	0.226
	Upper limit	-0.015	0.288
	Non-declining		
	Estimate	0.018	0.182
	Lower limit	-0.077	0.140
	Upper limit	0.113	0.235
P-value		<0.01	0.02
Dh vs Dap	*Declining*		
	Estimate	10.847	0.202
	Lower limit	10.382	0.184
	Upper limit	11.312	0.221
	Non-declining		
	Estimate	9.919	0.194
	Lower limit	9.437	0.167
	Upper limit	10.400	0.226
P-value		<0.001	0.67
Log CAph vs Dap	*Declining*		
	Estimate	4.485	0.030
	Lower limit	4.242	0.023
	Upper limit	4.728	0.040
	Non-declining		
	Estimate	4.106	0.029
	Lower limit	3.817	0.018
	Upper limit	4.395	0.045
P-value		<0.01	0.82

Discussion

In this study, we performed xylem and phloem anatomical analyses at the treetop of declining and non-declining Scots pine trees of similar height. Dendro-anatomical analyses of wood cores extracted at breast height revealed that declining trees started to produce narrower tracheids long before the emergence of signs of vigor loss (Pellizzari et al. 2016). Conversely, our results for the wood produced after the drought of 2012, revealed exactly the opposite pattern at the treetop, where larger tracheids and sieve elements were found in declining trees. Soil drought limits photosynthesis and growth because the water transpired by leaves cannot be supplied with water absorbed by roots and then flowing through the xylem in the stem. This results into reduced leaf hydration, with negative effects on stomatal conductance (Scoffoni et al. 2017), meristem activity and CO_2 fixation (Brodribb & Jordan 2008). Under drought also there is the need to increase tissue osmoregulation (O'Brien et al. 2014), and more abundant losses of organic compounds to the environment in the form of root exudates (Preece et al. 2018), and VOCs (Peñuelas & Llusià 2003) that can further limit the C resources available for plant growth.

A retrospective dendro-ecological meta-analysis on radial growth preceding mortality (Cailleret et al. 2017) suggested that rapid mortality events associated with an abrupt reduction of growth could be triggered by intense drought events determining driving widespread xylem embolization and plant desiccation by hydraulic failure. On the contrary, a long-term growth decline could be associated with a progressive deterioration in hydraulic performance coupled with a depletion in carbon reserves. Our study system represents trees in long-term growth decline. The studied Scots pine tree population analyzed in this and another study (Pellizzari et al. 2016) revealed that the long-term (>30 years) reduction in radial growth measured at the stem base in declining trees was coupled with a reduction in the average tracheid lumen area in the stem. In contrast, we found that the reduction in stem elongation was coupled with an increase in the tracheid lumen area, and a decrease in their cell wall thickness at the treetop. Moreover, the treetops of declining trees were characterized by phloem sieve elements with larger diameters compared to non-declining trees. However, both declining and non-declining trees followed similar axial scaling patterns in xylem and phloem showing that allometric relationships not only remain similar independently of plant size and age, but also across different degrees of vigor. Our scaling exponent of tracheid hydraulic

diameter (Table 2) is slightly lower than that commonly reported for different tree species (Anfodillo et al. 2013). On the contrary, the axial widening of phloem sieve elements was significant but not much pronounced (b=0.03) (Table 2) as that reported for entire plants (*b~0.14-0.22*) (Petit & Crivellaro 2014).

Considering that most of the total hydraulic resistance is concentrated at the treetop due to the local presence of the smallest conduits of the whole hydraulic path, a reduction in tracheid lumen area at the stem base would have a negligible effect on the total xylem conductance (i.e., xylem hydraulic efficiency) (Petit et al. 2010, Prendin et al. 2018). On the contrary, the slight enlargement of the tracheids' lumen areas at the treetop had theoretically great hydraulic consequences, with the release of the plant's hydraulic bottleneck and the consequent improvement in the total xylem conductance. The likely side cost of this strategy is the increase in the vulnerability to drought-induced embolism (Prendin et al. 2018), not just for the larger apical tracheids, but also for their thinner cell walls more prone to bending and air seeding under tension (Sperry et al. 2006). Understanding which the role is of this higher xylem vulnerability in the long-term process of vigor decline in our trees is difficult. Nevertheless, our results suggest that declining trees invested their limited C budget to build-up a low-cost xylem architecture, i.e., wide conduits at the treetop, in the attempt to maintain the total xylem conductance. This would reasonably seem a possible way to increase the chances of survival under drought stress. Indeed, attaining a positive C balance is subordinated to a sufficient C assimilation, and thus to a sufficient stomata opening together with an efficient xylem sap flow supplying the transpiring leaves. In this respect, it has been recently reported that trees acclimated to drier soil conditions can even load more leaf than xylem biomass along their branches compared to trees from more mesic conditions (Anfodillo et al. 2016, Petit et al. 2016, Kiorapostolou & Petit 2018). In such a way, they likely compensate for the negative effects of prolonged stomata closure on C assimilation, and thus covering the seasonal C costs for maintenance, osmoregulation, transfers of organic compounds to the rhizosphere and atmosphere, growth and reproduction. It is worth underlying that the presence of branch loading higher leaf biomass might be crucial in species shedding leaves during harsh summer droughts, when plant metabolism is sustained by the C reserves accumulated during favorable conditions (McDowell et al. 2008).

The development of a gradient of water potential along the xylem and the maintenance of leaf hydration are important not only for stomatal conductance and gas exchanges, but also for an efficient transport of photosynthetic products along the phloem (Mencuccini & Holtta 2010). Our anatomical analyses of phloem traits revealed that declining trees produced a more conductive phloem at the treetop. Similar to the xylem, the phloem architecture is characterized by conductive sieve elements that progressively increase in diameter from the stem apex towards the stem base (Petit & Crivellaro 2014, Jyske & Hölttä 2015, Savage et al. 2017, Kiorapostolou & Petit 2018), so that the treetop results to be the hydraulic bottleneck also for the long-distance sugar transport system (Ryan & Robert 2017, Savage et al. 2017). Consistent with the hypothesis that limitations to phloem transport under drought arouse from the higher phloem sap viscosity due to tissue dehydration (Sevanto 2014), we observed a larger conductive phloem area with wider sieve elements at the treetop of our declining, drought-stressed Scots pine trees.

Our analyses demonstrated that the anatomical modifications of both xylem and phloem architecture can be different and respond to different requirements depending of the position along the hydraulic path. In particular, modifications that occurred towards the stem base seemed to respond to contingent conditions of low C resource availability: allocation to this region is not prioritized, until the extreme case of no allocation at all (i.e., missing ring, Novak et al. 2016), because of its minor importance for the overall hydraulic properties (Petit & Anfodillo 2009, Savage et al. 2017). On the contrary, modifications at the hydraulic headquarters, i.e., at the treetop, where most of the total hydraulic resistance is concentrated (Petit & Anfodillo 2009, Savage et al. 2017), and the xylem tensions are the highest (Venturas et al. 2017), would result very effective for the overall xylem and phloem conductance and realizable at a low C cost. As unavoidable side effects, these modifications may pay the cost of a higher vulnerability to embolism formation, thus exposing declining trees to even a higher risk of hydraulic failure (Prendin et al. 2018).

Differently from a large body of published literature, our analyses and interpretations re-evaluate the role of the xylem embolism resistance as no longer central in the prioritized processes of acclimation and adaptation to soil drought conditions, especially in declining trees. Substantially, the tree reaction to drought unlikely produces a xylem more resistant to embolism, because this cannot be equally efficient

(Gleason et al. 2016). In other words, for a declining tree it would be counterproductive to allocate the reduced C resources in producing more embolism-resistant xylem (e.g., narrow conduits), when the resulting conductance is not sufficient to sustain leaf transpiration, and therefore to assimilate CO_2.

In conclusion, we demonstrated that the treetop is the region where low-cost but hydraulically effective anatomical modifications can be realized under drought stress, meristem impairment and shortage of C resources. Safeguarding the total xylem and phloem conductance seems a risk worth taking to increase the chances of survival, even though this may come at the cost of a higher vulnerability of embolism formation and the relative higher risk of death by hydraulic failure.

Chapter 7. More studies in short

1.Hydraulic recovery from xylem embolism in excised branches of angiosperms is related to the amount of xylem parenchyma and the occurrence of phloem

Introduction

Water transport in plants is realized through elongated dead xylem conduits following a gradient of water potentials developed from the transpiring leaves. According to the cohesion-tension mechanism, water is under tension and, although below its vapor pressure, it remains in liquid phase. Under such a metastable state, water is prone to cavitation, resulting in xylem embolism, especially under drought conditions, on the basis of the air-seeding hypothesis. Xylem embolism can spread leading in extensive water transport blockage and, ultimately, in hydraulic failure and mortality. The vulnerability of species to embolism formation can be evaluated by the species-specific *P50* values (the water potential at which xylem loses 50% of its total conductivity). Species with lower *P50* value (more negative) are less vulnerable to xylem embolism and they can operate hydraulically under more negative soil water potentials (drier soils). However, plants operate near critical thresholds of their hydraulic dysfunctions, especially angiosperms. For this reason, it is expected that plants have developed mechanisms to recover hydraulic functionality after embolism formation. However, the actual mechanism of embolism recovery has not yet been provided. According to the theory of Zwieniecki & Holbrook (2009), embolism recovery is a metabolic process according to which sugars accumulate in the embolised conduits attracting water from parenchyma cells and/or phloem. We hypothesized that (i) in case of the existence of this mechanism, there should be a link between the species' ability to recover from high percentage loss of conductivity and the amount of parenchyma in the wood, and (ii) phloem may have an important role in this mechanism because can act as source of water and solutes.

Materials and methods

We performed experiments on 12 angiosperm species (Table 1) growing in the Mediterranean region. The species were characterized by different: a) xylem embolism vulnerability, as estimated by species-specific *P50* values (= xylem tension inducing a Percentage Loss of hydraulic Conductivity, *PLC* = 50%, ranging between – 0.9 and – 4.6 MPa), and b) total wood parenchyma fraction (*RAP*, ranging between

Species	Family	*Abbr*	P_{50} (MPa)	*MVL* (m)	*RAP* (%)
Arbutus unedo L.	Ericaceae	Au	−3.1 (Martínez-Vilalta et al., 2002)	0.24 ± 0.01	19.2 ± 1.0
Ceratonia siliqua L.	Fabaceae	Cs	−2.6 (Trifilò et al., 2015)	0.36 ± 0.005	25.6 ± 4.0
Cercis siliquastrum L.	Fabaceae	Csq	−1.8 (Nardini et al., 2003)	0.20 ± 0.01	17.4 ± 2.2
Eucalyptus camaldulensis Dehnh	Myrtaceae	Ec	−4.6 (Trifilò et al., 2015)	0.90 ± 0.005	14.8 ± 0.2
Laurus nobilis L.	Lauraceae	Ln	−2.5 (Trifilò et al., 2015)	0.42 ± 0.01	17.1 ± 0.5
Morus alba L.	Moaraceae	Ma	−0.9	0.32 ± 0.01	28.6 ± 1.9
Myrtus communis L.	Myrtaceae	Mc	−3.1 (Trifilò et al., 2015)	0.31 ± 0.02	23.0 ± 1.6
Nerium oleander L.	Apocynaceae	No	−1.5 (Trifilò et al., 2015)	0.30 ± 0.02	14.0 ± 1.3
Olea europaea L.	Oleaceae	Oe	−2.1 (Trifilò et al., 2015)	0.66 ± 0.005	16.8 ± 0.8
Phillyrea latifolia L.	Oleaceae	Phi	−6.5 (Martínez-Vilalta et al., 2002)	0.26 ± 0.03	20.0 ± 1.7
Pistacia lentiscus L.	Anacardacieae	Pl	−4.1 (Trifilò et al., 2015)	0.32 ± 0.03	13.7 ± 1.5
Quercus ilex L.	Fagaceae	Qi	−3.3 (Trifilò et al., 2015)	0.91 ± 0.01	28.0 ± 4.0

13.7 and 28.6 %) (Table 1). In order to avoid possible excision artefacts during hydraulic measurements, branches at least 2 times longer than the species-specific maximum vessel length (*MVL*) were collected and bench dehydrated. Before hydraulic measurements, the basal end of the branches was immerged into a water-filled tray and cut several times from the base under water, until obtaining subsamples shorter than the *MVL*. This experimental procedure allowed avoiding spurious embolism in terminal shoot during dehydration, as well as to reconnect xylem with water and relax xylem tension before hydraulic measurements. A subset of these samples was measured immediately to estimate the initial *PLC* and another subset was maintained with the basal end in water for 1h before re-measuring *PLC* to estimate the ability for embolism recovery. Measurements were performed in both intact and girdled samples (with the phloem removed), and a xylem recovery index was calculated (*ΔPLC = PLC initial – PLC* after 1 h rehydration) to test the potential embolism repair ability.

Table 1. Name of species, family, abbreviations (*Abbr*), xylem pressure values inducing ~50% loss of xylem hydraulic conductivity (*P50*), mean values of maximum vessel length (*MVL*, n = 3) and the percentage of wood parenchyma cells (*RAP*, n = 3).

We also obtained radial and transverse wood micro sections and analysed some of the xylem's anatomical characteristics of the branches, i.e. the % axial parenchyma (PA_A), the % radial parenchyma (PA_R), and the area of the pith (*Apith*). Then we estimated the % total parenchyma volume ($PA_{TOT} = PA_A + PA_R + Apith$).

Results and discussion

We found a significant relationship between the recovery ability (*ΔPLC*) and the area of the pith (*Apith*) (Figure 1) and also a significant relationship between the *ΔPLC* the amount of total parenchyma (R^2 = 0.60; $P < 0.05$). These results indicate that parenchyma cells, and thus the amount of non-structural carbohydrates may have an important role in the hydraulic recovery process of the branches. In total 8 out of 12 species decreased significantly *PLC* within one hour in the water (Figure 2). In addition, when comparing the intact and girdled branches, we saw that girdled branches did not significantly decrease their *PLC* after one hour of rehydration (Figure 2). This suggests that also phloem has a role in the xylem embolism repair mechanism.

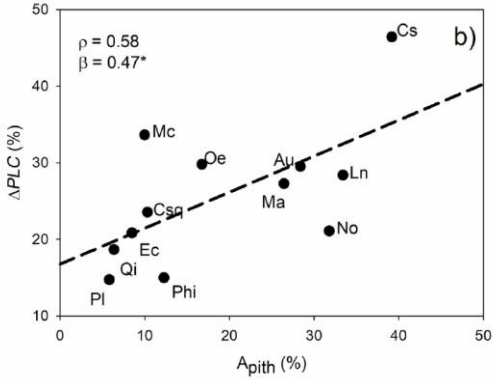

Figure 1. Relationship between recovery ability (*ΔPLC*) of the branches and pith area (*Apith*). Regression lines (dotted lines) and related β coefficients values are reported. Significance level: $*P < 0.05$.

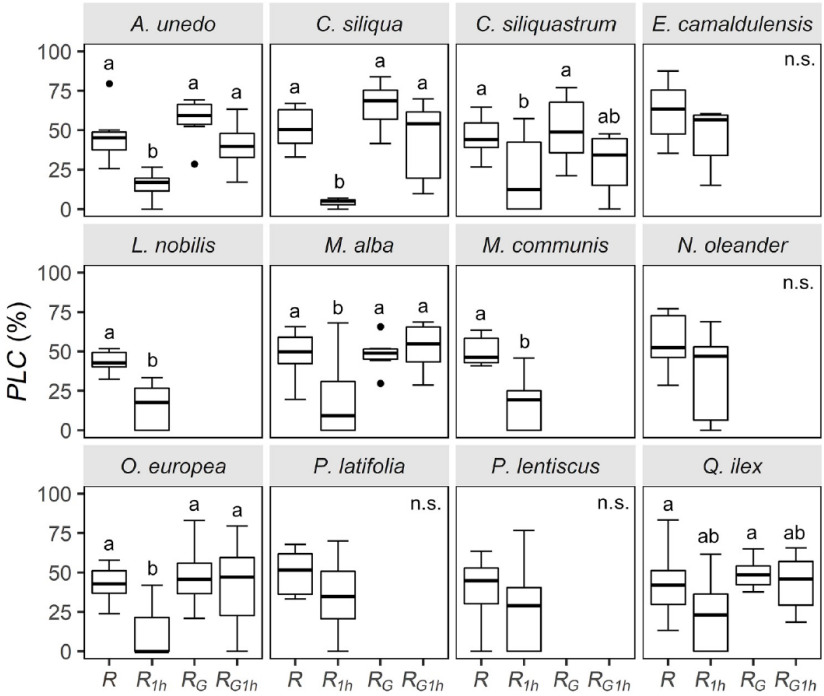

Figure 2. Mean values ± SEM of the percentage loss of hydraulic conductivity (PLC) as recorded in relaxed samples (*R*), in *R* samples after 1 h rehydration (R_{1h}), in girdled samples (*RG*), and in *RG* samples after 1 h rehydration (R_{G1h}). Different letters indicate significant differences from Tukey's pairwise comparisons or t-test ($n \geq 6$).

The measurements and results shown in this chapter is only part of this study. For the whole study:
Trifilò, P., Kiorapostolou, N., Petruzzellis, F., Vitti, S., Petit, G., Gullo, M. A. L., ... & Casolo, V. (2019). Hydraulic recovery from xylem embolism in excised branches of twelve woody species: Relationships with parenchyma cells and non-structural carbohydrates. Plant Physiology and Biochemistry, 139, 513-520.

2.Xylem parenchyma fraction and cell characteristics in three Fagaceae species along an environmental gradient in water availability

Introduction

Parenchyma cells within the xylem of woody plants play an important role in the storage of non-structural carbohydrates (*NSC*) (Plavcova et al. 2016) since stored *NSC* are responsible for plant maintenance and growth (Plavcova et al. 2016) and possibly have a role in embolism recovery (Zwieniecki and Holbrook 2009). However, they do have energy costs for maintenance since they are living cells (De Vries 1975). Therefore, the amount of parenchyma within wood, but also phloem are expected to affect the plant carbon balance.

We studied the fraction of xylem axial and radial parenchyma and the axial and radial parenchyma cell size and density along gradients in water availability in twenty-seven populations of three Fagaceae species. We hypothesized that trees from the same species that thrive under differing water availability conditions and that different species show differences in parenchyma cell production (size and density) and in parenchyma fraction. We expected that more vulnerable to embolism species might need a higher parenchyma fraction, larger parenchyma cells or denser for maintenance and embolism recovery under dry than under wet conditions, while species with a safer hydraulic system will not alter their parenchyma traits under conditions limiting carbon uptake in order to keep low costs of maintenance.

Materials and methods

Branch material

Branch samples from three species (*Fagus sylvatica*, *Quercus humilis*, *Quercus ilex*) were collected from 36 (nine per species) populations in the region of Catalonia (NE Spain). For each species, the populations were divided in dry, medium, and wet based on their water availability index. This index was calculated as the ratio of precipitation over potential evapotranspiration (*P/PET*) of the spring and summer months of the years 1951-2010 according to the Hargreaves-Samani method (Hargreaves and Samani 1982) with dry plots having a $P/PET < 33$ percentile, medium plots having $33 < P/PET < 66$ and wet plots having $P/PET > 66$ percentile. Three individuals per population were used in this parenchyma analysis (n=81). We did cell and tissue measurements on stained micro-sections that were made at 60 cm from the branch

apex. Images were analysed on ImageJ version 2.0.0 (Schneider et al. 2012). For each image, an area of approximately 0.5 mm^2 was selected within the intact tissues (i.e., tissues not affected by artificial cracks caused by cutting) of the 2-3 latest xylem rings (i.e., most current growth) herewith avoiding compression wood when possible.

Estimation of parenchyma fraction

On each image the areas occupied by parenchyma cells were outlined manually. The fractions of axial and radial parenchyma were measured as sum of outlined areas per total area of the analysed image. The total parenchyma fraction was calculated as the sum of axial and radial parenchyma fractions.

Parenchyma cell area and density

Two diameters (a - height and b - width) were measured in approximately 50-60 axial and 25 radial cells per image (n=81). Cell area was calculated as elliptic shape (*area = pi*a*b*) and the average of all cells per individual tree was calculated after log- transformation. In addition, in a small section of the image of approximately 0.02-0.05 μm^2, the axial and radial parenchyma cells were counted to calculate cell axial and radial cell density as number of cells per analysed area.

Data analysis

Before averages per tree and per plot were calculated, square root and natural logarithm transformations were performed for percentages and natural numbers respectively to meet the assumptions of normality and homoscedasticity. We used Spearman's correlations to test for relationships between the measured variables. Furthermore, to test for effects of the water availability gradient on the parenchyma traits we used type I regressions (lm in R) with as y-variables the measured traits (axial, radial and total parenchyma fractions, axial and radial cell area, axial and radial cell density) and as x-variable the *P/PET* values for spring and summer. One way ANOVA with Tukey post-hoc test was performed to test for differences in the parenchyma traits across species and conditions. Graphs, calculations and statistics were done in R version 3.4.2 (R Core Team 2017).

Results and discussion

Axial and radial parenchyma fractions were negatively correlated to each other (Table 1). Similar results were found also for axial cell area

and radial cell area, as well as for axial cell density and radial cell density (Table 1). These results suggest that the studied species arrange the available space within the xylem as such that *NSC* can be stored while leaving enough space for water transporting cells supporting leaf evapotranspiration (conduits) and cells for mechanical support (fibers). Opposite to our expectations, *P/PET* was not significantly related to the parenchyma fractions neither to the size or density of the parenchyma cells (Figure 1a and 1b; only results for total parenchyma shown). These results suggest that species do not adjust their xylem parenchyma fractions or cell traits to the local water availability conditions. This might indicate that the studied species do not invest in parenchyma cells under drier conditions probably because they are not in a need of more parenchyma to support maintenance or to recover embolised vessels, but instead they maintain their carbon balance by keeping a low amount of cells having high carbon costs.

Table 1. Spearman's correlation coefficients between the different parenchyma traits at population level: axial parenchyma fraction (%axial), radial parenchyma fraction (%radial), total parenchyma fraction (%total), axial parenchyma cell density (CDax), radial parenchyma cell density (CDrad), axial parenchyma cell area (CAax), radial parenchyma cell area (CArad). * $P < 0.05$, ** $P < 0.01$, *** $P < 0.001$.

	%radial	**%total**	**CDax**	**CDrad**	**CAax**	**CArad**
%axial	-0.71 ***	0.47 **	0.86***	-0.40**	0.85***	-0.51**
%radial		0.27*	-0.66***	0.42**	-0.56***	0.72***
%total			0.30*	-0.055	0.41*	0.16
CDax				-0.28*	0.72***	-0.60***
CDrad					-0.55***	0.096
CAax						-0.18

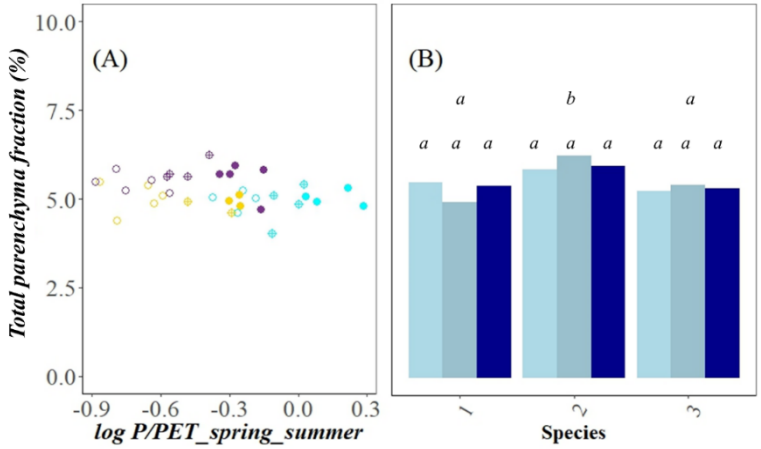

Figure 1. **(a)** Total parenchyma fraction (%) against the precipitation over potential evapotranspiration ratio of the spring and summer months (*P/PET_spring_summer)* for the 36 studied population. Shapes: open circles = dry conditions, crossed circles = medium conditions, solid circles = wet conditions. Colours: yellow = *F. sylvatica*, purple = *Q. humilis*, cyan = *Q. ilex*. **(b)** Total parenchyma fraction (%) in different species and conditions. Species : 1 = *F. sylvatica*, 2 = *Q. humilis*, 3 = *Q. ilex*. Colours: very light blue = dry, light blue = medium, dark blue = wet. Letters show the results of the Tukey post-hoc tests. Upper line letters show a comparison between species. Lower line letters show a comparison within species across the different sites. Similar letters mean no significant differences.

This work frames within the PHLOEMAP project (EU Horizon 2020 Programme – Marie Skłodowska-Curie individual fellowship – No 659191) lead by Dr. Elisabeth M.R. Robert and Prof. Dr. Jordi Martínez Vilalta of the Centre for Ecological Research and Forestry Applications (CREAF) in Barcelona, Spain.

3.Differences and similarities in the xylem anatomy of alive and dead Pinus nigra

Short introduction

Severe droughts affect the survival of tree species, especially when they occur during the growing season. After a drought occurred in 2012 in the Karst region of Trieste (Italy), individuals of the *Pinus nigra* population started defoliating and dying. However, other individuals growing very close to the dying trees are vigorous. We expected that there are xylem anatomical differences between the two groups of trees (dead vs. vigorous) that would allow us to understand the reason of mortality.

Materials and methods

Stem segments from two trees (one dead and one alive) of similar height and age were collected at different distances from the stem apex for the whole axial profile. Transverse micro-sections were obtained at 12 um using a rotary microtome LEICA RM 2245 (Leica Biosystems, Nussloch, Germany), stained with safranin 1% in distilled water, and permanently fixed on glass slides with Eukitt (BiOptica, Milan, Italy). Images were acquired at 100x magnification using a D-sight slide scanner (Menarini Group, Florence, Italy). The images were analysed in ROXAS v 3.0.139 for the automatic measurements of the hydraulic diameter (*Dh*) and ring area (*RA*). For the apical 1 m we also calculated the Cell Wall Thickness (*CWT*). We tested if there are differences in the allometric scaling of *Dh* against the distance from the tree apex (*Dap*), and of *CWT* against *Dap* between dead and alive trees.

Results and discussion

Both dead and alive trees showed an increasing tracheid hydraulic diameter (*Dh*) with increasing distance from the stem apex (*Dap*) (Figure 1). The allometric constants of the relationship did not differ significantly between the dead and alive tree (Figure 1). However, the exponent (*b*) of the relationship was significantly different between the two trees (Figure 1). When looking only at the apical 1 m, we found that the dead tree had narrower and thicker tracheids (Figure 2a and 2b) than the alive tree, and steeper slopes in both relationships. Our results suggest that the alive tree produced wider tracheids near the transpiring tissue to maintain an efficient water transportation to sustain transpiration at a low cost of carbon (thinner conduits). Furthermore,

our results demonstrate that wood anatomy is quite rigid between the two trees and conduits are widening from the stem apex downwards. These results are somehow in contrast to the results of the Chapter 6 of this thesis. As described in Chapter 6, declining *Pinus sylvestris* trees produced wider xylem and phloem cells near the stem apex in order to survive. Contrary, in this subchapter, *Pinus nigra* alive tree had wider and thinner tracheids and not the dead tree.

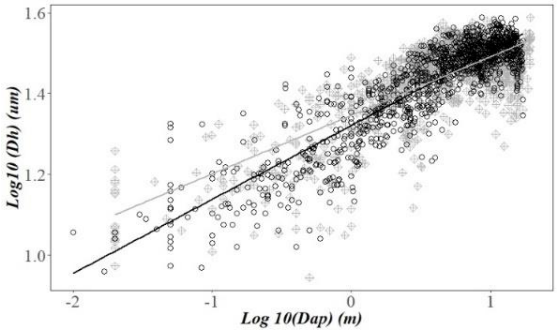

Figure 1: The hydraulic diameter (*Dh*) against the distance from the stem apex in dead (black color) and alive (gray color) *P. nigra* trees.

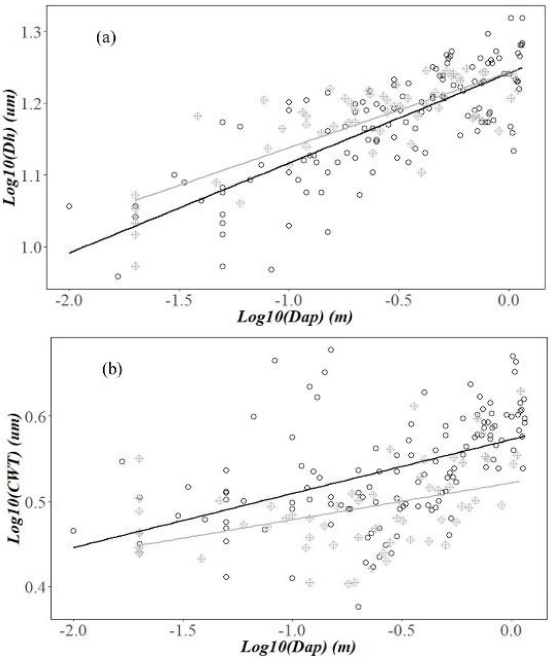

Figure 2: (a) Apical tracheid hydraulic diameter (*Dh*) against the distance from the stem apex (*Dap*) in dead (black) and alive (gray) *P. nigra*. **(b)** Apical tracheid cell wall thichness (*CWT*) against the distance from the stem apex (*Dap*) in dead (black) and alive (gray) *P. nigra* for the apical part.

These results belong to an individual study conducted in our group.

Chapter 8. Overall conclusion

Ongoing climatic changes impose limitations to tree growth and affect tree vigor. In this thesis, several independent studies were presented aiming to investigate how trees respond under different environmental conditions. The research questions answered in this thesis were related to the xylem and phloem anatomical traits and the allocation of biomass at the intraspecific level, the interspecific level and between declining/dead and non-declining/alive trees.

A positive carbon balance is crucial for tree survival. Under dry conditions trees have lower growth rates since the necessary resources are limited (e.g. Weemstra et al. 2013). These reduced growth rates allow for less carbon costs possibly being significant in the maintenance of the carbon balance since the stomata are open for a shorter period reaching the minimum leaf water potential earlier during the day.

In Chapter 2, we showed that *T. platyphyllos* - a relatively anisohydric species that maintains transpiration even under lower soil water potentials - produced less biomass with decreasing soil water availability. Nevertheless, under the same study, the relatively isohydric *P. sylvestris* produced a higher leaf biomass for a given amount of stem and branch biomass to compensate for the reduced time of stomata opening by having more needles and thus an efficient carbon uptake.

The maintenance of a positive carbon balance is linked to an efficient carbon uptake. Trees in order to sustain transpiration need an efficient water transport from roots to leaves; however, water transport efficiency is reduced under drought. According to the results of the Chapters 3, 6, and 7 included in this thesis, trees produce wider xylem cells near the stem apex under drier conditions to compensate for the reduced efficiencies at a relatively low cost of carbon for cell production. To produce more narrower and thicker cells costs more than producing fewer wider and thinner cells. These results were in contrast to earlier studies demonstrating that trees produce narrower conduits (and thus safer in terms of embolism vulnerability) in dry conditions to maintain a safe transport system (e.g. von Arx et al. 2012; Pfautsch et al. 2016). However, these studies did not look at the axial scaling of plant traits. Our results suggest that a few wider conduits near the stem apex, would allow for an efficient water transport to sustain transpiration at a reduced cost of carbon for cell production.

Plant carbon balance also depends on the transportation of sugars from the sources to the sinks. Dry conditions impose also limitations to sugar transportation since the phloem viscosity is higher. Therefore, it could

be expected that a higher phloem conductivity would be needed to transfer efficiently the necessary amount of sugars at a given time under drought. Indeed, in Chapter 3 of this thesis, *Fraxinus ornus* trees produced wider phloem sieve elements when growing at sites with lower soil water availability to compensate for the higher phloem viscosity.

Similar adjustments were also found as survival strategies in declining *Pinus sylvestris* trees that produced more efficient xylem and phloem (Chapter 6), and in the vigorous *Pinus nigra* tree when compared to a dead one (Chapter 7). Briefly, our results demonstrate that under drier conditions, when the resources are limited, the only way for a tree to survive might be to produce more efficient water transport system at a reduced cost of carbon for production, even if this decreases the hydraulic safety risking for a higher vulnerability to embolism formation.

Since plants operate close to their limits of hydraulic functionality, supposedly they can recover embolised conduits. In Chapter 4, a link between parenchyma fraction and vulnerability to embolism in angiosperms were presented, suggesting that parenchyma has a role in the embolism recovery process. In Chapter 7, the ability of angiosperm branches to recover from 50% loss of conductivity was subsequently tested and was linked to their parenchyma fraction, as well as the presence of the phloem. Possibly species prioritize in hydraulic efficiency since they are able to risk for embolism vulnerability as they can recover the embolised conduits.

Additionally, the scaling relationships in all related chapters showed that cell widening is quite rigid across different levels of soil water availability. The scaling exponents where similar to those reported in previous literature (Anfodillo et al. 2013). Considering conduit widening, in Chapter 5 it is shown that the most of the plant's hydraulic resistance is concentrated in the leaves, where the water potentials are highly negative, maintaining a quite safe water transport near the transpiring leaves, while the water status of the stem depends on soil conditions.

Concisely, according to the results of the studies presented in this thesis, trees invest in biomass according to their needs and adjust their anatomical characteristics to maintain the efficiency of the transport systems. However, the allometric relationships between traits are very similar across different conditions. This thesis provides valuable input to our current understanding of tree growth responses to droughts and

particularly as regards the tree water and sugar transportations. Future similar studies are highly recommended especially considering the axial trends of plant traits.

Additional information
Chapter 3.

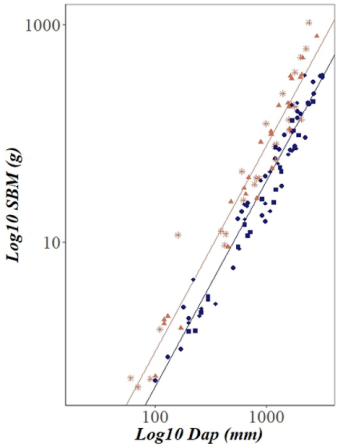

Supplementary Figure 1. Stem and branch mass (*SBM*, g) against the distance from the stem apex (*Dap*, mm) across the different sites. Blue colour for wet and orange for dry sites. Site symbols are shown in Table 1.

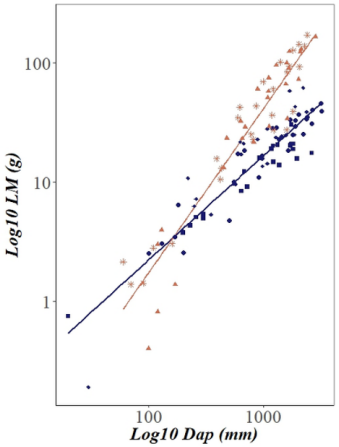

Supplementary Figure 2. Leaf mass (*LM*, g) against the distance from the stem apex (*Dap*, mm) across the different sites. Blue colour for wet and orange for dry sites. Site symbols are shown in Table 1.

Chapter 4.

For Supplementary: Tables: 1,2 and Figures: 1,2,3,4 please look online in Tree Physiology.

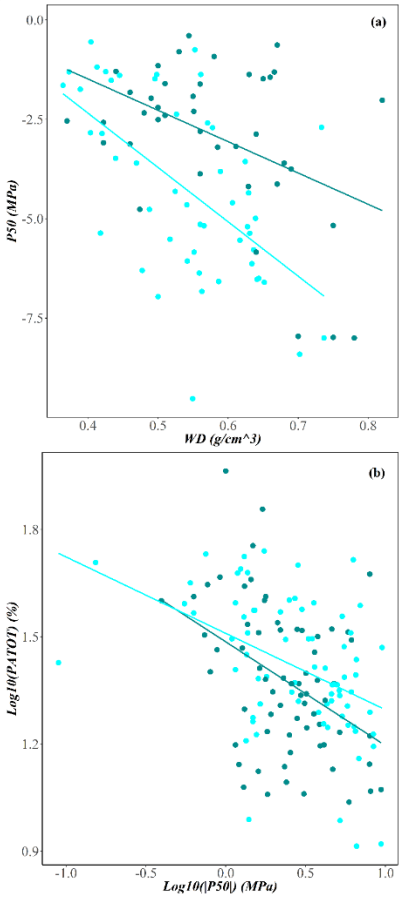

Supplementary Figure 5. (a) Vulnerability to embolism (*P50*) against the Wood Density (*WD*) for angiosperms of our dataset in light cyan and global dataset in dark cyan color. **(b)** *P50* against the total parenchyma amount (PA_{TOT}) for angiosperm of our dataset in light cyan and global dataset in dark cyan color.

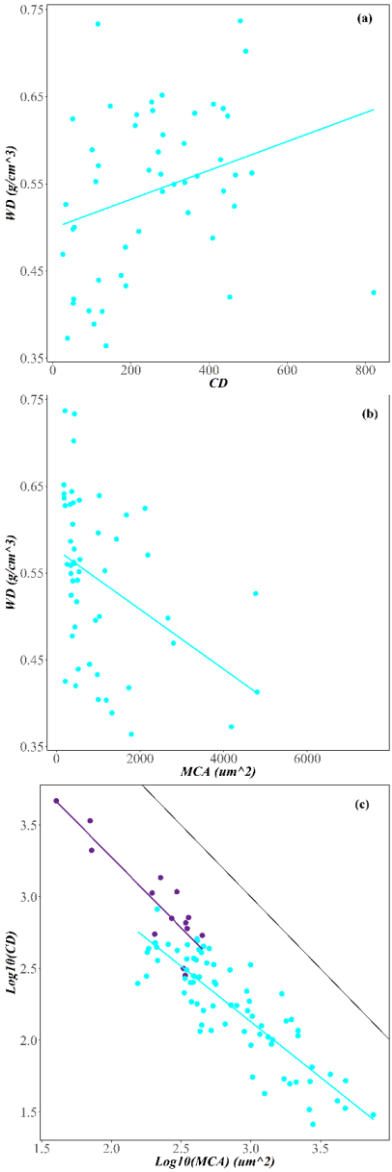

Supplementary Figure 6. (a) Wood Density (*WD*) against the Conduit Density (CD) for angiosperm species. **(b)** Wood Density (*WD*) against Mean Conduit Area (*MCA*) for angiosperm species. **(c)** Conduit Density (*CD*) against the Mean Conduit Area (*MCA*) for angiosperms in light cyan and gymnosperms in dark purple. The black line represents the xylem packing.

Acknowledgements

I would like to thank my supervisor, Giai Petit for his support, guidance, collaboration, and his fruitful ideas. I have learnt a lot from Giai. I am thanking Jozica Gricar and Lenka Plavkova for their time reviewing this thesis and for their positive comments. I appreciated the collaboration and support of Andrea Nardini, and the collaboration and encouragement of Patrizia Trifilò, with whom we had an amazing "crazy" time in the lab doing hydraulic experiments. I am also thanking Elisabeth Robert, Jordi Martínez-Vilalta, and Mauricio Mencuccini. I welcomed the collaboration of Lucía Galiano-Pérez, Georg von Arx, and Arthur Gessler and the other co-authors. Thanks to Vinicio Carraro and Enrico Marcolin for some help in the lab. A special thanks to Angela for all her company, for her help in lab work and questions about analysis in ROXAS in the beginning of my PhD, considering that she was under time pressure as she was submitting her PhD thesis, and for her suggestion to add some anatomical images at the end of this thesis. Thanks also to my office mates Silvia, Gaia, Arturo, Giacomo for their company. Moreover, I am thanking Francesco Petruzzellis for his help in the sampling of *Fraxinus ornus* trees, for his statistical advices on our paper, and the positive thinking on our paper. I am grateful also to Tadeja Savi for our short collaboration, her prompt and positive replies. I would like to thank the students Luca and Brigita for all the work they have done. Lastly, warm thanks to my parents and brother for their care, comprehension, and for all their moral support during these years. Huge special thanks to Ilias for his care, affection, and especially for his patience. Thank you!

Anatomical images
Chapter 3.

Figure 2. Transverse micro section of *Fraxinus ornus* focused on the phloem.

Figure 1. Transverse micro section of *Fraxinus ornus*.

Chapter 4.

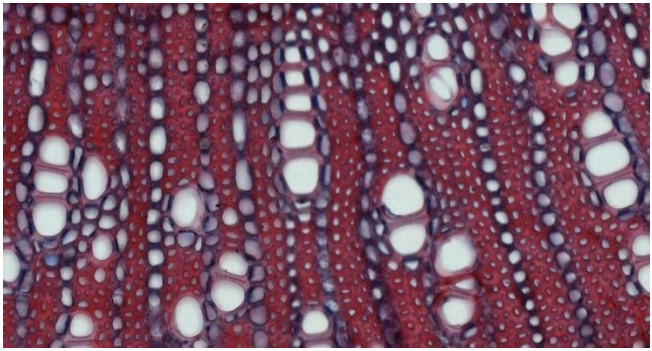

Figure 1. Transverse micro section of *Olea europaea*.

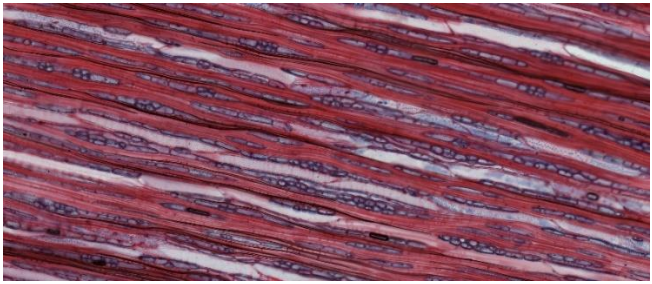

Figure 2. Tangential micro section of *Olea europaea*.

Chapter 5.

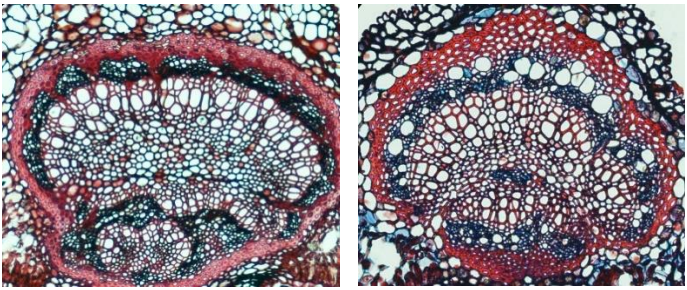

Figure 1. Left: Leaf micro section of *Fagus sylvatica*.
Right: Leaf microsection of *Acer pseudoplatanus*.

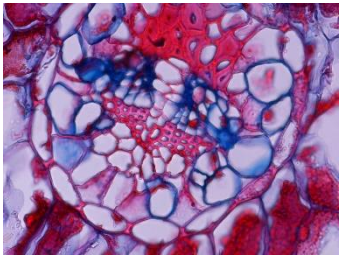

Figure 2. Needle micro section of *Picea abies.*

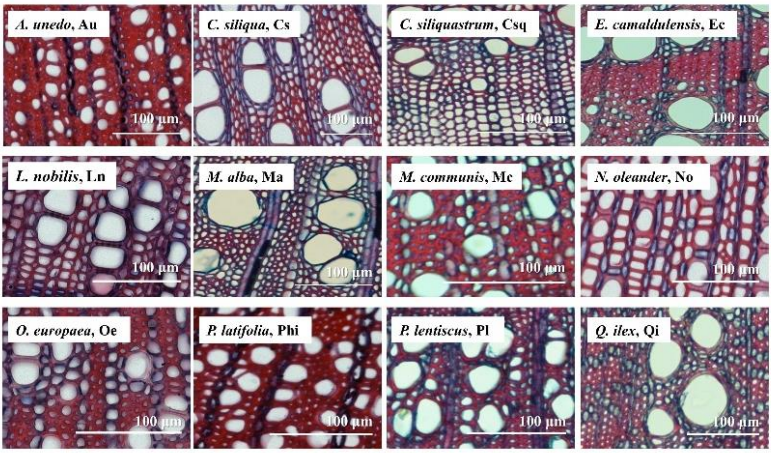

Figure 1. Transverse micro sections of 12 angiosperm species in Messina, Sicily. Scale bars at 100 µm.

Literature cited

Chapter 1.

Allen CD, Macalady AK, Chenchouni H, Bachelet D, McDowell N, Vennetier M, … Gonzalez P (2010) A global overview of drought and heat-induced tree mortality reveals emerging climate change risks for forests. Forest Ecol Manag 259: 660–684.

Anderegg WR, Konings AG, Trugman AT, Yu K, Bowling DR, Gabbitas R, ... Zenes N (2018) Hydraulic diversity of forests regulates ecosystem resilience during drought. Nature 561: 538.

Anfodillo T, Petit G, Crivellaro A (2013) Axial conduit widening in woody species: A still neglected anatomical pattern. IAWA J 34: 352–364.

Anfodillo T, Petit G, Sterck F, Lechthaler S, Olson ME (2016) Allometric trajectories and "stress": A quantitative approach. Front Plant Sci 7: 1681-1687.

Attia Z, Domec JC, Oren R, Way DA, Moshelion M (2015) Growth and physiological responses of isohydric and anisohydric poplars to drought. J Exp Bot 66: 4373-4381.

Brodersen C, McElrone A (2013) Maintenance of xylem network transport capacity: a review of embolism repair in vascular plants. Front Plant Sci 4: 108.

Choat B, Brodribb TJ, Brodersen CR, Duursma RA, López R, Medlyn BE (2018) Triggers of tree mortality under drought. Nature 558: 531.

Choat B, Jansen S, Brodribb TJ, Cochard H, Delzon S, Bhaskar R, … Zanne AE (2012) Global convergence in the vulnerability of forests to drought. Nature, doi: https://doi.org/10.1038/nature11688

De Schepper V, De Swaef T, Bauweraerts I, Steppe K (2013) Phloem transport: a review of mechanisms and controls. J Exp Bot 64: 4839-4850. doi: 10.1093/jxb/ert302

Dixon HH, Joly J (1895) On the ascent of sap. Philosophical Transactions of the Royal Society (London) 57B: 563.

Hacke UG, Sperry JS (2001) Functional and ecologycal xylem anatomy. Persp Plant Ecol Evol System 4: 97–115.

Hartmann H, Moura CF, Anderegg WR, Ruehr NK, Salmon Y, Allen CD, ... Ruthrof KX (2018) Research frontiers for improving our understanding of drought-induced tree and forest mortality. New Phytol 218: 15-28.

Hölttä T, Vesala T, Sevanto S, Perämäki M, Nikinmaa E (2006) Modeling xylem and phloem water flows in trees according to cohesion theory and Münch hypothesis. Trees 20: 67-78. doi: 10.1007/s00468-005-0014-6

IPCC (2014) Climate Change 2014- Impacts, Adaptation, and Vulnerability: Regional Aspects. Cambridge University Press.

Jensen KH, Liesche J, Bohr T, Schulz A (2012) Universality of phloem transport in seed plants. Plant, Cell & Environment 35: 1065-1076. doi:10.1111/j.1365-3040.2011.02472.x

Lack AJ, Evans DE (2005) Plant Biology. Garland Science.

Larter M, Pfautsch S, Domec J, Trueba S, Nagalingum N, Delzon S (2017) Aridity drove the evolution of extreme embolism resistance and the radiation of conifer genus *Callitris*. New Phytol 215: 97-112.

Martínez-Vilalta J, Garcia-Forner N (2017) Water potential regulation, stomatal behaviour and hydraulic transport under drought : deconstructing the iso/anisohydric concept. Plant Cell Environ 40: 962–976.
McDowell NG (2011) Mechanisms linking drought, hydraulics, carbon metabolism, and vegetation mortality. Plant Physiol 155: 1051-1059.
Mcdowell N, Pockman WT, Allen CD, Breshears DD, Cobb N, Kolb T, … Yepez EA (2008) Mechanisms of Plant Survival and Mortality during Drought : Why Do Some Plants Survive while Others Succumb to Drought ? New Phytol 178: 719–739.
Nardini A, Salleo S (2000) Limitation of stomatal conductance by hydraulic traits: sensing or preventing xylem cavitation? Trees 15: 14–24.
Petit G, Crivellaro A (2014) Comparative axial widening of phloem and xylem conduits in small woody plants. Trees 28: 915-921. doi: 10.1007/s00468-014-1006-1
Pfautch S, Harbusch M, Wesolowski A, Smith R, Macfarlane C, Tjoelker MG, Reich PB, Adams MA (2016) Climate determines vascular traits in the ecologically diverse genus *Eucalyptus*. Ecol Lett 19: 240–248.
Pratt RB, Ewers FW, Lawson MC, Jacobsen AL, Brediger MM, Davis SD (2005) Mechanisms for tolerating freeze–thaw stress of two evergreen chaparral species: Rhus ovata and Malosma laurina (Anacardiaceae). Am J Bot 92: 1102-1113.
Reich PB, Sendall KM, Stefanski A, Rich RL, Hobbie SE, Montgomery RA (2018) Effects of climate warming on photosynthesis in boreal tree species depend on soil moisture. Nature 562: 263.
Savage JA, Clearwater MJ, Haines DF, Klein T, Mencuccini M, Sevanto S, Turgeon R, Zhang C (2016) Allocation, stress tolerance and carbon transport in plants: how does phloem physiology affect plant ecology? Plant Cell Environ 39: 709-725. doi:10.1111/pce.12602
von Arx G, Archer SR, Hughes MK (2012) Long-term functional plasticity in plant hydraulic architecture in response to supplemental moisture. Annals Bot 109: 1091–1100.
Zwieniecki MA, Holbrook NM (2009) Confronting Maxwell's demon: biophysics of xylem embolism repair. Trends Plant Sci 14: 530–534.

Chapter 2.

Aguadé D, Poyatos R, Gómez M, Oliva J, Martínez-Vilalta J (2015) The role of defoliation and root rot pathogen infection in driving the mode of drought-related physiological decline in Scots pine (*Pinus sylvestris* L.). Tree physiol 35: 229-242.
Allen CD, Macalady AK, Chenchouni H et al (2010) A global overview of drought and heat-induced tree mortality reveals emerging climate change risks for forests. For Ecol Manage 259: 660-684.
Anfodillo T, Petit G, Crivellaro A (2013) Axial conduit widening in woody species: A still neglected anatomical pattern. IAWA J 34: 352-364.
Anfodillo T, Petit G, Sterck F, Lechthaler S, Olson ME (2016) Allometric trajectories and "stress": A quantitative approach. Front Plant Sci 7: 1681-1687.
Attia Z, Domec JC, Oren R, Way DA, Moshelion M (2015) Growth and physiological responses of isohydric and anisohydric poplars to drought. J Exp Bot 66: 4373-4381.

Becker P, Gribben RJ, Lim CM (2000) Tapered conduits can buffer hydraulic conductance from path-length effects. Tree Physiol 20: 965-967.
Brunner I, Herzog C, Dawes MA, Arend M, Sperisen C (2015) How tree roots respond to drought. Front Plant Sci 6: 547.
De Micco V, Aronne G (2012) Morpho-anatomical traits for plant adaptation to drought, In Plant Responses to Drought Stress. Springer, Heidelberg pp. 37-62.
Galiano L, Timofeeva G, Saurer M, Siegwolf R, Martínez-Vilalta J, Hommel R, Gessler A (2017) The fate of recently fixed carbon after drought release: towards unravelling C storage regulation in *Tilia platyphyllos* and *Pinus sylvestris*. Plant Cell Environ 40: 1711-1724.
Hacke UG, Spicer R, Schreiber SG, Plavcová L (2017) An ecophysiological and developmental perspective on variation in vessel diameter. Plant Cell Environ 40: 831-845.
Hacke UG, Sperry JS (2001) Functional and ecological xylem anatomy. Per Plant Ecol Evol System 4: 97-115.
IPCC (2014) Climate Change 2014- Impacts, Adaptation, and Vulnerability: Regional Aspects. Cambridge University Press.
Irvine J, Perks MP, Magnani F, Grace J (1998) The response of *Pinus sylvestris* to drought: stomatal control of transpiration and hydraulic conductance. Tree Physiol 18: 393-402.
Jump AS, Penuelas J (2005) Running to stand still : adaptation and the response of plants to rapid climate change. Ecol Lett 8: 1010-1020.
Larter M, Pfautsch S, Domec JC, Trueba S, Nagalingum N, Delzon S (2017) Aridity drove the evolution of extreme embolism resistance and the radiation of conifer genus Callitris. New Phytol 215: 97-112.
Lens F, Baas P, Jansen S, Smets E (2007) A search for phylogenetically informative wood characters within Lecythidaceae sl. Am J Bot 94: 483-502.
Leuzinger S, Zotz G, Asshoff R, Körner C (2005) Responses of deciduous forest trees to severe drought in Central Europe. Tree Physiol 25: 641-650.
Martínez-Vilalta J, Garcia-Forner N (2017) Water potential regulation, stomatal behaviour and hydraulic transport under drought: deconstructing the iso/anisohydric concept. Plant Cell Environ 40: 962-976.
Maseda PH, Fernández RJ (2016) Growth potential limits drought morphological plasticity in seedlings from six Eucalyptus provenances. Tree Physiol 36: 243-251.
McDowell N, Pockman WT, Allen CD et al (2008) Mechanisms of plant survival and mortality during drought: Why do some plants survive while others succumb to drought? New Phytol 178: 719-739.
McDowell NG (2011) Mechanisms linking drought, hydraulics, carbon metabolism, and vegetation mortality. Plant Physiol 155: 1051-1059.
Mencuccini M, Hölttä T, Petit G, Magnani F (2007) Sanio's laws revisited. Size-dependent changes in the xylem architecture of trees. Ecol Lett 10: 1084-1093.
Mencuccini M (2014) Temporal scales for the coordination of tree carbon and water economies during droughts. Tree Physiol 34: 439-442.
Menzel A, Fabian P (1999) Growing season extended in Europe. Nature 397: 659.
Mitchell PJ, O'Grady AP, Tissue DT, White DA, Ottenschlaeger ML, Pinkard EA (2013) Drought response strategies define the relative contributions of hydraulic dysfunction and carbohydrate depletion during tree mortality. New Phytol 197: 862-872.

Mitchell PJ, O'Grady AP, Tissue DT, Worledge D, Pinkard EA (2014) Co-ordination of growth, gas exchange and hydraulics define the carbon safety margin in tree species with contrasting drought strategies. Tree Physiol 34: 443-458.
Olson ME, Anfodillo T, Rosell JA et al (2014) Universal hydraulics of the flowering plants: Vessel diameter scales with stem length across angiosperm lineages, habits and climates. Ecol Lett 17: 988-997.
Petit G, Anfodillo T (2009) Plant physiology in theory and practice: An analysis of the WBE model for vascular plants. J Theor Biol 259: 1-4.
Petit G, Anfodillo T (2011) Comment on "The blind men and the elephant: the impact of context and scale in evaluating conflicts between plant hydraulic safety and efficiency" by Meinzer et al. (2010). Oecologia 165: 271-274.
Petit G, Anfodillo T, Carraro V, Grani F, Carrer M (2011) Hydraulic constraints limit height growth in trees at high altitude. New Phytol 189: 241-252.
Petit G, Savi T, Consolini M, Anfodillo T, Nardini A (2016) Interplay of growth rate and xylem plasticity for optimal coordination of carbon and hydraulic economies in Fraxinus ornus trees. Tree Physiol 36: 1310-1319.
Pfautch S, Harbusch M, Wesolowski A, Smith R, Macfarlane C, Tjoelker MG, Reich PB, Adams MA (2016) Climate determines vascular traits in the ecologically diverse genus Eucalyptus. Ecol Lett 19: 240-248.
Prendin AL, Petit G, Fonti P, Rixen C, Dawes MA, von Arx G (2018) Axial xylem architecture of Larix decidua exposed to CO2 enrichment and soil warming at the treeline. Funct Ecol 32: 273-287.
Reich PB, Tjoelker MG, Pregitzer KS, Wright IJ, Oleksyn J, Machado JL (2008) Scaling of respiration to nitrogen in leaves, stems and roots of higher land plants. Ecol Lett 11: 793-801.
Rosell JA, Olson ME, Anfodillo T (2017) Scaling of xylem vessel diameter with plant size: Causes, predictions, and outstanding questions. Current Forestry Reports 3: 46-59.
Rossi S, Deslauriers A, Anfodillo T, Morin H, Saracino A, Motta R, Borghetti M (2006) Conifers in cold environments synchronize maximum growth rate of tree-ring formation with day length. New phytol 170: 301-310.
Schweingruber FH (1990) Microscopic wood anatomy: structural variability of stems and twigs in recent and subfossil woods from Central Europe. Swiss Federal Institute for Forest, Snow and Landscape Research.
Sterck F, Zweifel R (2016) Trees maintain a similar conductance per leaf area through integrated responses in growth, allocation, architecture and anatomy. Tree Physiol 36: 1307-1309.
Tyree MT, Ewers FW (1991) The hydraulic architecture of trees and other woody plants. New Phytol 119: 345-360.
von Arx G, Dietz H (2005) Automated image analysis of annual rings in the roots of perennial forbs. Int J Plant Sci 166: 723-732.
von Arx G, Archer SR, Hughes MK (2012) Long-term functional plasticity in plant hydraulic architecture in response to supplemental moisture. Ann Bot 109: 1091-1100.
von Arx G, Carrer M (2014) ROXAS -A new tool to build centuries-long tracheid-lumen chronologies in conifers. Dendrochronologia 32: 290-293.
von Arx G, Crivellaro A, Prendin AL, Čufar K, Carrer M (2016) Quantitative wood anatomy- practical guidelines. Front Plant Sci 7: 781.

Weiner J (2004) Allocation, plasticity and allometry in plants. Perspect Plant Ecol Syst 6: 207–215.
West GB, Brown JH, Enquist BJ (1999) A general model for the structure and allometry of plant vascular systems. Nature 400: 664-667.
Wheeler JK, Sperry JS, Hacke UG, Hoang N (2005) Inter-vessel pitting and cavitation in woody Rosaceae and other vesselled plants: a basis for a safety versus efficiency trade-off in xylem transport. Plant Cell Environ 28: 800-812.
Yang S, Tyree MT (1993) Hydraulic resistance in Acer saccharum shoots and its influence on leaf water potential and transpiration. Tree Physiol 12: 231-242.
Zar JH (1999) Biostatistical Analysis. Pearson Education India.

Chapter 3.

Anfodillo T, Carraro V, Carrer M, Fior C, Rossi S (2006) Convergent tapering of xylem conduits in different woody species. New Phytol 169: 279-290. doi: 10.1111/j.1469-8137.2005.01587.x
Anfodillo T, Petit G, Crivellaro A (2013) Axial conduit widening in woody species: a still neglected anatomical pattern. IAWA 34: 352-364. doi: 10.1163/22941932-00000030
Anfodillo T, Petit G, Sterck F, Lechthaler S, Olson ME (2016) Allometric trajectories and "stress": a quantitative approach. Frontiers in Plant Science 7: doi: 10.3389/fpls.2016.01681
Aston MJ, Lawlor DW (1979) The relationship between transpiration, root water uptake, and leaf water potential. J Exp Bot 30: 169-181. doi: 10.1093/jxb/30.1.169
Brodersen CR, McElrone AJ (2013) Maintenance of xylem Network Transport Capacity: A Review of Embolism Repair in Vascular Plants. Front Plant Sci 4: 1-11. doi:10.3389/fpls.2013.00108
Cai J, Tyree MT (2010) The impact of vessel size on vulnerability curves: data and models for within-species variability in saplings of aspen, Populus tremuloides Michx. Plant Cell Environ 33: 1059-1069. doi: 10.1111/j.1365-3040.2010.02127.x
De Micco V, Aronne G (2012) Morpho-anatomical traits for plant adaptation to drought, In Plant Responses to Drought Stress. Springer, Heidelberg pp. 37-62.
De Schepper V, De Swaef T, Bauweraerts I, Steppe K (2013) Phloem transport: a review of mechanisms and controls. J Exp Bot 64: 4839-4850. doi: 10.1093/jxb/ert302
Evert RF (1990) Dicotyledons. In *Sieve elements* (pp. 103-137). Springer, Berlin, Heidelberg
Franks PJ, Cowan IR, Farquhar GD (1998) A study of stomatal mechanics using the cell pressure probe. Plant Cell Environ 21: 94-100. doi:10.1046/j.1365-3040.1998.00248.x
Gortan E, Nardini A, Gascó A, Salleo S (2009) The hydraulic conductance of Fraxinus ornus leaves is constrained by soil water availability and coordinated with gas exchange rates. Tree Physiol 29: 529-539. doi: 10.1093/treephys/tpn053
Hacke UG, Sperry JS, Pockman WT, Davis SD, McCulloch KA (2001) Trends in wood density and structure are linked to prevention of xylem implosion by negative pressure. Oecologia 126: 457-461. doi: 10.1007/s004420100628

Hacke UG, Spicer R, Schreiber SG, Plavcová L (2017) An ecophysiological and developmental perspective on variation in vessel diameter. Plant, Cell & Environment 40: 831-845. doi: 10.1111/pce.12777

Hölttä T, Mencuccini M, Nikinmaa E (2009) Linking phloem function to structure: Analysis with a coupled xylem-phloem transport model. J Theor Biol 259: 325-337. doi: 10.1016/j.jtbi.2009.03.039

Hölttä T, Vesala T, Sevanto S, Perämäki M, Nikinmaa E (2006) Modeling xylem and phloem water flows in trees according to cohesion theory and Münch hypothesis. Trees 20: 67-78. doi: 10.1007/s00468-005-0014-6

Jensen KH, Liesche J, Bohr T, Schulz A (2012) Universality of phloem transport in seed plants. Plant, Cell & Environment 35: 1065-1076. doi:10.1111/j.1365-3040.2011.02472.x

Jyske T, Hölttä T (2015) Comparison of phloem and xylem hydraulic architecture in *Picea abies* stems. New Phytol 205: 102-115. doi:10.1111/nph.12973

Kiorapostolou N, Galiano-Pérez L, von Arx G, Gessler A, Petit G (2018) Structural and anatomical responses of *Pinus sylvestris* and *Tilia platyphyllos* seedlings exposed to water shortage. Trees- Struct Funct: doi: 10.1007/s00468-018-1703-2

Klein T, Hoch G (2015) Tree carbon allocation dynamics determined using a carbon mass balance approach. New Phytol 205: 147-159. doi:10.1111/nph.12993

Larter M, Pfautsch S, Domec JC, Trueba S, Nagalingum N, Delzon S (2017) Aridity drove the evolution of extreme embolism resistance and the radiation of conifer genus Callitris. New Phytol 215: 97-112. doi: 10.1111/nph.14545

Lechthaler S, Turnbull T, Gelmini Y, Pirotti F, Anfodillo T, Adams MA, Petit G (2018) A standardization method to disentangle environmental information from axial trends of xylem anatomical traits. Tree Physiol: under revision

Lintunen A, Paljakka T, Jyske T, Peltoniemi M, Sterck F, Von Arx G, Cochard H, Copini P, Caldeira MC, Delzon S, Gebauer R, Grönlund L, Kiorapostolou N, Lechthaler S, Lobo-do-Vale R, Peters RL, Petit G, Prendin AL, Salmon Y, Steppe K, Urban J, Roig Juan S, Robert EMR, Hölttä T (2016) Osmolality and non-structural carbohydrate composition in the secondary phloem of trees across a latitudinal gradient in Europe. Front Plant Sci 7: doi: 10.3389/fpls.2016.00726

Maier CA (2001) Stem growth and respiration in loblolly pine plantations differing in soil resource availability. Tree Physiol 21: 1183-1193. doi: 10.1093/treephys/21.16.1183

Marron N, Dreyer E, Boudouresque E, Delay D, Petit JM, Delmotte FM, Brignolas F (2003) Impact of successive drought and re-watering cycles on growth and specific leaf area of two Populus×canadensis (Moench) clones, 'Dorskamp' and 'Luisa_Avanzo'. Tree physiology 23: 1225-1235. doi: 10.1093/treephys/23.18.1225

Mencuccini M, Höltta T, Petit G, Magnani F (2007) Sanio's laws revisited. Size-dependent changes in the xylem architecture of trees. Ecol Lett 10: 1084-1093. doi: 10.1111/j.1461-0248.2007.01104.x

Mencuccini M, Minunno F, Salmon Y, Martínez-Vilalta J, Hölttä T (2015) Coordination of physiological traits involved in drought-induced mortality of woody plants. New Phytol 208: 396-409. doi: doi:10.1111/nph.13461

Nardini A, Savi T, Losso A, Petit G, Pacilè S, Tromba G, Mayr S, Trifilò P, Lo Gullo MA, Salleo S (2017) X-ray microtomography observations of xylem embolism in stems of Laurus nobilis are consistent with hydraulic measurements of

percentage loss of conductance. New Phytol 213: 1068-1075. doi: 10.1111/nph.14245
Olson ME, Anfodillo T, Rosell JA, Petit G, Crivellaro A, Isnard S, León-Gómez C, Alvarado-Cárdenas LO, Castorena M (2014) Universal hydraulics of the flowering plants: vessel diameter scales with stem length across angiosperm lineages, habits and climates. Ecol Lett 17: 988-997. doi: 10.1111/ele.12302
Petit G, Anfodillo T (2009) Plant physiology in theory and practice: An analysis of the WBE model for vascular plants. J Theor Biol 259: 1-4. doi: 10.1016/j.jtbi.2009.03.007
Petit G, Crivellaro A (2014) Comparative axial widening of phloem and xylem conduits in small woody plants. Trees 28: 915-921. doi: 10.1007/s00468-014-1006-1
Petit G, Pfautsch S, Anfodillo T, Adams MA (2010) The challenge of tree height in Eucalyptus regnans: when xylem tapering overcomes hydraulic resistance. New Phytol 187: 1146-1153. doi: 10.1111/j.1469-8137.2010.03304.x
Petit G, Savi T, Consolini M, Anfodillo T, Nardini A (2016) Interplay of growth rate and xylem plasticity for optimal coordination of carbon and hydraulic economies in Fraxinus ornus trees. Tree Physiol 36: 1310-1319. doi: 10.1093/treephys/tpw069
Petit G, von Arx G, Kiorapostolou N, Lechthaler S, Prendin AL, Anfodillo T, Caldeira MC, Cochard H, Copini P, Crivellaro A, Delzon S, Gebauer R, Gričar J, Grönholm L, Hölttä T, Jyske T, Lavrič M, Lintunen A, Lobo do Vale R, Peltoniemi M, Peters RL, Robert EMR, Roig Juan S, Senfeldr M, Steppe K, Urban J, Van Camp J, Sterck F (2018) Tree differences in primary and secondary growth drive convergent scaling in leaf area to sapwood area across Europe. New Phytol 218: 1383-1392. doi: doi:10.1111/nph.15118
Pfautsch S, Harbusch M, Wesolowski A, Smith R, Macfarlane C, Tjoelker MG, Reich PB, Adams MA (2016) Climate determines vascular traits in the ecologically diverse genus Eucalyptus. Ecol Lett 19: 240-248. doi: 10.1111/ele.12559
Plavcová L, Hoch G, Morris H, Ghiasi S, Jansen S (2016) The amount of parenchyma and living fibers affects storage of nonstructural carbohydrates in young stems and roots of temperate trees. Am J Bot 103: 603-612. doi:10.3732/ajb.1500489
Prendin AL, Mayr S, Beikircher B, von Arx G, Petit G (2018a) Xylem anatomical adjustments prioritize hydraulic efficiency over safety as Norway spruce trees grow taller. Tree Physiol: accepted
Prendin AL, Petit G, Fonti P, Rixen C, Dawes MA, von Arx G (2018b) Axial xylem architecture of Larix decidua exposed to CO2 enrichment and soil warming at the tree line. Funct Ecol 32: 273-287. doi: 10.1111/1365-2435.12986
R Core Team (2017) R: A language and environment for statistical computing. R Foundation for Statistical Computing, Vienna, Austria. URL https://www.R-project.org/.
Savage JA, Beecher SD, Clerx L, Gersony JT, Knoblauch J, Losada JM, Jensen KH, Knoblauch M, Holbrook NM (2017) Maintenance of carbohydrate transport in tall trees. Nature Plants 3: 965-972. doi: 10.1038/s41477-017-0064-y
Savage JA, Clearwater MJ, Haines DF, Klein T, Mencuccini M, Sevanto S, Turgeon R, Zhang C (2016) Allocation, stress tolerance and carbon transport in plants: how does phloem physiology affect plant ecology? Plant Cell Environ 39: 709-725. doi:10.1111/pce.12602

Schindelin J, Arganda-Carreras I, Frise E, et al. (2012) Fiji: an open-source platform for biological-image analysis. Nature methods 9: 676-682, PMID 22743772, doi:10.1038/nmeth.2019

Sevanto S (2014) Phloem transport and drought. J Exp Bot 65: 1751-1759. doi: 10.1093/jxb/ert467

Sevanto S, Ryan M, Turin DL, Derome D, Patera A, Defraeye T, Pangle RE, Hudson PJ, Pockman WT (2018) Is desiccation tolerance and avoidance reflected in xylem and phloem anatomy of two co-existing arid-zone coniferous trees? Plant Cell Environ: doi:10.1111/pce.13198

Sperry JS, Stiller V, Hacke UG (2003) Xylem hydraulics and the soil–plant–atmosphere continuum. Agronomy Journal 95: 1362-1370. doi: 10.2134/agronj2003.1362

Sterck F, Zweifel R (2016) Trees maintain a similar conductance per leaf area through integrated responses in growth, allocation, architecture and anatomy. Tree Physiol 36: 1307-1309. doi: 10.1093/treephys/tpw100

Thompson MV, Holbrook NM (2003) Scaling phloem transport: water potential equilibrium and osmoregulatory flow. Plant Cell Environ 26: 1561-1577. doi: 10.1046/j.1365-3040.2003.01080.x

Tyree MT, Ewers FW (1991) The hydraulic architecture of trees and other woody plants. New Phytol 119: 345-360. doi: 10.1111/j.1469-8137.1991.tb00035.x

Venturas MD, Sperry JS, Hacke UG (2017) Plant xylem hydraulics: What we understand, current research, and future challenges. J Integr Plant Biol 59: 356-389. doi: 10.1111/jipb.12534

von Arx G, Archer SR, Hughes MK (2012) Long-term functional plasticity in plant hydraulic architecture in response to supplemental moisture. Ann Bot 109: 1091-1100. doi: 10.1093/aob/mcs030

von Arx G, Carrer M (2014a) ROXAS - a new tool to build centuries-long tracheid-lumen chronologies in conifers. Dendrochronologia 32: 290-293. doi:

von Arx G, Carrer M (2014b) ROXAS – A new tool to build centuries-long tracheid-lumen chronologies in conifers. Dendrochronologia 32: 290-293. doi: https://doi.org/10.1016/j.dendro.2013.12.001

von Arx G, Crivellaro A, Prendin AL, Čufar K, Carrer M (2016) Quantitative wood anatomy- practical guidelines. Front Plant Sci 7: 781. doi: 10.3389/fpls.2016.00781

Wright, I. J., Reich, P. B., & Westoby, M. (2001). Strategy shifts in leaf physiology, structure and nutrient content between species of high- and low-rainfall and high- and low-nutrient habitats. Funct Ecol 15: 423-434. doi: 10.1046/j.0269-8463.2001.00542.x

Chapter 4.

Becker P, Gribben RJ, Schulte PJ (2003) Incorporation of transfer resistance between tracheary elements into hydraulic resistance models for tapered conduits. Tree Physiol 23: 1009–1019.

Brodersen CR, McElrone AJ (2013) Maintenance of xylem Network Transport Capacity: A Review of Embolism Repair in Vascular Plants. Front Plant Sci. doi: https://doi.org/10.3389/fpls.2013.00108

Chave J, Coomes D, Jansen S, Lewis SL, Swenson NG, Zanne AE (2009) Towards a worldwide wood economics spectrum. Ecol Lett 12: 351–366.

Choat B, Nolf M, Lopez R, Peters JM, Carins-Murphy MR, Creek D, Brodribb TJ (2018) Non-invasive imaging shows no evidence of embolism repair after drought in tree species of two genera. Tree Physiol 39: 113-121.

Choat B, Jansen S, Brodribb TJ, Cochard H, Delzon S, Bhaskar R, … Zanne AE (2012) Global convergence in the vulnerability of forests to drought. Nature, doi: https://doi.org/10.1038/nature11688

Christman MA, Sperry JS, Smith DD (2012) Rare pits, large vessels and extreme vulnerability to cavitation in a ring-porous tree species. New Phytol. doi: https://doi.org/10.1111/j.1469-8137.2011.03984.x

Cochard H, Badel E, Herbette S, Delzon S, Choat B, Jansen S (2013) Methods for measuring plant vulnerability to cavitation: a critical review. J Exp Bot 64: 4779-4791.

Cochard H, Delzon S (2013) Hydraulic failure and repair are not routine in trees. Ann For Sci 70: 659–661.

Cochard H, Tyree MT (1990) Xylem dysfunction in Quercus: vessel sizes, tyloses, cavitation and seasonal changes in embolism. Tree Physiol 6: 393–407.

Creek D, Blackman CJ, Brodribb TJ, Choat B, Tissue DT (2018) Coordination between leaf, stem, and root hydraulics and gas exchange in three arid-zone angiosperms during severe drought and recovery. Plant Cell Environ 41: 2869-2881.

Domec JC, Scholz FG, Bucci SJ, Meinzer FC, Goldstein G, Villalobos-Vega R (2006) Diurnal and seasonal variation in root xylem embolism in neotropical savanna woody species: impact on stomatal control of plant water status. Plant Cell Environ 29: 26–35.

Duursma R, Choat B (2017) fitplc - an R package to fit hydraulic vulnerability curves. J Plant Hydraul. doi: https://doi.org/10.20870/jph.2017.e002

Ennajeh M, Simões F, Khemira H, Cochard H (2011) How reliable is the double-ended pressure sleeve technique for assessing xylem vulnerability to cavitation in woody angiosperms? Physiol Plant 142: 205–210.

Fox J, Bouchet-Valat M (2018) Rcmdr: R Commander. R package version 2.4-4.

Fox J (2017) Using the R Commander: A Point-and-Click Interface or R. Boca Raton FL: Chapman and Hall/CRC Press.

Fox J (2005) The R Commander: A Basic Statistics Graphical User Interface to R. J Stat Soft 14: 1-42.

Hacke UG, Sperry JS (2001) Functional and ecologycal xylem anatomy. Persp Plant Ecol Evol System 4: 97–115.

Hacke UG, Sperry JS, Pockman WT, Davis SD, McCulloh KA (2001) Trends in wood density and structure are linked to prevention of xylem implosion by negative pressure. Oecologia 126: 457–461.

Hacke UG, Sperry JS, Wheeler JK, Castro L (2006) Scaling of angiosperm xylem structure with safety and efficiency. Tree Physiol 26: 689–701.

Hacke UG, Venturas MD, MacKinnon ED, Jacobsen AL, Sperry JS, Pratt RB (2015) The standard centrifuge method accurately measures vulnerability curves of long-vesselled olive stems. New Phytol 205: 116-127.

Hacke UG, Spicer R, Schreiber SG, Plavcová L (2017) An ecophysiological and developmental perspective on variation in vessel diameter. Plant Cell Environ 40: 831-845.

Jacobsen AL, Ewers FW, Brandon Pratt R, Paddock III WA, Davis SD (2005) Do Xylem Fibers Affect Vessel Cavitation Resistance? Plant Physiol 139: 546–556.

Jacobsen AL, Pratt RB, Venturas MD, Hacke UW (2019) Large volume vessels are

vulnerable to water-stress-induced embolism in stems of poplar. IAWA. doi: 10.1163/22941932-40190233
Jacobsen AL, Pratt RB (2012) No evidence for an open vessel effect in centrifuge-based vulnerability curves of a long-vesselled liana (*Vitis vinifera*). New Phytol 194: 982-990.
Johnson KM, Jordan GJ, Brodribb TJ (2018) Wheat leaves embolized by water stress do not recover function upon rewatering. Plant Cell Environ 41: 2704-2714.
Johnson DM, McCulloh KA, Woodruff DR, Meinzer FC (2012) Hydraulic safety margins and embolism reversal in stems and leaves: Why are conifers and angiosperms so different? Plant Sci. doi: https://doi.org/10.1016/j.plantsci.2012.06.010
Jupa R, Plavcová L, Gloser V, Jansen S (2016) Linking xylem water storage with anatomical parameters in five temperate tree species. Tree Physiol 36: 756-769.
Klein T, Zeppel M, Anderegg W, Bloemen J, De Kauwe M, Hudson P, … Nardini A (2018) Xylem embolism refilling and resilience against drought-induced mortality in woody plants: Processes and trade-offs. Ecol Res. doi: https://doi.org/10.1007/s11284-018-1588-y
Lachenbruch B, McCulloh KA (2014) Traits, properties, and performance: how woody plants combine hydraulic and mechanical functions in a cell, tissue, or whole plant. New Phytol 204: 747–764.
Larter M, Pfautsch S, Domec J, Trueba S, Nagalingum N, Delzon S (2017) Aridity drove the evolution of extreme embolism resistance and the radiation of conifer genus Callitris. New Phytol215: 97–112.
Lazzarin M, Crivellaro A, Williams CB, Dawson TE, Mozzi G, Anfodillo T (2016) Tracheid and pit anatomy vary in tandem in a tall Sequoiadendron giganteum tree. IAWA J 37: 172–185.
Lechthaler S, Turnbull TL, Gelmini Y, Pirotti F, Anfodillo T, Adams MA, Petit G (2018) A standardization method to disentangle environmental information from axial trends of xylem anatomical traits. Tree Physiol. doi: https://doi.org/10.1093/treephys/tpy110
Lens F, Tixier A, Cochard H, Sperry JS, Jansen S, Herbette S (2013) Embolism resistance as a key mechanism to understand adaptive plant strategies. Curr Opin Plant Biol 16: 287–292.
Martínez-Cabrera HI, Jones CS, Espino S, Jochen Schenk H (2009) Wood anatomy and wood density in shrubs: Responses to varying aridity along transcontinental transects. Am J Bot 96: 1388–1398.
Martinez-Vilalta J, Mencuccini M, Alvarez X, Camacho J, Loepfe L, Pinol J (2012) Spatial distribution and packing of xylem conduits. Am J Bot 99: 1189–1196.
Mayr S, Schmid P, Laur J, Rosner S, Charra-Vaskou K, Damon B, Hacke UG (2014) Uptake of Water via Branches Helps Timberline Conifers Refill Embolized Xylem in Late Winter. Plant Physiol 164: 1731–1740.
Morris H, Plavcová L, Cvecko P, Fichtler E, Gillingham MAF, Martínez-Cabrera HI, … Jansen S (2016) A global analysis of parenchyma tissue fractions in secondary xylem of seed plants. New Phytol 209: 1553–1565.
Nardini A, Savi T, Trifilò P, Lo Gullo MA (2017) Drought Stress and the Recovery from Xylem Embolism in Woody Plants. Prog Bot. doi:https://doi.org/10.1007/124_2017_11
Nardini A, Lo Gullo MA, Salleo S (2011) Refilling embolized xylem conduits: Is it a matter of phloem unloading? Plant Sci 180: 604–611.

Nardini A, Salleo S (2000) Limitation of stomatal conductance by hydraulic traits: sensing or preventing xylem cavitation? Trees 15: 14–24.

Ogasa M, Miki NH, Murakami Y, Yoshikawa K (2013) Recovery performance in xylem hydraulic conductivity is correlated with cavitation resistance for temperate deciduous tree species. Tree Physiol 33: 335–344.

Petit G, Savi T, Consolini M, Anfodillo T, Nardini A (2016) Interplay of growth rate and xylem plasticity for optimal coordination of carbon and hydraulic economies in Fraxinus ornus trees. Tree physiol 36: 1310-1319.

Plavcova L, Hoch G, Morris H, Ghiasi S, Jansen S (2016) The amount of parenchyma and living fibers affects storage of nonstructural carbohydrates in young stems and roots of temperate trees. Am J Bot 103: 603–612.

Pratt RB, Jacobsen AL, Ewers FW, Davis SD (2007) Relationships among xylem transport, biomechanics and storage in stems and roots of nine Rhamnaceae species of the California chaparral. New Phytol 174: 787-798.

Pratt RB, Ewers FW, Lawson MC, Jacobsen AL, Brediger MM, Davis SD (2005) Mechanisms for tolerating freeze–thaw stress of two evergreen chaparral species: Rhus ovata and Malosma laurina (Anacardiaceae). Am J Bot 92: 1102-1113.

R Core Team (2017) R: A language and environment for statistical computing. R Foundation for Statistical
Computing, Vienna, Austria. URL: https://www.R-project.org/.

RStudio Team (2015) RStudio: Integrated Development for R. RStudio, Inc., Boston, MA URL http://www.rstudio.com/.

Rosner S, Heinze B, Savi T, Dalla-Salda G (2018) Prediction of hydraulic conductivity loss from relative water loss: new insights into water storage of tree stems and branches. Physiol Plant. doi: 10.1111/ppl.12790.

Rosner S (2017) Wood density as a proxy for vulnerability to cavitation: Size matters. J Plant Hydraul. doi: https://doi.org/10.20870/jph.2017.e001

Salleo S, Lo Gullo MA, Trifilò P, Nardini A (2004) New evidence for a role of vessel-associated cells and phloem in the rapid xylem refilling of cavitated stems of Laurus nobilis L. Plant Cell Environ 27: 1065–1076.

Savi T, Tintner J, Da Sois L, Grabner M, Petit G, Rosner S (2018) The potential of Mid-Infrared spectroscopy for prediction of wood density and vulnerability to embolism in woody angiosperms. Tree Physiol. doi:10.1093/treephys/tpy112

Schneider CA, Rasband WS, Eliceiri KW (2012) NIH Image to ImageJ: 25 years of image analysis. Nature methods 9: 671.

Secchi F, Pagliarani C, Zwieniecki MA (2017) The functional role of xylem parenchyma cells and aquaporins during recovery from severe water stress. Plant Cell Environ 40: 858–871.

Secchi F, Zwieniecki MA (2011) Sensing embolism in xylem vessels: The role of sucrose as a trigger for refilling. Plant Cell Environ 34: 514–524.

Sperry JS, Christman MA, Torres-Ruiz JM, Taneda H, Smith DD (2012) Vulnerability curves by centrifugation: is there an open vessel artefact, and are ‘r’shaped curves necessarily invalid? Plant Cell Environ 35: 601-610.

Sperry JS, Meinzer FC, McCulloh KA (2008) Safety and efficiency conflicts in hydraulic architecture: Scaling from tissues to trees. Plant Cell Environ 31: 632–645.

Sperry JS, Tyree MT (1988) Mechanism of Water Stress-Induced Xylem Embolism. Plant Physiol 88: 581–587.

Spicer R (2014) Symplasmic networks in secondary vascular tissues: parenchyma distribution and activity supporting long-distance transport. J Exper Bot 65: 1829–1848.

Tomasella M, Häberle KH, Nardini A, Hesse B, Machlet A, Matyssek R (2017) Post-drought hydraulic recovery is accompanied by non-structural carbohydrate depletion in the stem wood of Norway spruce saplings. Sci Rep 7: 14308.

Trifilò P, Kiorapostolou N, Petruzzellis F, Vitti S, Petit G, Gullo MAL, Nardini A & Casolo V (2019) Hydraulic recovery from xylem embolism in excised branches of twelve woody species: Relationships with parenchyma cells and non-structural carbohydrates. Plant Physiol Biochem. doi: https://doi.org/10.1016/j.plaphy.2019.04.013

Trifilò P, Nardini A, Lo Gullo MA, Barbera PM, Savi T, Raimondo F (2015) Diurnal changes in embolism rate in nine dry forest trees: relationships with species-specific xylem vulnerability, hydraulic strategy and wood traits. Tree Physiol 35: 694–705.

Tyree MT (1997) The Cohesion-Tension theory of sap ascent: current controversies. J Exper Bot 48: 1753–1765.

Tyree MT, Sperry JS (1989) Vulnerability of Xylem to Cavitation and Embolism. Ann Rev Plant Physiol Plant Mol Biol 40: 19–36.

Venturas MD, Sperry JS, Hacke UG (2017) Plant xylem hydraulics: What we understand, current research, and future challenges. J Integr Plant Biol 59: 356–389.

Vilagrosa A, Chirino E, Peguero-Pina JJ, Barigah TS, Cochard H, Gil-Pelegrín E (2012) Plant Responses to Drought Stress. Plant Responses to Drought Stress: From Morphological to Molecular Features. doi: https://doi.org/10.1007/978-3-642-32653-0

von Arx G, Carrer M (2014) ROXAS – A new tool to build centuries-long tracheid-lumen chronologies in conifers. Dendrochronologia 32: 290–293.

von Arx G, Dietz H (2005) Automated Image Analysis of Annual Rings in the Roots of Perennial Forbs. Int J Plant Sci 166: 723–732.

Wang R, Zhang L, Zhang S, Cai J, Tyree MT (2014) Water relations of *Robinia pseudoacacia* L.: do vessels cavitate and refill diurnally or are R-shaped curves invalid in *Robinia*? Plant Cell Environ 37: 2667-2678.

Wheeler JK, Huggett BA, Tofte AN, Rockwell FE, Holbrook NM (2013) Cutting xylem under tension or supersaturated with gas can generate PLC and the appearance of rapid recovery from embolism. Plant Cell Environ 36: 1938–1949.

Zanne AE, Lopez-Gonzalez G, Coomes DA, Illic J, Jansen SL, Lewis SL, Miller RB, Swenson NG, Wiemann MCCJ (2009) Data from: Towards a worldwide wood economics spectrum. Dryad Digital Repository. doi: https://doi.org/https://doi.org/10.5061/dryad.234

Zwieniecki MA, Holbrook NM (2009) Confronting Maxwell's demon: biophysics of xylem embolism repair. Trends Plant Sci 14: 530–534.

Chapter 5.

Anderson, G., & Bancroft, J. 2002. Tissue processing and microtomy including frozen. In Bancroft Gamble,J.D., J. (ed.), *Theory and Practice of Histological Techniques*, pp. 87–107. Churchill Livingstone, London.

Anfodillo, T., Carraro, V., Carrer, M., Fior, C., & Rossi, S. 2006. Convergent tapering of xylem conduits in different woody species. *New Phytologist* 169: 279–290.

Anfodillo, T., Petit, G., & Crivellaro, A. 2013. Axial conduit widening in woody species: A still neglected anatomical pattern. *IAWA Journal* 34: 352–364.

Angeles, G., Bond, B., Boyer, J.S., Brodribb, T., Brooks, J.R., Burns, M.J., Cavender-Bares, J., Clearwater, M., Cochard, H., Comstock, J., Davis, S.D., Domec, J.C., Donovan, L., Ewers, F., Gartner, B., Hacke, U., Hinckley, T., Holbrook, N.M., Jones, H.G., Kavanagh, K., Law, B., Lopez-Portillo, J., Lovisolo, C., Martin, T., Martinez-Vilalta, J., Mayr, S., Meinzer, F.C., Melcher, P., Mencuccini, M., Mulkey, S., Nardini, A., Neufeld, H.S., Passioura, J., Pockman, W.T., Pratt, R.B., Rambal, S., Richter, H., Sack, L., Salleo, S., Schubert, A., Schulte, P., Sparks, J.P., Sperry, J., Teskey, R., & Tyree, M. 2004. The Cohesion-Tension theory. *New Phytologist* 163: 451–452.

von Arx, G., & Carrer, M. 2014. ROXAS - a new tool to build centuries-long tracheid-lumen chronologies in conifers. *Dendrochronologia* 32: 290–293.

von Arx, G., & Dietz, H. 2005. Automated Image Analysis of Annual Rings in the Roots of Perennial Forbs. *International Journal of Plant Sciences* 166: 723–732.

Becker, P., Gribben, R.J., & Schulte, P.J. 2003. Incorporation of transfer resistance between tracheary elements into hydraulic resistance models for tapered conduits. *Tree Physiology* 23: 1009–1019.

Brown, H.R. 2013. The Theory of the Rise of Sap in Trees: Some Historical and Conceptual Remarks. *Physics in Perspective* 15: 320–358.

Brown, R.W., & van Haveren, B.P. 1972. The properties and behavior of water in the soil-plant-atmosphere continuum. In *Psychrometry in water relations research*, Logan: Utah State University.

Buckley, T.N., & Sack, L. 2019. The humidity inside leaves and why you should care: implications of unsaturation of leaf intercellular airspaces. *American Journal of Botany* 106: 618–621.

Choat, B., Cobb, A.R., & Jansen, S. 2008. Structure and function of bordered pits: new discoveries and impacts on whole-plant hydraulic function. *New Phytologist* 177: 608–626.

Christman, M.A., & Sperry, J.S. 2010. Single-vessel flow measurements indicate scalariform perforation plates confer higher flow resistance than previously estimated. *Plant Cell and Environment* 33: 431–443.

Cochard, H., Nardini, A., & Coll, L. 2004. Hydraulic architecture of leaf blades: where is the main resistance? *Plant, Cell and Environment* 27: 1257–1267.

Coomes, D.A., Heathcote, S., Godfrey, E.R., Shepherd, J.J., & Sack, L. 2008. Scaling of xylem vessels and veins within the leaves of oak species. *Biol. Lett* 4: 302–306.

Dixon, H.H., & Joly, J. 1895. On the Ascent of Sap. *Philosophical Transactions of the Royal Society of London* 186: 563–576.

Hacke, U.G., & Sperry, J.S. 2001. Functional and ecological xylem anatomy. *Perspectives in Plant Ecology, Evolution and Systematics* 4: 97–115.

Jacobsen, A.L., Valdovinos-Ayala, J., Rodriguez-Zaccaro, F.D., Hill-Crim, M.A., Percolla, M.I., & Venturas, M.D. 2018. Intra-organismal variation in the structure of plant vascular transport tissues in poplar trees. *Trees* 32: 1335–1346.

Johnson, D.M., Wortemann, R., McCulloh, K.A., Jordan-Meille, L., Ward, E., Warren, J.M., Palmroth, S., & Domec, J.-C. 2016. A test of the hydraulic vulnerability segmentation hypothesis in angiosperm and conifer tree species (N. Phillips, Ed.). *Tree Physiology* 36: 983–993.

Lazzarin, M., Crivellaro, A., Williams, C.B., Dawson, T.E., Mozzi, G., & Anfodillo, T.

2016. Tracheid and pît anatomy vary in tandem in a tall Sequoiadendron giganteum tree. *IAWA Journal* 37: 172–185.

Lintunen, A., & Kalliokoski, T. 2010. The effect of tree architecture on conduit diameter and frequency from small distal roots to branch tips in Betula pendula, Picea abies and Pinus sylvestris. *Tree Physiology* 30: 1433–1447.

Lintunen, A., Kalliokoski, T., & Niinemets, Ü. 2010. The effect of tree architecture on conduit diameter and frequency from small distal roots to branch tips in *Betula pendula*, *Picea abies* and *Pinus sylvestris*. *Tree Physiology* 30: 1433–1447.

Losso, A., Anfodillo, T., Ganthaler, A., Kofler, W., Markl, Y., Nardini, A., Oberhuber, W., Purin, G., & Mayr, S. 2018. Robustness of xylem properties in conifers: analyses of tracheid and pit dimensions along elevational transects. *Tree Physiology* 38: 212–222.

Martin-StPaul, N., Delzon, S., & Cochard, H. 2017. Plant resistance to drought depends on timely stomatal closure (H. Maherali, Ed.). *Ecology Letters* 20: 1437–1447.

Martínez-Vilalta, J., Prat, E., Oliveras, I., & Piñol, J. 2002. Xylem hydraulic properties of roots and stems of nine Mediterranean woody species. *Oecologia* 133: 19–29.

Martre, P., Durand, J.-L., & Cochard, H. 2000. Changes in axial hydraulic conductivity along elongating leaf blades in relation to xylem maturation in tall fescue. *New Phytologist* 146: 235–247.

McElrone, A.J., Pockman, W.T., Martinez-Vilalta, J., & Jackson, R.B. 2004. Variation in xylem structure and function in stems and roots of trees to 20 m depth. *New Phytologist* 163: 507–517.

Nardini, A., & Salleo, S. 2000. Limitation of stomatal conductance by hydraulic traits: sensing or preventing xylem cavitation? *Trees* 15: 14–24.

Nobel, P.S. 2012. *Physicochemical and Environmental Plant Physiology*. Academic Press.

Olson, M.E., Anfodillo, T., Rosell, J.A., Petit, G., Crivellaro, A., Isnard, S., León-Gómez, C., Alvarado-Cárdenas, L.O., & Castorena, M. 2014. Universal hydraulics of the flowering plants: Vessel diameter scales with stem length across angiosperm lineages, habits and climates. *Ecology Letters* 17: 988–997.

Olson, M.E., Soriano, D., Rosell, J.A., Anfodillo, T., Donoghue, M.J., Edwards, E.J., León-Gómez, C., Dawson, T., Camarero Martínez, J.J., Castorena, M., Echeverría, A., Espinosa, C.I., Fajardo, A., Gazol, A., Isnard, S., Lima, R.S., Marcati, C.R., & Méndez-Alonzo, R. 2018. Plant height and hydraulic vulnerability to drought and cold. *Proceedings of the National Academy of Sciences* 115: 7551–7556.

Petit, G., & Anfodillo, T. 2009. Plant physiology in theory and practice: An analysis of the WBE model for vascular plants. *Journal of Theoretical Biology* 259: 1–4.

Petit, G., & Anfodillo, T. 2013. Widening of xylem conduits and its effect on the diurnal course of water potential gradients along leaf venations. *Acta Horticulturae* 991: 239–244.

Petit, G., Anfodillo, T., & Mencuccini, M. 2008. Tapering of xylem conduits and hydraulic limitations in sycamore (*Acer pseudoplatanus*) trees. *New Phytologist* 177: 653–664.

Petit, G., Anfodillo, T., & De Zan, C. 2009. Degree of tapering of xylem conduits in stems and roots of small Pinus cembra and Larix decidua trees. *Botany* 87: 501–508.

Petit, G., Pfautsch, S., Anfodillo, T., & Adams, M.A. 2010. The challenge of tree height in Eucalyptus regnans: When xylem tapering overcomes hydraulic resistance.

New Phytologist 187: 1146–1153.
Pittermann, J., Sperry, J.S., Hacke, U.G., Wheeler, J.K., & Sikkema, E.H. 2006. Inter-tracheid pitting and the hydraulic efficiency of conifer wood: The role of tracheid allometry and cavitation protection. *American Journal of Botany* 93: 1265–1273.
Pratt, R.B., North, G.B., Jacobsen, A.L., Ewers, F.W., & Davis, S.D. 2010. Xylem root and shoot hydraulics is linked to life history type in chaparral seedlings. *Functional Ecology* 24: 70–81.
Prendin, A.L., Petit, G., Fonti, P., Rixen, C., Dawes, M.A., & von Arx, G. 2018. Axial xylem architecture of Larix decidua exposed to CO2 enrichment and soil warming at the tree line. *Functional Ecology* 32: 273–287.
Reid, D.E.B., Silins, U., Mendoza, C., & Lieffers, V.J. 2005. A unified nomenclature for quantification and description of water conducting properties of sapwood xylem based on Darcy's law. *Tree Physiology* 25: 993–1000.
Sack, L., & Holbrook, N.M. 2006. Leaf Hydraulics. *Annual Review of Plant Biology* 57: 361–381.
Sack, L., Scoffoni, C., McKown, A.D., Frole, K., Rawls, M., Havran, J.C., Tran, H., & Tran, T. 2012. Developmentally based scaling of leaf venation architecture explains global ecological patterns. *Nature Communications* 3: 837.
Scoffoni, C., Albuquerque, C., Brodersen, C.R., Townes, S. V, John, G.P., Bartlett, M.K., Buckley, T.N., McElrone, A.J., & Sack, L. 2017. Outside-xylem vulnerability, not xylem embolism, controls leaf hydraulic decline during dehydration. *Plant Physiology* 173: 1197–1210.
Sobrado, M. a. 2007. Relationship of water transport to anatomical features in the mangrove Laguncularia racemosa grown under contrasting salinities. *New Phytologist* 173: 584–591.
Sperry, J.S., Hacke, U.G., & Pittermann, J. 2006. Size and function in conifer tracheids and angiosperm vessels. *American Journal of Botany* 93: 1490–1500.
Sperry, J.S., Hacke, U.G., & Wheeler, J.K. 2005. Comparative analysis of end wall resistivity in xylem conduits. *Plant, Cell and Environment* 28: 456–465.
Steudle, E., & Peterson, C. a. 1998. How does water get through roots ? *Journal of Experimental Botany* 49: 775–788.
Trifiló, P., Raimondo, F., Savi, T., Lo Gullo, M.A., & Nardini, A. 2016. The contribution of vascular and extra-vascular water pathways to drought-induced decline of leaf hydraulic conductance. *Journal of Experimental Botany* 67: 5029–5039.
Tsuda, M., & Tyree, M.T. 1997. Whole-plant hydraulic resistance and vulnerability segmentation in Acer saccharinum. *Tree Physiology* 17: 351–357.
Tyree, M., & Ewers, F. 1991. The hydraulic architecture of trees and other woody plants. *New Phytologist* 119: 345–360.
Tyree, M.T., Sinclair, B., Lu, P., & Granier, A. 1993. Whole shoot hydraulic resistance in quercus species measured with a new high-pressure flowmeter. *Annales Des Sciences Forestieres* 50: 417–423.
Tyree, M.T., & Zimmermann, M.H. 2002. *Xylem structure and the ascent of sap*. Springer, Berlin.
Venturas, M.D., Sperry, J.S., & Hacke, U.G. 2017. Plant xylem hydraulics: What we understand, current research, and future challenges. *Journal of Integrative Plant Biology* 59: 356–389.
West, G.B., Brown, J.H., & Enquist, B.J. 1999. A general model for the structure and allometry of plant vascular systems. *Nature* 400: 664–667.

Yang, S.D., & Tyree, M.T. 1994. HYDRAULIC ARCHITECTURE OF ACER-SACCHARUM AND A-RUBRUM - COMPARISON OF BRANCHES TO WHOLE TREES AND THE CONTRIBUTION OF LEAVES TO HYDRAULIC RESISTANCE. *Journal of Experimental Botany* 45: 179–186.

Yang, S., & Tyree, M.T. 1993. Hydraulic resistance in Acer saccharum shoots and its influence on leaf water potential and transpiration. *Tree physiology* 12: 231–42.

Chapter 6.

Adams HD, Zeppel MJ, Anderegg WR, Hartmann H, Landhäusser SM, Tissue DT, ... Anderegg LD (2017) A multi-species synthesis of physiological mechanisms in drought-induced tree mortality. Nat Ecol Evol 1: 1285.

Allen CD, Breshears DD, McDowell NG (2015) An underestimation of global vulnerability to tree mortality and forest die-off from hotter drought in the Anthropocene. Ecosphere 6: 1-55.

Allen CD, Macalady AK, Chenchouni H, Bachelet D, McDowell N, Vennetier M, ... Gonzalez P (2010) A global overview of drought and heat-induced tree mortality reveals emerging climate change risks for forests. Forest Ecol Manag 259: 660-684.

Ameye M, Allmann S, Verwaeren J, Smagghe G, Haesaert G, Schuurink RC, Audenaert K (2018) Green leaf volatile production by plants: a meta-analysis. New Phytol 220: 666-683.

Anfodillo T, Petit G, Crivellaro A (2013) Axial conduit widening in woody species: a still neglected anatomical pattern. Iawa J 34: 352-364.

Anfodillo T, Petit G, Sterck F, Lechthaler S, Olson ME (2016) Allometric trajectories and "stress": a quantitative approach. Front Plant Sci 7: 1681.

Brodribb TJ, Jordan GJ (2008) Internal coordination between hydraulics and stomatal control in leaves. Plant Cell Environ 31: 1557-1564.

Cailleret M, Jansen S, Robert EM, Desoto L, Aakala T, Antos JA, ... Čada V (2017) A synthesis of radial growth patterns preceding tree mortality. Global Change Biol 23: 1675-1690.

Camarero JJ, Gazol A, Sangüesa-Barreda G, Oliva J, Vicente-Serrano SM (2015) To die or not to die: early warnings of tree dieback in response to a severe drought. J Ecol 103: 44-57.

Cochard H (2006) Cavitation in trees. Comptes Rendus Physique 7: 1018-1026.

Dai A (2013) Increasing drought under global warming in observations and models. Nature Climate Change 3: 52.

Dannoura M, Epron D, Desalme D, Massonnet C, Tsuji S, Plain C, ... Gérant D (2018) The impact of prolonged drought on phloem anatomy and phloem transport in young beech trees. Tree physiol 39: 201-210.

De Schepper V, De Swaef T, Bauweraerts I, Steppe K (2013) Phloem transport: a review of mechanisms and controls. J Exp Bot 64: 4839-4850.

Gaylord ML, Kolb TE, McDowell NG (2015) Mechanisms of piñon pine mortality after severe drought: a retrospective study of mature trees. Tree physiol 35: 806-816.

Gleason SM, Westoby M, Jansen S, Choat B, Hacke UG, Pratt RB, ... Cochard H (2016) Weak tradeoff between xylem safety and xylem-specific hydraulic efficiency across the world's woody plant species. New Phytol 209: 123-136.

Hacke UG, Sperry JS, Wheeler JK, Castro L (2006) Scaling of angiosperm xylem structure with safety and efficiency. Tree physiol 26: 689-701.

Hölttä T, Mencuccini M, Nikinmaa E (2009) Linking phloem function to structure: analysis with a coupled xylem–phloem transport model. J Theor Biol 259: 325-337.

Hölttä T, Vesala T, Sevanto S, Perämäki M, Nikinmaa E (2006) Modeling xylem and phloem water flows in trees according to cohesion theory and Münch hypothesis. Trees 20: 67-78.

Jones DL, Nguyen C, Finlay RD (2009) Carbon flow in the rhizosphere: carbon trading at the soil–root interface. Plant Soil 321: 5-33.

Jyske T, Hölttä T (2015) Comparison of phloem and xylem hydraulic architecture in *Picea abies* stems. New Phytol 205: 102-115.

Kiorapostolou N, Galiano-Pérez L, von Arx G, Gessler A, Petit G (2018) Structural and anatomical responses of *Pinus sylvestris* and *Tilia platyphyllos* seedlings exposed to water shortage. Trees 32: 1211-1218.

Kiorapostolou N, Petit G (2018) Similarities and differences in the balances between leaf, xylem and phloem structures in *Fraxinus ornus* along an environmental gradient. Tree Physiol 39: 234-242.

Larter M, Pfautsch S, Domec JC, Trueba S, Nagalingum N, Delzon S (2017) Aridity drove the evolution of extreme embolism resistance and the radiation of conifer genus *Callitris*. New Phytol 215: 97-112.

Lechthaler S, Turnbull TL, Gelmini Y, Pirotti F, Anfodillo T, Adams MA, Petit G (2018) A standardization method to disentangle environmental information from axial trends of xylem anatomical traits. Tree Physiol 39: 495-502.

Maier CA (2001) Stem growth and respiration in loblolly pine plantations differing in soil resource availability. Tree Physiol 21: 1183-1193.

Martínez-Sancho E, Dorado-Liñán I, Hacke UG, Seidel H, Menzel A (2017) Contrasting hydraulic architectures of Scots pine and sessile oak at their southernmost distribution limits. Front Plant Sci 8: 598.

McDowell N, Pockman WT, Allen CD, Breshears DD, Cobb N, Kolb T, ... Yepez EA (2008) Mechanisms of plant survival and mortality during drought: why do some plants survive while others succumb to drought? New Phytol 178: 719-739.

McDowell NG, Fisher RA, Xu C, Domec JC, Hölttä T, Mackay DS, ... Limousin JM (2013) Evaluating theories of drought-induced vegetation mortality using a multimodel–experiment framework. New Phytol 200: 304-321.

Mencuccini M, Hölttä T, Petit G, Magnani F (2007) Sanio's laws revisited. Size-dependent changes in the xylem architecture of trees. Ecol Lett 10: 1084-1093.

Mencuccini M, Hölttä T (2010) The significance of phloem transport for the speed with which canopy photosynthesis and belowground respiration are linked. New Phytol 185: 189-203.

Novak K, De Luis M, Saz MA, Longares LA, Serrano-Notivoli R, Raventós J, ... Rathgeber CB (2016) Missing rings in *Pinus halepensis*–the missing link to relate the tree-ring record to extreme climatic events. Front Plant Sci 7: 727.

O'Brien MJ, Leuzinger S, Philipson CD, Tay J, Hector A (2014) Drought survival of tropical tree seedlings enhanced by non-structural carbohydrate levels. Nature Climate Change 4: 710.

Pellizzari E, Camarero JJ, Gazol A, Sangüesa-Barreda G, Carrer M (2016) Wood anatomy and carbon-isotope discrimination support long-term hydraulic deterioration as a major cause of drought-induced dieback. Global change Biol 22: 2125-2137.

Peñuelas J, Llusià J (2003) BVOCs: plant defense against climate warming? Trends

Plant Sci 8: 105-109.
Petit G, Anfodillo T (2009) Plant physiology in theory and practice: an analysis of the WBE model for vascular plants. J Theor Biol 259: 1-4.
Petit G, Anfodillo T, De Zan C (2009) Degree of tapering of xylem conduits in stems and roots of small *Pinus cembra* and *Larix decidua* trees. Botany 87: 501-508.
Petit G, Crivellaro A (2014) Comparative axial widening of phloem and xylem conduits in small woody plants. Trees 28: 915-921.
Petit G, Pfautsch S, Anfodillo T, Adams MA (2010) The challenge of tree height in *Eucalyptus regnans*: when xylem tapering overcomes hydraulic resistance. New Phytol 187: 1146-1153.
Petit G, Savi T, Consolini M, Anfodillo T, Nardini A (2016) Interplay of growth rate and xylem plasticity for optimal coordination of carbon and hydraulic economies in *Fraxinus ornus* trees. Tree Physiol 36: 1310-1319.
Pfautsch S, Harbusch M, Wesolowski A, Smith R, Macfarlane C, Tjoelker MG, ... Adams MA (2016) Climate determines vascular traits in the ecologically diverse genus *Eucalyptus*. Ecol Lett 19: 240-248.
Preece C, Farré-Armengol G, Llusià J, Peñuelas J (2018) Thirsty tree roots exude more carbon. Tree Physiol 38: 690-695.
Prendin AL, Mayr S, Beikircher B, von Arx G, Petit G (2018) Xylem anatomical adjustments prioritize hydraulic efficiency over safety as Norway spruce trees grow taller. Tree Physiol 38: 1088-1097.
R Development Core Team (2017) R: A language and environment for statistical computing. R Foundation for Statistical Computing, Vienna, Austria. URL https://www.R-project.org/
Ryan MG, Robert EM (2017) Zero-calorie sugar delivery to roots. Nature plants 3: 922.
Savage JA, Beecher SD, Clerx L, Gersony JT, Knoblauch J, Losada JM, ... Holbrook NM (2017) Maintenance of carbohydrate transport in tall trees. Nature plants 3: 965.
Schuldt B, Knutzen F, Delzon S, Jansen S, Müller-Haubold H, Burlett R, ... Leuschner C (2016) How adaptable is the hydraulic system of European beech in the face of climate change-related precipitation reduction? New Phytol 210: 443-458.
Scoffoni C, Albuquerque C, Brodersen CR, Townes SV, John GP, Bartlett MK, ... Sack L (2017) Outside-xylem vulnerability, not xylem embolism, controls leaf hydraulic decline during dehydration. Plant Physiol 173: 1197-1210.
Sevanto S (2014) Phloem transport and drought. J Exper Bot 65: 1751-1759.
Sevanto S, McDowell NG, Dickman LT, Pangle R, Pockman WT (2014) How do trees die? A test of the hydraulic failure and carbon starvation hypotheses. Plant Cell Environ 37: 153-161.
Sevanto S, Ryan M, Dickman LT, Derome D, Patera A, Defraeye T, ... Pockman WT (2018) Is desiccation tolerance and avoidance reflected in xylem and phloem anatomy of two coexisting arid-zone coniferous trees? Plant Cell Environ 41: 1551-1564.
Sperry JS, Hacke UG, Pittermann J (2006) Size and function in conifer tracheids and angiosperm vessels. Am J Bot 93: 1490-1500.
Taiz L, Zeiger E (2006) Plant Physiology, Respiration and Lipid Matebolism.
Tixier A, Herbette S, Jansen S, Capron M, Tordjeman P, Cochard H, Badel E (2014) Modelling the mechanical behaviour of pit membranes in bordered pits with respect to cavitation resistance in angiosperms. An Bot 114: 325-334.

Tyree MT (1997) The cohesion-tension theory of sap ascent: current controversies. J Exp Bot 48: 1753-1765.
Tyree MT, Ewers FW (1991) The hydraulic architecture of trees and other woody plants. New Phytol 119: 345-360.
Venturas MD, Sperry JS, Hacke UG (2017) Plant xylem hydraulics: what we understand, current research, and future challenges. J Integ Plant Biol 59: 356-389.
Von Arx G, Archer SR, Hughes MK (2012) Long-term functional plasticity in plant hydraulic architecture in response to supplemental moisture. An Bot 109: 1091-1100.
Von Arx G, Carrer M (2014) ROXAS–A new tool to build centuries-long tracheid-lumen chronologies in conifers. Dendrochronologia 32: 290-293.
Walter J (2018) Effects of changes in soil moisture and precipitation patterns on plant-mediated biotic interactions in terrestrial ecosystems. Plant Ecol 219: 1449-1462.
Waring RH, Landsberg JJ, Williams M (1998) Net primary production of forests: a constant fraction of gross primary production? Tree physiol 18: 129-134.
Warton DI, Wright IJ, Falster DS, Westoby M (2006) Bivariate line-fitting methods for allometry. Biol Reviews 81: 259-291.
Warton DI, Duursma RA, Falster DS, Taskinen S (2012) smatr 3–an R package for estimation and inference about allometric lines. Methods Ecology Evol 3: 257-259.
Weemstra M, Eilmann B, Sass-Klaassen UG, Sterck FJ (2013) Summer droughts limit tree growth across 10 temperate species on a productive forest site. Forest Ecol Manag 306: 142-149.

Chapter 7.

De Vries FP (1975) The cost of maintenance processes in plant cells. *Ann Bot 39*: 77-92.
Hargreaves HG, Z.A. Samani ZA (1982) Estimating Potential Evapotranspiration. *J Irrigation Drainage Division - ASCE* 108 (January):225–30.
Plavcova L, Hoch G, Morris H, Ghiasi S, Jansen S (2016) The amount of parenchyma and living fibers affects storage of nonstructural carbohydrates in young stems and roots of temperate trees. Am J Bot 103: 603–612.
R Core Team (2017) R: A language and environment for statistical computing. R Foundation for Statistical Computing, Vienna, Austria. URL: https://www.R-project.org/.
Schneider CA, Rasband WS, Eliceiri KW (2012) NIH Image to ImageJ: 25 years of image analysis. Nature methods 9: 671.
Zwieniecki MA, Holbrook NM (2009) Confronting Maxwell's demon: biophysics of xylem embolism repair. Trends Plant Sci 14: 530–534.

Chapter 8.

Anfodillo T, Petit G, Crivellaro A (2013) Axial conduit widening in woody species: a still neglected anatomical pattern. IAWA 34: 352-364. doi: 10.1163/22941932-00000030
Pfautsch S, Harbusch M, Wesolowski A, Smith R, Macfarlane C, Tjoelker MG, Reich PB, Adams MA (2016) Climate determines vascular traits in the ecologically diverse genus *Eucalyptus*. Ecol Lett 19:240–248.

von Arx G, Archer SR, Hughes MK (2012) Long-term functional plasticity in plant hydraulic architecture in response to supplemental moisture. Ann Bot 109:1091–1100.

Weemstra M, Eilmann B, Sass-Klaassen UG, Sterck FJ (2013) Summer droughts limit tree growth across 10 temperate species on a productive forest site. *Forest Ecol Manag* 306: 142-149.